Hochschule für Angewandte Wissenschaften Hamburg
Hamburg University of Applied Sciences

Hamburg University of Applied Science

Faculty Life Sciences

Sex specific differences in *Leishmania* infection and treatment of human primary macrophages

Master Thesis

In Pharmaceutical Biotechnology

Handed in by

Max Hüppner

[redacted]

Hamburg

11.11.2022

Table of content

List of abbreviations

AmpB	Amphotericin B
APC	allophycocyanin
APC	antigen-presenting cell
BNITM	Bernhard-Nocht-Institute for Tropical Medicine
BSA	bovine serum albumin
BUV	brilliant ultraviolet
BV	brilliant violet
CCL	chemokine (C-C motif) ligand
CD	Cluster of differentiation
CR	complement receptor
CXCL	chemokine (C-X-C motif) ligand
DAMP	damage associated molecular pattern
DAPI	4',6-Diamidino-2-phenylindol
DC	dendritic cell
DHT	5α-Dihydrotestosterone
DMSO	dimethyl sulfoxide
(D)PBS	(Dulbeccos) phosphate buffered saline
e.g.	lat.: exempli gratia engl.: for example
E2	17β-Estradiol
EDTA	Ethylenediaminetetraacetic acid
Eh	*Entamoeba histolytica*
et al.	lat.: *et aliis* engl.: and others
FACS	fluorescent activated cell sorting

FCS	fetal calf serum
FDA	(united states) food and drug administration
FITC	fluorescein-5-isothiocyanate
GPI	glycosylphosphatidylinositol
h.p.i.	hours post infection
HCS	high content screening
HEPES	4-(2-hydroxyethyl)-1-piperazineethanesulfonic acid
HLA-DR	human leukocyte antigen – DR isotype
hMDM	human monocyte derived macrophages
HSC	hematopoietic stem cell
HSP	heat shock protein
HSP90	heat shock protein 90
Ig	Immunglobulin
IL	interleukin
Imi	Imiquimod
(i)NOS	(cytokine - inducible) nitric oxide synthase
ISDA	Infectious Disease Society of America
LPS	Lipopolysaccharides
MACS	magnetic cell separation
M-CSF	macrophage colony stimulation factor
MHC	major histocompatibility complex
Mil	Miltefosine
MOI	multiplicity of infection
MPO	myeloperoxidase
NA	numerical aperture

NADPH	nicotinamide adenine dinucleotide phosphate
NF	nuclear factor
NK	natural killer
NLR	NOD-like receptor
NO	nitric oxide
NOD	nucleotide-binding oligomerization domain
PAMP	pathogen associated molecular pattern
PBMC	peripheral blood mononuclear cells
PE	phycoerythrin
PerCP	pridinin chlorophyll protein
PFA	paraformaldehyde
PI	phosphatidylinositol
PRR	pattern recognition receptor
RLR	retinoid acid-inducible gene I-like receptor
RNS	reactive nitrogen species
ROS	reactive oxygen species
RPMI	Roswell Park Memorial Institute
RT	room temperature
TCR	T cell receptor
Th1/2	$CD4^+$ T helper cells type 1/2
TLR	toll-like receptor
TNF	tumor necrosis factor
U	units
UV	ultraviolet
WHO	World Health Organisation

Abstract

Leishmaniasis is a group of neglected tropical diseases with around 1,4 million new cases each year. Depending on *Leishmania* species, different clinical manifestations of the disease can be observed, with symptoms varying from cutaneous lesions (“cutaneous Leishmaniasis) to visceral organ damage (“visceral Leishmaniasis”) with high lethality when left untreated. With the current rise in temperature induced by anthropogenic climate change and a globalized world as we see it today, in the future it is not unlikely that *Leishmania* parasites also migrate to northern western world countries. Increasing resistance of parasites to current treatment methods generates the need for new drugs or new therapy strategies. Given that the development of disease is highly dependent on the characteristics of host immune response, combining leishmanicidal drugs with immune response modifiers is an intriguing option for combination treatments in the future to lower the doses of toxic drugs and to ameliorate adverse effects and increase treatment efficacy by circumventing drug resistance mechanisms. The research groups of groups of Prof. Meier (University of Hamburg) and Prof. Lotter (BNITM) have developed six chemically synthesized analoga of a glycosylphosphatidylinositol anchor derived from lipopeptidephosphoglycan found in the membrane of *Entamoeba histolytica*, called Eh-1 - Eh-6 which show immune modulatory functions and protection during *Leishmania* infection making them interesting drug candidates for combination therapy of Leishmaniasis. A male bias of infection and disease severity can be observed in Leishmaniasis and other parasitic diseases indicating a background of sex specific immunity.

During this work different strategies for the treatment of human monocyte-derived macrophages infected with *Leishmania (L.) major* and *L. infantum* have been tested in *in vitro* models of cutaneous and visceral Leishmaniasis (**Figure 0-1**). Mono and combination therapy strategies with Amphotericin B, Miltefosine, Imiquimod and drug candidate Eh-1 were tested using high content drug screening assays identifying Miltefosine or Amphotericin B with Imiquimod as combinations with cooperative potential. Eh-1 did not provide convincing evidence for combination therapy. Still, in cytokine analyses of *L. major* infection, Eh-1 showed expression of protective cytokines indicating increased inflammasome mediated oxidative clearance of

parasites, which was amplified in combination with Amphotericin B to provide cooperative protection. In *L. infantum* infection Eh-1 also showed protection, but independent of protective cytokine production. During infection experiments several instances of sex specific immunity were observed, as females showed higher degree of inflammatory cytokine production, stronger pro inflammatory phenotype and lower overall infection with *L. infantum*. In this context Estradiol was identified as mediator of protection against *L. infantum* infection and Dihydrotestosterone mediated higher susceptibility to infection for female human monocyte-derived macrophages.

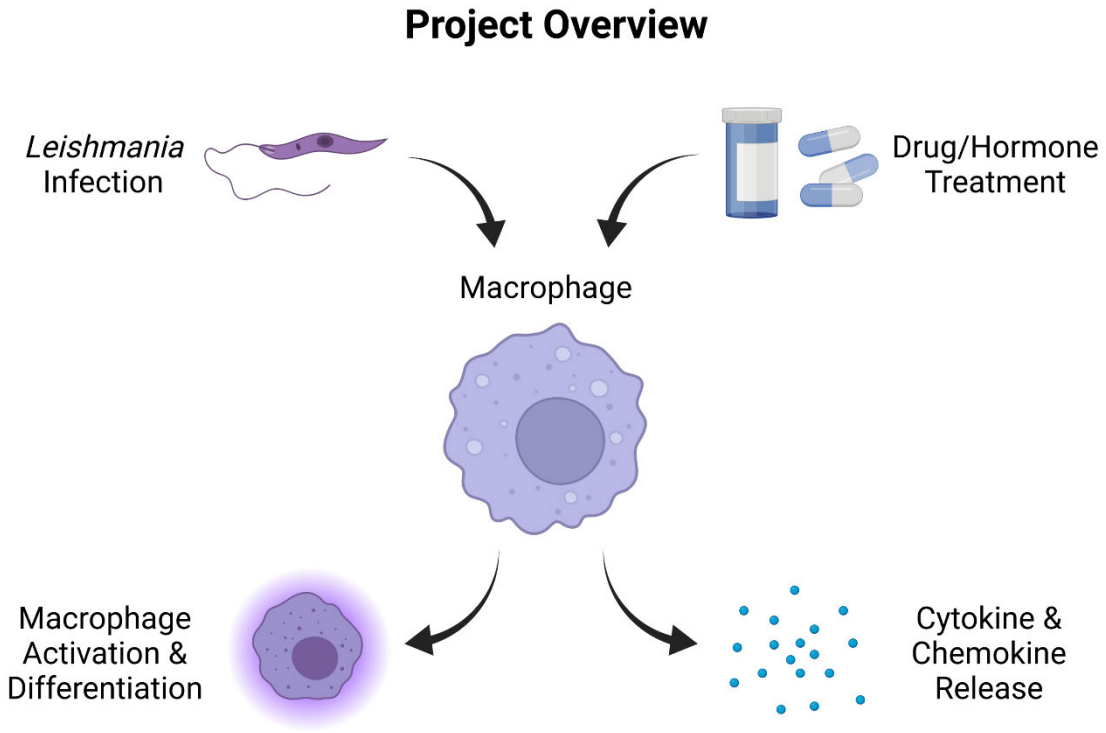

Figure 0-1: Basic overview of the Project. Macrophages are infected with *Leishmania* parasites and treated with different drug combinations or hormones inducing macrophage activation and differentiation, and the release of cytokines and chemokines, which are analyzed subsequently. (Created with BioRender)

1 Introduction

Humans encounter various infections with pathogens during their lifetime. Therefore, the human body has evolved a great number of ways of fighting pathogens before they can exert their destructive properties. This complex interplay of leukocyte cells and effector molecules is termed the immune system (Murphy and Weaver 2016).

1.1 Human Immune System

The human immune system often is broadly categorized into two branches: innate and adaptive immune system (Murphy and Weaver 2016).

Cells of the innate immune system act immediately to recognize pathogens, initiate a defensive response via phagocytosis or release of antimicrobial granola and promote inflammatory responses by enabling monocyte and lymphocyte migration via chemokine and cytokine production (Murphy and Weaver 2016).

Cells of the adaptive immune system are activated by binding of specific (pathogen-associated) antigens to one of a huge number of invariant surface receptors of T or B lymphocytes and signals of innate immune cells, acting after four to seven days to provide a tailored, pathogen-specific response. This includes polyclonal antibody responses induced by activated B lymphocytes and diverse enhancing as well as regulatory mechanisms induced by activated T lymphocytes (Murphy and Weaver 2016).

1.1.1 Macrophage origin and distribution

Macrophages are innate immune cells of myeloid lineage, that show a great degree of plasticity in their genotype and function (Murphy and Weaver 2016, Gasteiger, D'Osualdo et al. 2017). They originate in the bone marrow where pluripotent hematopoetic stem cells mature to monocytes during hematopoeises (Murphy and Weaver 2016). Monocytes are released into the bloodstream, where they can circulate for up to seven days depending on their functional role (Patel, Ginhoux et al. 2021). They can migrate into tissues via positive chemotaxis upon chemokine stimulation and

differentiate into macrophages to fulfill various functions not only in the immediate response to pathogen invasion, but also in tissue integrity and homeostasis (Gasteiger, D'Osualdo et al. 2017).

Human peripheral blood monocytes show heterogeneity in their surface receptor composition indicating subsets with distinct functions (Yang, Zhang et al. 2014). These are often categorized into three subsets: classical, intermediate, and non-classical monocytes (Yang, Zhang et al. 2014). These subsets can be identified by their degree of cluster of differentiation (CD)14/CD16 expression.

In both, steady state conditions and inflammation, classical CD14+ monocytes can migrate into tissues to become tissue resident macrophages or dendritic cells (DCs) (Italiani and Boraschi 2014). Monocyte differentiation into macrophages in tissue environments is driven by macrophage colony-stimulating factor (M-CSF), which, in a tissue context, is expressed by stromal cells and binds to colony-stimulating factor 1 receptor (CSF-1R) expressed on monocytes (Italiani and Boraschi 2014). Importantly, for *in vitro* studies this differentiation process can be reproduced by cultivation in the presence of M-CSF (Rey-Giraud, Hafner et al. 2012). Isolation of human primary macrophages is highly impracticable, since it requires tissue samples with low yield, and macrophages do not proliferate in culture (Merck 2022). Depending on the media composition, macrophages can be polarized into different activation states (Rey-Giraud, Hafner et al. 2012).

1.1.2 Macrophage roles in pathogen response and inflammation

Next to neutrophils, macrophages are among the first cells pathogens encounter when they enter a tissue environment (Murphy and Weaver 2016). They are involved in pathogen removal, wound healing, and immune regulation (Italiani and Boraschi 2014).

They can fight pathogens directly by reactive oxygen species (ROS), nitric oxide (NO) and myeloperoxidase (MPO) production and engulf them via phagocytosis to process and present (pathogen associated) antigens via major histocompatibility complex (MHC) II (Eiz-Vesper and Schmetzer 2020). Before an oxidative response, pathogens trigger a signaling cascade in macrophages upon recognition by pathogen-specific cell surface receptors (Mogensen 2009).

Macrophages have a variety of different pathogen recognition and binding systems. They can recognize pathogen invasion by toll-like receptors (TLRs) on their cell surface. Binding of pathogen-associated molecular patterns (PAMPs) to TLRs induces oligomerization of intracellular signaling domains resulting in the induction of inflammatory pathways (e.g. Myeloid differentiation primary response 88 (Myd88)-pathway) (Mogensen 2009, Chavez-Galan, Olleros et al. 2015). Intracellular pattern-recognition receptors (PRRs) in the form of retinoid acid-inducible gene I-like receptors (RLRs) or nucleotide-binding oligomerization domain (NOD)-like receptors (NLRs) give additional aid in the induction of inflammatory reactions (Mogensen 2009).

Macrophages exert functions in signal transduction and cell communication. They secrete several cytokines, chemokines, microvesicles and growth factors and act in direct signal transduction via diverse surface receptor interactions and communication via gap junctions (Gasteiger, D'Osualdo et al. 2017). This enables macrophages to be “immune modulatory switches” in facilitating T helper type 1 (Th1) or T helper type 2 (Th2) responses by driving the functional polarization of tissue resident $CD4^+$ T cells, which do not act in pathogen recognition themselves (Italiani and Boraschi 2014).

Since they can display different activation states that differ in proteome and can show contradicting roles during inflammation and its resolution, macrophages are often categorized into two broad categories: M1 (“classically activated”) and M2 (“alternatively activated”) macrophages, which act pro- (or Th1-related) and anti-inflammatory (or Th2-related), respectively (Italiani and Boraschi 2014). In **Table 1-1** characteristic properties of the different activation states are summarized.

The pro-inflammatory M1 state is characterized by the expression of interleukin (IL)-1β, tumor necrosis factor (TNF)-α, IL-12, IL-6 & IL-23 as well as upregulation of inducible nitric oxide synthase (iNOS) and subsequent NO production facilitating the killing of pathogens (Italiani and Boraschi 2014, Chavez-Galan, Olleros et al. 2015). The release of NO can damage surrounding tissue. Upregulation of MHC II, cluster of differentiation (CD) 68 and CD80 surface proteins enables efficient activation of T cells (Broeren, Gray et al. 2000, Buxade, Huerga Encabo et al. 2018). M1 macrophage polarization and Th1 responses are closely related and influence each other in a positive feedback loop (Italiani and Boraschi 2014, Buxade, Huerga Encabo et al. 2018). Triggered by PAMP binding, macrophages produce cytokines and present antigens via MHC II, which are bound by T cell receptors (TCRs) of resident $CD4^+$ T

cells driving Th1 polarization (Mogensen 2009, Italiani and Boraschi 2014). Th1 T cells in turn express interferon (IFN)-γ, which is a potent inducer of M1 macrophage polarization (Italiani and Boraschi 2014).

The anti-inflammatory M2 state has been subcategorized into M2a, M2b and M2c with varying action profiles depending on the stimuli inducing the respective state (Italiani and Boraschi 2014).

Stimulation by IL-4 or IL-13 suppresses IFN-γ signaling and leads to a phenotype with high expression of IL-10, transforming growth factor (TGF)-β and signal transducer and activator of transcription (STAT) 6 transcription factor, which actively suppress inflammatory reactions on a transcription level and drive Th2 differentiation, CD206 expression and Arginase1 (Arg1) production (Italiani and Boraschi 2014, Chavez-Galan, Olleros et al. 2015, Viola, Munari et al. 2019). CD206, or macrophage mannose receptor, can bind proteins with mannose modifications like e.g. myeloperoxidase, but also surface proteins of pathogens like lipophosphoglycan (LPG) of *Leishmania donovani* leading to phagocytosis of pathogens and clearance of damaging enzymes (Chakraborty, Ghosh et al. 2001, Lee, Evers et al. 2002). This state is called M2a (Italiani and Boraschi 2014, Chavez-Galan, Olleros et al. 2015, Viola, Munari et al. 2019). M2a macrophages show activity in tissue remodeling and angiogenesis (Zizzo, Hilliard et al. 2012, Viola, Munari et al. 2019).

M2b state is induced by simultaneous binding of TLR ligands and fragment crystallizable (FC)γ receptor activation by immunocomplexes. It is characterized by a phenotype similar to M1 with CD86 as well as MHC II on the cell surface (Viola, Munari et al. 2019). By expressing IL-6R and IL-12R on their surface, these macrophages are drawn to sites of high inflammation and show important functions in controlling immune reactions by driving Th2 response via IL-10 and Arg1 expression (Zizzo, Hilliard et al. 2012, Italiani and Boraschi 2014, Viola, Munari et al. 2019).

M2c state, which is induced by stimulation with glucocorticoids and IL-10, shows high immunosuppression by abundant IL-10 and TGF-β expression enabling tissue regeneration (Viola, Munari et al. 2019). They express the apoptotic cell receptor Mer tyrosine kinase and are associated with the removal and degradation of apoptotic cells and debris, which is an important factor in tissue homeostasis (Zizzo, Hilliard et al. 2012, Gasteiger, D'Osualdo et al. 2017).

Table 1-1: Overview of macrophage activation states and their characteristic properties. The pro-inflammatory M1 state is related to Th1 response and is characterized by diverse inflammatory cytokines as well as NO production by iNOS. M2 states are associated with anti-inflammatory cytokines, Th2 response and immunosuppression. Source: (Viola, Munari et al. 2019), modified

Polarization	Stimuli	Released cytokines	Surface markers	Metabolic enzymes	Transcription factors	Functions
M1	LPS + IFN-γ	TNF-α, IL-1β, IL-6, IL-12, IL-23	CD80, CD86, CIITA, MHC-II	iNOS, PFKFB3, PKM2, ACOD1	NF-κB (p65), STAT1, STAT3, IRF-4, HIF1α, AP1	Bacterial killing, tumor resistance, Th1 response
M2a	IL-4/IL-13	IL-10, TGF-β	CD206, CD36, IL1Ra, CD163	ARG1, CARKL	STAT6, GATA3, SOCS1, PPARγ	Anti-inflammatory response, tissue remodeling, wound healing
M2b	IC, TLR ligands/IL-1Ra	IL-10, IL-1β, IL-6, TNF- α	CD86, MHC II	ARG1, CARKL	STAT3, IRF4, NF-κB (p50)	Tumor progression, immunoregulation, Th2 response
M2c	Glucocorticoids/IL-10	IL-10, TGF- β	CD163, TLR1, TLR8	ARG1, GS	STAT3, STAT6, IRF4, NF-κB (p50)	Phagocytosis of apoptotic bodies, tissue remodeling, immunosuppresion

A2R, adenosine receptor 2; ACOD1, aconitate decarboxylase 1; AP-1, Activator proten 1; ARG1, Arginase 1; CARKL, carbohydrate kinase- like; IC, immunocomplexes; IDO, indoleamine dioxygenase; iNOS, inducible Nitric Oxide Synthase; GATA3, GATA binding protein 3; GS, glutamine synthetase; HIF1α, Hypoxia-inducible factor 1-alpha; IFN-γ, Interferon gamma; IL-, interleukin; IRF, interferon regulatory factor; MHC-II, major histocompatibility complex class 2; NF-κB, nuclear factor kappa-light-chain-enhancer of activated B cells; PPARγ, Peroxisome proliferator-activated receptor gamma; SOCS1, Suppressor of cytokine signaling 1; STAT, Signal transducer and activator of transcription; TNF-α, Tumor necrosis factor alpha; TGF-β, transforming growth factor beta; TLR, toll like receptor; VEGF, Vascular endothelial growth factor.

All M2 substates are characterized by the expression of scavenger receptors, which can recognize damage-associated molecular patterns (DAMPs) drawing M2 macrophages to sites of tissue damage (Italiani and Boraschi 2014, Komai, Shichita et al. 2017). Together with Arg1 activity as a competitor for iNOS substrate L-arginine and its ability to produce polyamines and collagen, these properties allow for the effective containment and replenishment of M1 and Th1 induced oxidative damage (Caldwell, Rodriguez et al. 2018).

Although M1/M2 classification does not display the real, dynamic plasticity of macrophage activation very accurately, it can still be used to get a general idea of activation and action profile tendencies. In *in vivo* tissue context, delicate changes in the microenvironment induce subtle changes in proteome leading to a much greater range of genotypes than *in vitro* polarization can display (Italiani and Boraschi 2014). It is important to note that in transcription studies *in vitro* polarized macrophages and *in vivo* stimulated macrophages of the same activation state showed deviating transcriptomes and often, data generated in *in vitro* models cannot be transferred to animal models directly (Orecchioni, Ghosheh et al. 2019).

1.2 Leishmaniasis

Leishmaniasis, a disease affecting humans and other vertebrates, is transmitted by phlebotomine sand flies during blood meals (Global Health 2020). It is caused by protozoan parasites of the genus *Leishmania* (Global Health 2020). Twenty different human pathogenic *Leishmania* species can be found in around 90 countries, mainly in tropical or subtropical areas as well as in southern Europe (Mann, Frasca et al. 2021). Disease forms and respective causative parasites are grouped in three categories: cutaneous (infection of the skin/dermis), mucosal/muco-cutaneous (infection of mucosal tissues) and visceral (infection of inner organs) Leishmaniasis (Mann, Frasca et al. 2021). Leishmaniasis is classified as a neglected tropical disease by the World Health Organisation (WHO) with approximately 1 million cases of its cutaneous and < 100.000 cases for its visceral manifestation each year (Global Health 2020, WHO 2022)

1.2.1 Parasites and human disease

The obligate intracellular *Leishmania* parasites can be found in two main phenotypes during their life cycle (**Figure 1-1**), promastigotes and amastigotes (Mann, Frasca et al. 2021).

Metacyclic promastigotes, that form inside the vector, are injected into human skin during the blood meal of sand flies, where they are phagocytized by mononuclear cells, often macrophages (Bates 2007, Mann, Frasca et al. 2021). Subsequently in response to environmental changes in phagolysosomes, intracellular parasites transform into their amastigote form changing their metabolism and phenotype (Besteiro, Williams et al. 2007). They reproduce by cell division inside a “parasitophorous vacuole”, which can be compared to a phagosome, while interfering with host cell metabolism and can also be transported through the bloodstream or lymph system to infect other tissues than the skin (Mann, Frasca et al. 2021). When a critical number is reached, host cells are lysed and *Leishmania* amastigotes are released to be phagocytized again (Inc. 2022). Amastigote infected cells can be taken up during the blood meal of sand flies where *Leishmania* transform into promastigotes in sand fly gut (Besteiro, Williams et al. 2007). After multiplication they migrate to the proboscis from where they can be transmitted to a new host (Besteiro, Williams et al. 2007, Global Health 2020).

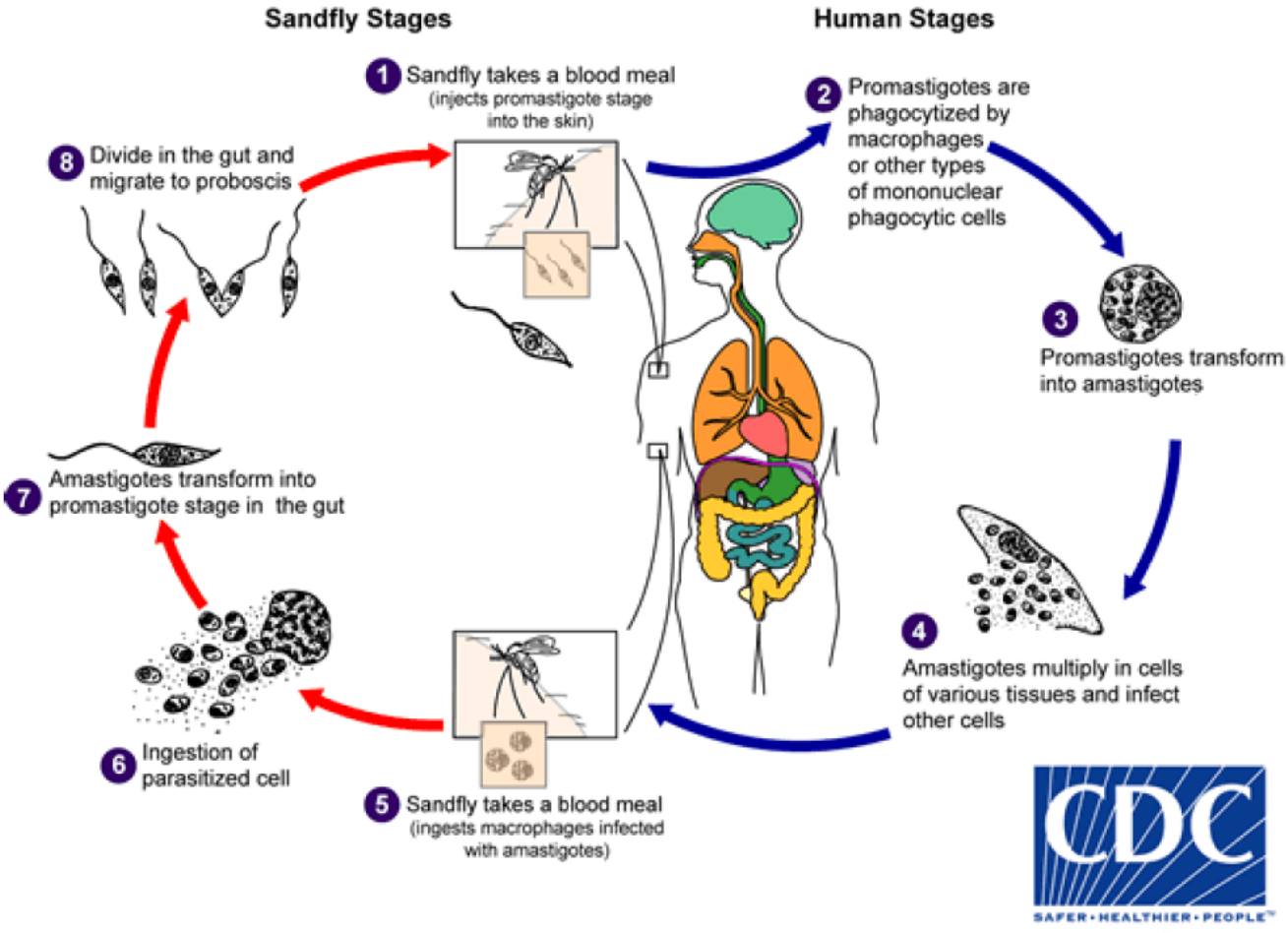

Figure 1-1: Schematic overview of Leishmania life cycle. Leishmania promastigotes are transferred to the human host via sand fly blood meal (1) where they are phagocytized by macrophages (2). They shift their metabolism and respond to their new environment in amastigote form (3), in which they proliferate until the host cell is lysed (4). They can be transferred back into the sand fly vector by their blood meal (5) as intracellular amastigotes. Inside the sand fly gut, they transform back into promastigotes (7) enabling them to move to the proboscis for new transmission (8). Source: (Global Health 2020)

Leishmaniasis can develop different clinical manifestations depending on the infecting *Leishmania* species and immune response of the host (Mann, Frasca et al. 2021): cutaneous, mucocutaneous and visceral disease. During the work for this thesis *Leishmania (L.) major* and *L. infantum* were used. *L. major* is the main endemic species causing cutaneous disease in the new world and *L. infantum* is the prevalent species found in the mediterranean area and southern Europe causing cutaneous and visceral disease (Pigott, Bhatt et al. 2014).

Development of cutaneous Leishmaniasis starts with papules on the skin at the site of the sand fly bite, that over weeks to months can develop into lesions (Mann, Frasca et

al. 2021). Lesion manifestations vary substantially. Some individuals show no clinical symptoms at all, while others develop acute skin ulcers that can heal spontaneously over months to years and cause scars strongly influencing quality of life (Mann, Frasca et al. 2021).

Visceral Leishmaniasis represents the most severe form of the disease, since its systemic distribution of parasites leads to infection of liver, spleen, hematogenous and lymphatic system causing hepatosplenomegaly, weight loss and pancytopenia (Mann, Frasca et al. 2021). Untreated, visceral Leishmaniasis is often lethal (Mann, Frasca et al. 2021).

The course of the malicious disease caused by *Leishmania* parasites is driven by differences in Th1 and Th2 responses (Mann, Frasca et al. 2021). Individuals with an immediate Th1 response show low parasite burden and better disease control, but a tendency toward an overshooting oxidative response and related tissue damage while humans with an immediate Th2 response are more prone to systemic distribution of parasites, diffuse disease and visceral Leishmaniasis (Mann, Frasca et al. 2021).

It is important to note that parasite strains show different clinical symptoms, ways of interaction with host immune system, and metabolism (Westrop, Williams et al. 2015).

1.3 Macrophage response in the context of *Leishmania* infection

As mentioned in **1.2.1**, macrophages are the main replicating niche for *Leishmania* parasites (Bogdan 2020), even though most parasites are phagocytized by neutrophil granulocytes upon host entry (Tomiotto-Pellissier, Bortoleti et al. 2018). Mouse model experiments have shown, that even when they are phagocytized by neutrophils upon host entry, *Leishmania* will eventually find their way into macrophages, since neutrophils will commit to apoptosis while secreting chemokine (C-C motif) ligand (CCL) 4, that draws macrophages to the site of action, where they phagocytize parasites while clearing cell debris (Bogdan 2020).

When Leishmania directly interact with macrophages, their uptake has been linked to interaction with complement receptor (CR) 1, CR 3 and mannose-fucose receptor (Liu and Uzonna 2012). Interestingly metacyclic promastigotes do not bind to mannose-

fucose receptor, while avirulent promastigotes induce an inflammatory response after mannose-fucose receptor interaction (Liu and Uzonna 2012). After binding to these receptors, parasites are internalized in phagosomes (Liu and Uzonna 2012).

Following phagocytosis, *Leishmania* are transported to lysosomes for degradation (Moradin and Descoteaux 2012). During this process, promastigotes have been observed to inhibit maturation of phagolysosomes leading to limited interaction with lysosomes and late endosomes (Moradin and Descoteaux 2012). Moreover, in phagosomes containing promastigotes, ROS generation by nicotinamide adenine dinucleotide phosphate (NADPH) oxidase is depleted, depriving macrophages of one of their efficient degradation mechanisms (Moradin and Descoteaux 2012). In this low oxidative, acidic environment of phagosomes, *Leishmania* then transform into amastigotes to form the parasitophorous vacuole, their main center of replication (Moradin and Descoteaux 2012). The inhibition of phagosome maturation has been linked to the abundantly expressed, membrane bound surface glycolipid lipophosphoglycan (LPG) of *Leishmania* (Moradin and Descoteaux 2012). This molecule is most likely involved in the disruption of lipid microdomains in the phagosome membrane causing impairment of fusion machinery (Moradin and Descoteaux 2012).

Without the direct, phagocytosis-mediated lysosomal degradation of *Leishmania* at their disposal, macrophages are required to combat parasites in another way. This is where macrophage polarization state and immune response modulation can be deciding factors.

1.3.1 Role of macrophage polarization states and cytokines in immune response to *Leishmania* infection

The most important role in killing intracellular *Leishmania* is fulfilled by iNOS, the enzyme responsible for the production of NO, which is toxic to parasites (Liu and Uzonna 2012). This enzyme is abundantly expressed in macrophages polarized into M1 state (Liu and Uzonna 2012). Induction of iNOS in macrophages is critically dependent on IFN-γ (Liu and Uzonna 2012). IFN-γ is usually found in the context of Th1 response, expressed by effector T cells after antigen presentation and cytokine stimulation (Khattak, Akbar et al. 2021). In Leishmaniasis, usually IL-12 expression by

dendritic cells (DCs) and macrophages leads to induction of IFN-γ expression by $CD4^+$ T cells and natural killer (NK) cells (s. **Figure 1-2**) (Khattak, Akbar et al. 2021). Interestingly, *in vitro* experiments have shown, that in mouse macrophages IL-12 expression is actively inhibited by *Leishmania* parasites (Carrera, Gazzinelli et al. 1996).

Generally, it is believed that the interplay of IFN-γ production by $CD4^+$ T cells and macrophages is required to contain *Leishmania* infection as it has been shown in mouse models (Bogdan 2020). In addition to IFN-γ expression, TNF-α expression is necessary for iNOS activity and parasite killing by mouse macrophages (Bogdan 2020). TNF-α has shown to epigenetically reduce the induction of Arg1 expression by IL-4 and induce expression of iNOS by activation of mitogen-activated protein kinases and the transcription factors activator protein (AP)-1 and NF-κB (Bogdan 2020). TNF-α production in macrophages can be induced by PAMP binding or TLR stimulation (Parameswaran and Patial 2010).

One of the most important players regarding parasite survival is the enzyme Arg1, that is produced upon induction of Th2 response in M2 macrophages. It acts antagonistic to iNOS as it competes for the substrate L-arginine (Liu and Uzonna 2012). While iNOS produces NO, arginase produces L-ornithine, which is a useful metabolic source for *Leishmania* facilitating parasite survival and reducing parasite killing (Liu and Uzonna 2012, Bogdan 2020). Th2 response, M2 state and related Arg1 expression are mainly driven by the cytokines IL-4, IL-10, TGF-β and IL-13 (Bogdan 2020).

Moreover, high IL-10 expression was found in hamsters and humans in bone marrow and spleen during active visceral disease (Melby, Chandrasekar et al. 2001). IL-10 is a cytokine expressed by M2 macrophages, that has been related to downregulated human T cell responses in infection with *L. donovani* and blocked NO production by human macrophages in *L. infantum* and *L. major* infection after IFN-γ stimulation (Vouldoukis, Becherel et al. 1997, Melby, Chandrasekar et al. 2001). This antagonistic role of IL-10 towards IFN-γ is also considered to shape the malicious course of disease (Kane and Mosser 2001, Schwarz, Remer et al. 2013). This is further supported by the fact that in mouse models chemokine (C-X-C motif) ligand (CXCL)10 reduced *L. infantum* parasite load mediated by reduction in IL-10 and TGF-β level (Figueiredo, Viana et al. 2017). Both, macrophages and T cells, express IL-10 in Leishmaniasis (Kane and Mosser 2001, Schwarz, Remer et al. 2013).

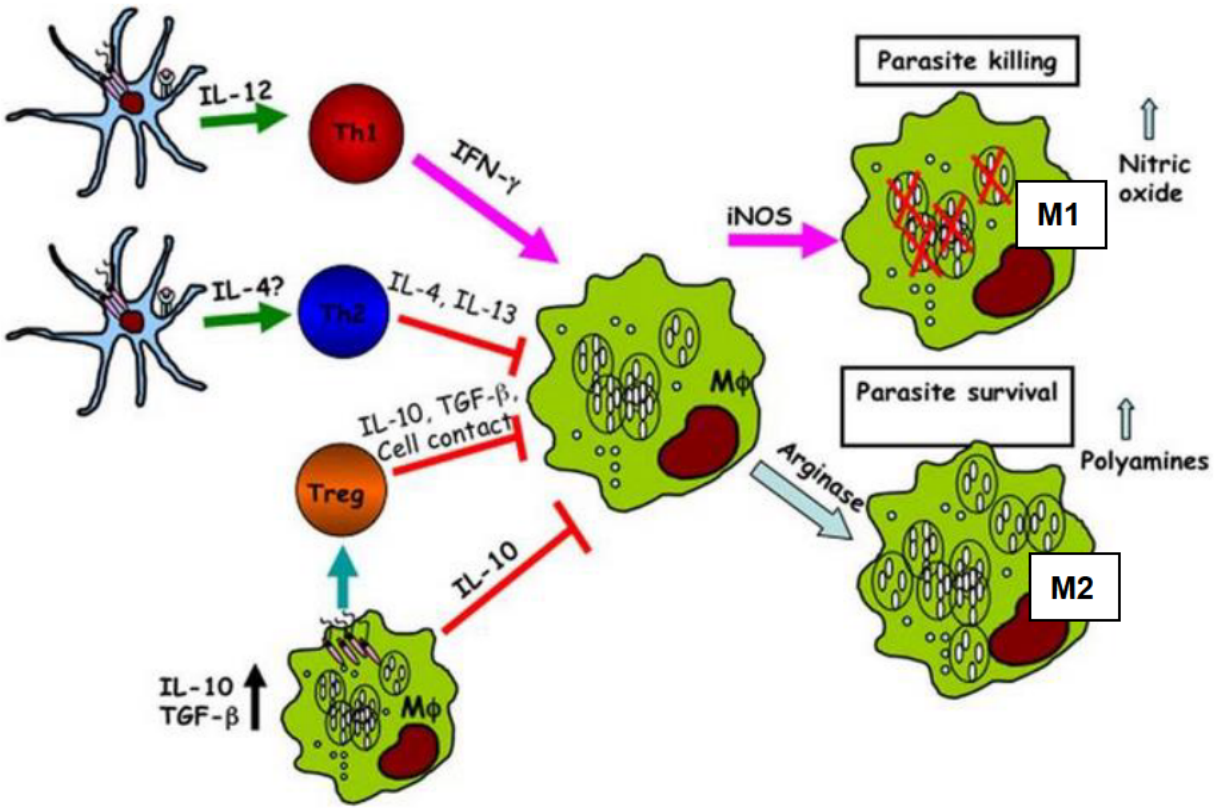

Figure 1-2: Role of cytokine stimulation in macrophage polarization and the impact of macrophage sate on parasites. Infected dendritic cells produce IL-12 leading to induction of a Th1 response in $CD4^+$ T cells. T cells produce IFN-γ polarizing resting macrophages into M1 state, which is related to NO production by iNOS and parasite killing. Induction of a Th2 response, which is driven by IL-4, IL13, IL-10 and TGF-b induces M2 state with upregulated Arginase (Arg1) expression and related production of polyamines connected to parasite survival. Source: (Liu and Uzonna 2012), edited

Clinical evidence also suggests a role for cytokines in shaping the course of disease. In human plasma samples of patients with cutaneous Leishmaniasis higher levels of Arg1 and TGF-β were detected (Bogdan 2020). Blood of humans with visceral disease showed elevated Arg1 levels and reduced amounts of NO (Tomiotto-Pellissier, Bortoleti et al. 2018). Moreover, IL-10 and IL-4 concentrations have been shown to be increased in plasma samples, while MHC II and IL-6 expression were downregulated (Bogdan 2020). This indicates that Th2 or M2 related cytokines are associated with disease progression while Th1 or M1 related cytokines suppress disease.

On the other hand, it has been shown, that very high levels of M1 differentiation can lead to a stronger disease in mouse models of *L. major* infection and higher amount of tissue damage caused by uncontrolled oxidative response (Tomiotto-Pellissier, Bortoleti et al. 2018). In line with this, IL-4 depletion experiments have shown that IFN-

γ and IL-4 play a cooperative role in the control of *Leishmania* infection (Alexander, Carter et al. 2000). It is also important to note that *in vivo* IFN-γ related cytokines lead to further recruitment of macrophages, which, especially during the early phase of infection, leads to a bigger pool of susceptible host cells (Carneiro, Lopes et al. 2020). Thus, although it is the main factor in NO production and parasite elimination, IFN-γ can also have effects in disease progression (Carneiro, Lopes et al. 2020). This highlights the importance of cooperative Th1 and Th2 response.

1.4 Treatment strategies for Leishmaniasis

Generally, Leishmaniasis must be treated depending on symptoms and parasite strain (Mann, Frasca et al. 2021). Infections with *Leishmania major* in immunocompetent individuals usually heal without treatment (Mann, Frasca et al. 2021). In cases of higher complexity such as e.g. intensive lesions (high area, number or duration), diffuse cutaneous Leishmaniasis, immunosuppressed individuals or mucosal Leishmaniasis, systemic or local treatment with leishmanicidal drugs is administered (Mann, Frasca et al. 2021). Local treatment methods include photo- or thermotherapy, topical treatment with paramomycin and injection of lesions with pentavalent antimonials (Mann, Frasca et al. 2021). Pentavalent antimonials have been implicated as the “gold standard” for cutaneous treatment in Latin America and has also been considered standard treatment for visceral cases by the Infectious Disease Society of America (IDSA) in previous years (Mann, Frasca et al. 2021). But with emerging drug resistance, Amphotericin B (AmpB) and Miltefosine (Mil) are now preferred and recommended, while pentavalent antimonials are only used as backup therapy for patients that cannot tolerate the former (Mann, Frasca et al. 2021). Miltefosine is the first leishmanicidal drug that can be administered orally via capsules, while Amphotericin B is mostly given as a liposomal formulation via injection (Soto and Soto 2006, Stone, Bicanic et al. 2016). For more information on the drugs mentioned above see **Table 1-2**.

During this thesis, Amphotericin B and Miltefosine (**Figure 1-5 A&B**) are used as U.S. Food and Drug Administration (FDA) approved examples of drugs with leishmanicidal effects (FDA 2014, FDA 2022).

Amphotericin B (**Figure 1-5 A**) was discovered as a fungicide that binds to ergosterol, an integral component of fungi membranes, forming transmembrane pores that lead to

efflux of essential cell metabolites and killing cells via membrane disruption (Ellis 2002). Generally, Amphotericin B is known to bind sterols of any composition, but it binds to ergosterol with much higher affinity than to cholesterol of mammalian cells enabling it for therapeutic use (Cohen 2016). Interestingly, formation of aqueous pores by sterol binding of Amphotericin B has been linked to a local reduction of membrane thickness causing reorganization of membrane structure (Cohen 2016). Membrane thinning events near lipid raft areas can induce steric movement in the transmembrane regions of TLRs, and Rat sarcoma (Ras) proteins inducing activation of their downstream signaling pathways and induction of an immune response in mammals (Cohen 2016).

Miltefosine (**Figure 1-5 B**), which is the only FDA approved drug for Leishmaniasis that can be administered orally, is a hexadecylphosphocholine that emits its leishmanicidal properties by inhibition of *Leishmania* phosphatidylcholine biosynthesis by phosphatidylethanolamine N-methyltransferase (Pinto-Martinez, Rodriguez-Duran et al. 2018). This effect was found to be 10 - 20 times stronger in protozoan parasites compared to mammalian cells, enabling the use of Miltefosine for Leishmaniasis therapy (Pinto-Martinez, Rodriguez-Duran et al. 2018). Moreover, it reduces generation of adenosine triphosphate (ATP) and oxygen catabolism in *Leishmania* by inhibition of mitochondrial cytochrome c oxidase inducing apoptosis-like cell death (Mollinedo 2014, Pinto-Martinez, Rodriguez-Duran et al. 2018).

The drugs mentioned above are not directly tailored to the treatment of Leishmaniasis, often have high production costs and parasites become increasingly resistant to treatment (Mann, Frasca et al. 2021). This generates a need for new drugs and treatment methods like combination therapy, which can effectively obviate drug resistance and increase effectiveness of treatment with lower doses and duration of toxic drug administration ameliorating adverse effects (Ahmed, Curtis et al. 2020). The combination of drugs with varying mechanisms of action, pharmacokinetics and pharmacodynamics can be used to target different pathways circumventing possible resistance mechanisms (Ahmed, Curtis et al. 2020).

Lots of testing is carried out and even clinical trials are done regarding combination therapy (van Griensven, Balasegaram et al. 2010). While most studies focus on combination of the drugs mentioned in **Table *1-2***, another important class of drugs that could be explored for combination therapy are immune modulating drugs. Given the

immune system dependent nature of Leishmaniasis, immune response modifiers could be a useful alternative to drugs focusing on the elimination of parasites directly (Buates and Matlashewski 1999). These molecules do not have antimicrobial properties themselves, but instead induce control of pathogen infections using the host immune system (Sauder 2004). This can be achieved by stimulating the pathogen recognition systems of immune cells to enhance protective immune response.

Table 1-2: Overview of different treatment methods with their route of administration, formulation, mechanism of action and problems.

DRUG	TYPE	ROUTE OF ADMINISTRATION	FORMULATION	MECHANISM OF ACTION	PROBLEMS / ADVERSE EFFECTS
SODIUM STIBOGLUCONATE ("PENTOSTAM") / MEGLUMINE ANTIMONIATE ("GLUCANTIME")	Pentavalent Antimonial (Herwaldt and Berman 1992)	Intravenous / intramuscular (Herwaldt and Berman 1992)	Liposome solution (Dar, Din et al. 2018)	Inhibition of parasite trypanothion reductase (redox metabolism) (Wyllie, Cunningham et al. 2004)	Headaches, fatigue, muscle aches, risk of pancreatitis for immunocompromised individuals, cytopenia, drug resistance (Dar, Din et al. 2018)
AMPHOTERICIN B ("AMBISOME")	Fungicide (Stone, Bicanic et al. 2016)	Intravenous (Stone, Bicanic et al. 2016)	Liposome solution (Stone, Bicanic et al. 2016)	Formation of pores in parasite membrane via binding to ergosterol (Cohen 2016)	High production cost, nephrotoxicity (Stone, Bicanic et al. 2016)
MILTEFOSINE ("IMPAVIDO")	Antineoplastic drug (Soto and Soto 2006)	Oral (Sunyoto, Potet et al. 2018)	Capsule (Sunyoto, Potet et al. 2018)	Interference in membrane anabolism, induction of apoptosis like cell death (Pinto-Martinez, Rodriguez-Duran et al. 2018)	Teratogenic, renal and hepatic toxicity, high cost (Sunyoto, Potet et al. 2018)
IMIQUIMOD ("ALDARA")	Immune response modifier (Buates and Matlashewski 1999)	Topical (Fuentes-Nava, Tirado-Sanchez et al. 2021)	Cream (Fuentes-Nava, Tirado-Sanchez et al. 2021)	Induces type 1 immune response by TLR 7/8 stimulation (Buates and Matlashewski 1999)	Severe Erythema, Headache, Back Pain (Cunha 2021)

During Leishmaniasis immune modulation can be used to induce elevated Th1 responses, that increase parasite killing mechanisms. In macrophages, this is achieved by inducing macrophage polarization into M1 state. TLRs are an important class of PRRs that can be targeted in macrophages to achieve immune modulation during Leishmaniasis, as it has been shown, that e.g. TLR2 mediates parasite control by IL-12, TNF-α and NO production after recognition of *Leishmania* surface protein LPG (Elmahallawy, Alkhaldi et al. 2021).

During this thesis, Imiquimod and Eh-1 a synthetic phosphatidylinositol (PI) analog derived from *Entamoeba histolytica* lipopeptidophosphoglycan (*Eh*LPPG), were used and compared for immune modulation treatment.

Imiquimod (Imi) (**Figure 1-5 C**) is an FDA approved imidazoquinolone amine commonly used for treatment of cutaneous malignancies (Bubna 2015). It binds to TLRs 7 & 8 of macrophages inducing inflammatory response and release of cytokines like IL-12, IFN-γ and TNF-α, but can also directly induce apoptosis by upregulation of Bax and Bak of the intrinsic apoptosis pathway (Bubna 2015). It has been successfully used for the treatment of cutaneous Leishmaniasis (Fuentes-Nava, Tirado-Sanchez et al. 2021) and has been shown to induce production of NO in the context of an *in vitro* murine model of visceral Leishmaniasis (Buates and Matlashewski 1999).

Eh-1 (**Figure 1-5 D**) is a chemically synthesized analog of the GPI-anchor *Eh*PIb, which is derived from *Eh*LPPG. In mouse model experiments it was discovered that *Eh*LPPG, derived from the membrane of the protozoan parasite *Entamoeba histolytica*, shows the capability to induce IFN-γ production in invariant natural killer T cells (iNKTs) and thus modulate immune response towards Th1 (Lotter, Gonzalez-Roldan et al. 2009). Building on this, the immune modulating effect of *Eh*LPPG was then identified to be induced by one of the two glycosylphosphatidylinositol (GPI)-anchors found in the molecule (*Eh*PIb) (Lotter, Gonzalez-Roldan et al. 2009). After the discovery of the immune modulating capabilities of the GPI-anchor *Eh*PIb, six analoga with differences in stereochemistry of the alkyl chains and the alcohol linker group were chemically synthesized (**Figure 1-3**) (Fehling, Choy et al. 2020). These analoga represent promising drug candidates for immune modulation in Leishmaniasis, as they have shown reduction of parasite load in *in vitro* experiments with hMDMs and reduction in cutaneous lesions in murine model associated with the production of Th1 cytokines (Fehling, Choy et al. 2020, Fehling, Niss et al. 2021). Eh-1 is one of these analoga,

which features a C_{16} alkyl chain instead of C_{28} or C_{30} found in *Eh*PIb (Fehling, Choy et al. 2020). The inositol of the molecule is arranged in D-configuration, while the glycerol linker group is R-configurated.

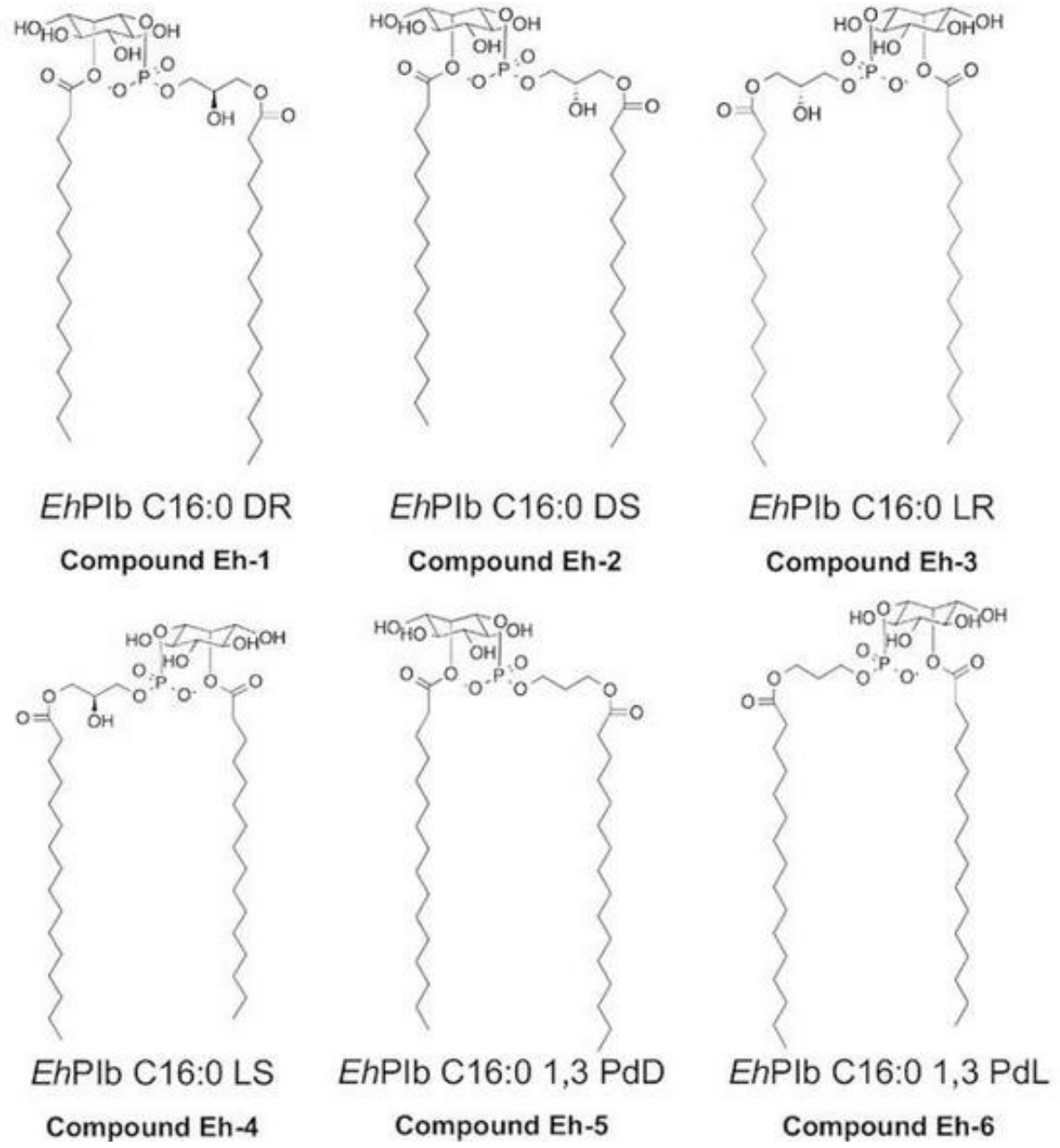

Figure 1-3: Schematic representations of molecular structures of chemically synthesized *Eh*PIb analoga. Two C16 alkyl chains are connected via alcohol and PI linker of different stereochemical composition. Compounds Eh-1, Eh-2, Eh-3 and Eh-4 contain a glycerol linker of R (Eh-1 and Eh-3) or S (Eh-2 and Eh-4) configuration, while Eh-5 and Eh-6 contain a propanediol in R (Eh-5) or S (Eh-6) configuration. The inositol moiety is either D (Eh-1, Eh-2, Eh-5) or L configurated (Eh-3, Eh-4, Eh-6) **S**ource: (Fehling, Choy et al. 2020)

1.5 Sex differences in immunity

Differences in the outcome of parasitic diseases have been observed between male and female including Leishmaniasis (Bernin and Lotter 2014). When addressing sex differences in humans, biological sex refers to the genetic and bodily foundations of an individual, not the gender identification in the context of society. Differences in chromosomes, gonads and sex hormones lead to differences in gene expression patterns and immune cell activity (Wilkinson, Chen et al. 2022). Male individuals have XY composition of sex chromosomes, develop testis and produce high levels of testosterone and its analogs. Female individuals show XX composition of sex chromosomes, develop ovaries and produce estrogens and progesterone (Wilkinson, Chen et al. 2022).

Females have two X chromosomes, one of which is transcriptionally inactivated during embryonic development via formation of heterochromatin (Wilkinson, Chen et al. 2022). However, for some X-chromosome specific genes, incomplete inactivation or escape from inactivation leads to higher expression of these genes in females (Wilkinson, Chen et al. 2022). One of these genes encodes TLR7, which is an endosomal receptor for ssRNA and leads to production of Th1 related interferons when activated (Wilkinson, Chen et al. 2022). This effect can be found in female monocytes enabling them for the possibility of stronger Th1 cytokine response (Wilkinson, Chen et al. 2022).

In mouse model transcriptome studies, many genes related to IFN-γ responsiveness and complement system have been identified, that show higher levels in unstimulated and stimulated macrophages from female mice compared to male mice. This indicates a higher potential for inflammatory response for females during Leishmaniasis (Gal-Oz et al. 2019).

Another key factor for sex differences in immunity is the presence of sex hormones. Both, male and female sex hormones show immune modulating effects in *in vitro* experiments. Testosterone and estrogen receptors are found on both, female and male monocytes and macrophages in humans (Snider, Lezama-Davila et al. 2009).

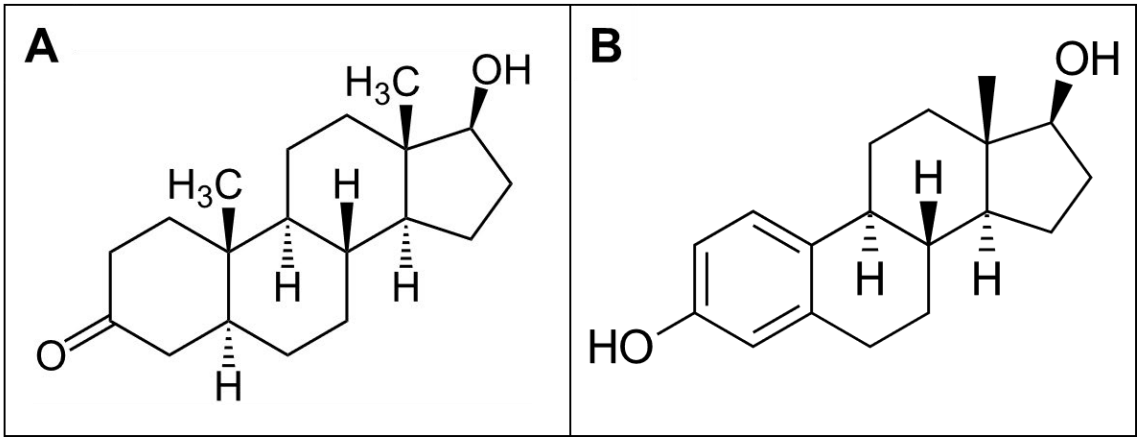

Figure 1-4: Schematic representations of molecular structures of 5α-Dihydrotestosterone (DHT) (A) and 17β-Estradiol (E2) (B). Sources: (NEUROtiker 2007, Jü 2020)

In Leishmaniasis, higher infection rate and more severe disease are observed for male individuals over the age of 15 compared to female individuals, while this is not observed for males under the age of 15 (Bernin and Lotter 2014). This correlates with the rise in testosterone production observed during puberty indicating a role of testosterone in disease susceptibility (Bernin and Lotter 2014). Moreover, in hamster models of cutaneous Leishmaniasis induced by *L. panamensis* and *L. mexicana*, testosterone administration in female hamsters led to significantly higher lesion size further supporting the role of testosterone in the male bias of Leishmaniasis (Travi, Osorio et al. 2002, Snider, Lezama-Davila et al. 2009).

Estrogens were observed to reduce expression of pro-inflammatory cytokines (IL-1β, TNF-α, IL-6) in macrophages via downregulation of CD16 expression in a human monocyte cell line (THP-1) (Fish 2008). After 17β-Estradiol (E2) stimulation of bone-marrow derived macrophages from male and female mice, macrophages from both sexes showed increased NO levels without increase in IL-6, IL-12 or TNF-α in *L. mexicana* infection (Snider, Lezama-Davila et al. 2009). In a hamster model of visceral Leishmaniasis induced by *L. donovani,* treatment with testosterone worsened course of disease for male and female hamsters while estradiol treatment led to increased parasite control in both sexes (Snider, Lezama-Davila et al. 2009). Moreover, castration of hamsters showed reduction in parasite burden and ovariectomy increased disease severity (Snider, Lezama-Davila et al. 2009).

These data indicate a protective role of E2 and a disease-enhancing role of testosterone in Leishmaniasis.

1.6 Aims of the Thesis

During this thesis, different strategies for the treatment of *Leishmania infantum* and *Leishmania major* infection of female and male human monocyte derived macrophages (hMDMs) are compared in *in vitro* high content drug screening experiments using automated confocal microscopy and image analysis. Macrophages are treated with the FDA approved Leishmaniasis drugs Amphotericin B and Miltefosine, and immune response modifier Imiquimod, as well as the immune stimulatory drug candidate Eh-1 in *in vitro* models of cutaneous and visceral Leishmaniasis. During the experiments mono and combination treatments should be compared regarding hMDM response in *L. major* and *L. infantum* infection and their effect on drug screening parameters to identify suitable treatment combinations.

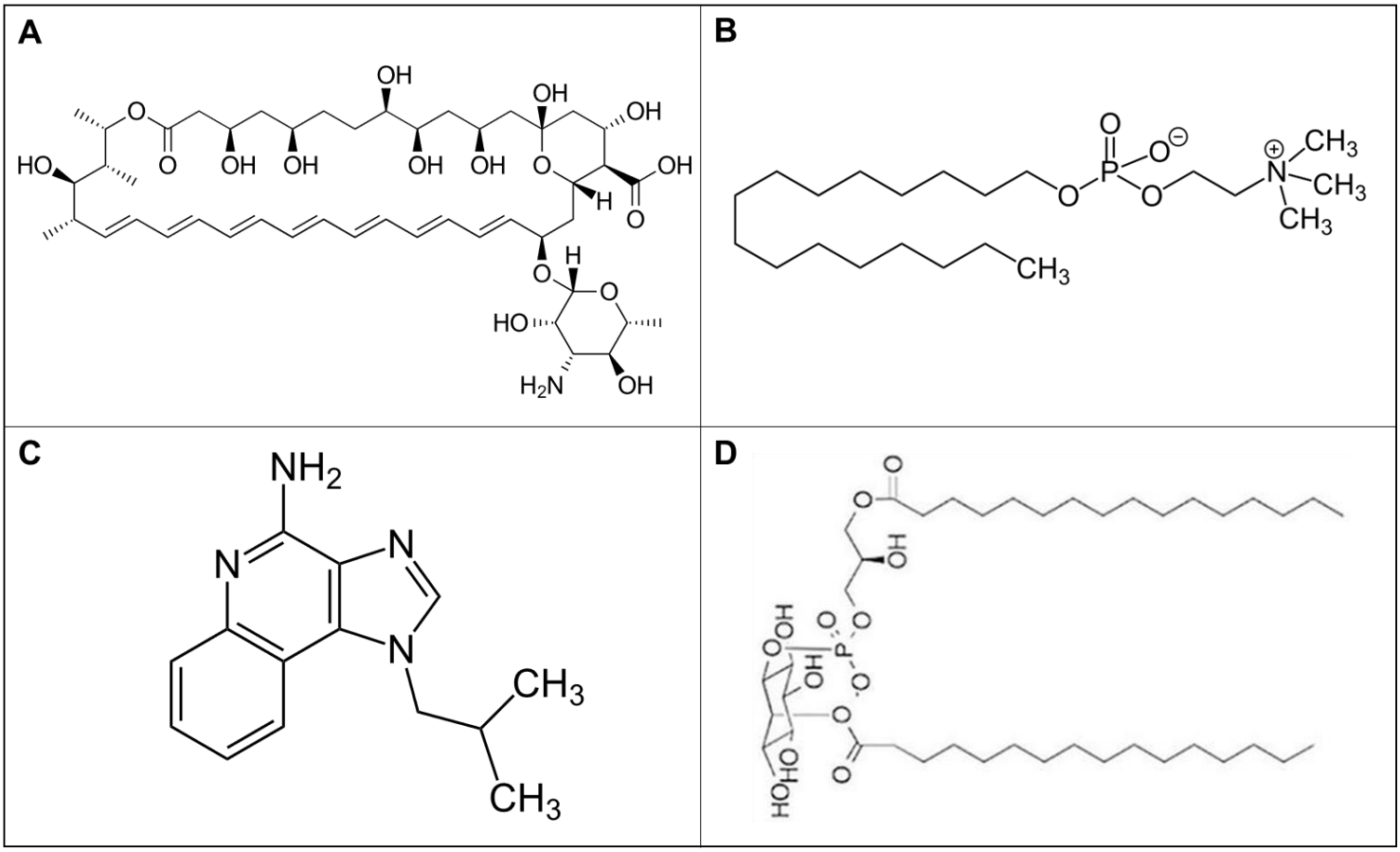

Figure 1-5: Chemical structures of the molecules used for treatment of *Leishmania*-infected macrophages during the thesis. Amphotericin B (A), Miltefosine (B), and Imiquimod (C) and Eh-1. Miltefosine and Amphotericin B are FDA approved drugs for the treatment of visceral Leishmaniasis. Imiquimod has been used as an immune response modifier for topical treatment of cutaneous Leishmaniasis and Eh-1 is an immune stimulatory compound that was developed as a chemical analog to the glycosylphosphatidylinositol (GPI) anchor EhPIb derived from *Entamoeba histolytica* lipopeptidophosphoglycan (EhLPPG). Sources: (chemistds 2012, Jü 2012, Jü 2013, Fehling, Choy et al. 2020)

Macrophage responses to *L. major* and *L. infantum* infection and treatment with Amphotericin B, Eh-1, and their combination are compared by analysis of extracellular cytokine profiles with immunoassays to characterize the role of cytokine response during treatment.

Sex differences are analyzed by the comparison of infection and treatment characteristics between female and male individuals including evaluation of drug screening parameters, phenotypical evaluation of macrophage polarization upon infection and extracellular cytokine profiles. Moreover, to shed a light on the role of sex hormones during *L. infantum* infection, male and female hMDMs were stimulated with 5α-Dihydrotestosterone (DHT) and 17β-Estradiol (E2) (**Figure 1-4**) during their titration for the establishment of a stimulation protocol.

2 Materials and methods

2.1 Materials

2.1.1 Chemicals, solutions and kits

Table 2-1: List of chemicals

Chemical	Manufacturer	Identification Nr.
BSA	SERVA	11926.03
EDTA	ROTH	8043.2
Tris	ROTH	4855.2
NH_4Cl	ROTH	K298.1
Charcoal, Dextran coated	Sigma-Aldrich	C6241-5G

Table 2-2: List of commercial solutions

Solution	Manufacturer	Identification Nr.
DPBS w/o calcium, w/o magnesium, sterile filtered	PAN Biotech	P04-361000
Biocoll Separation Solution	Bio & Sell	BS.L6115
Anti-human CD14 magnetic beads	BD Biosciences	557769
RPMI Medium	PAN Biotech	P04-17500
RPMI Medium w/o phenol red	PAN Biotech	P04-16516
M-CSF	BioLegend	574804
Fetal Bovine Serum Advanced	Capricorn	FBS-11A
L-Glutamine	PAN Biotech	P04-80100
Penicillin/Streptomycin	AppliChem	A8943
DMSO	ROTH	A994.1
DAPI	Sigma-Aldrich	D-9564
FIX/Perm Concentrate	invitrogen	00-5123-43
FIX/Perm Diluent	invitrogen	00-5223-56
PermWash	invitrogen	00-8333-56
Trypan Blue	invitrogen	T10282
Paraformaldehyde 4% in PBS	Thermo Scientific	J19943.K2
Medium 199	Sigma-Aldrich	51322C

Zombie UV Dye	Biolegend	77474
Triton X-100	ROTH	9002-93-1
CASYton	OLS	5651808

Table 2-3: List of utilized media and buffers

PBS (20x)

ddH_2O

+ 0,05 M KCl

+ 0,03 M KH_2PO_4

+ 0,16 M Na_2HPO_4

+ 2,74 M NaCl

cRPMI Medium

RPMI Medium

+ 10 % (v/v) FCS (heat-inactivated & hormone depleted via active charcoal stripping)

+100 U/ml Penicillin/Streptomycin

+ 2 mM L-Glutamine

+ 2,06 nM M-CSF

Erythrocyte Lysis Buffer

0,144 M NH_4Cl

0,01 M Tris pH 7,6

MACS Buffer

1x PBS pH 7,2

+ 2 mM EDTA

+ 75,2 µM BSA

FACS Buffer

1x PBS

+ 1% (v/v) FCS

Permeabilization Buffer

1x PBS pH 7,2
+ 50 mM NH_4Cl
+ 0,1 % (v/v) Triton X-100

Blocking Solution

1x PBS
+ 0,3 mM BSA
+ 0,1 % (v/v) Triton X-100

Washing Buffer

1x PBS pH 7,2
+ 0,1 % (v/v) Triton X-100

M199+ Medium

1x Medium 199
+ 20% (v/v) FCS (heat-inactivated)
+ 2 mM L-Glutamine
+ 100 U Penicillin
+ 0,17 mM Streptomycine
+ 40 mM HEPES pH 7,4
+ 15,3 µM Hemine
+ 100 µM Adenine
+ 5 µM Biopterine

Table 2-4: List of commercial ready-to-use kits

Kit	Manufacturer	Identification Nr.
LEGENDplex custom panel 12-plex	Biolegend	-

For the analysis of macrophage cytokine profiles in the context of Leishmaniasis, a custom cytokine panel was designed in cooperation with Biolegend containing the following analytes:

IL-12p70, TNF-α, IL-6, IL-10, IL-1β, Arginase, CCL17, IL-23, IFN-γ, CXCL10, IL-18, CCL2

2.1.2 Drugs, compounds and hormones

Table 2-5: Drugs used for macrophage treatment during high content screening analyses

Chemical/Solution	Manufacturer	Identification Nr.	Stock Concentration
Imiquimod in DMSO	Thermo Scientific	99011-02-6	20,8 mM
Miltefosine in cRPMI	Sigma-Aldrich	58066-85-6	5 mM
0,27 mM Amphotericin B/ 0,52 mM Natriumdeoxycholat	Gibco Life Technologies	15290018	0,27 mM / 0,52 mM
*Eh*Plb C16:0 DR („Eh-1) in DMSO	AG Prof. Chris Meier	-	6,25 mM
17β-Estradiol in Ethanol	Sigma-Aldrich	E2257	
5α-Dihydrotestosterone in Ethanol	Supelco	D-073	

2.1.3 Parasites

Leishmania parasites were kindly provided by PD Dr. Joachim Clos and his research group (RG) “Leishmania Molecular Genetics” at the BNITM.

Table 2-6: List of parasite strains

Parasite	Strain	Species classification
L. major	5ASKH	dermotropic
L. infantum	3511	viscerotropic

2.1.4 Cell source

All human primary cells were isolated from from buffy coats of healthy donors kindly provided by the institute of transfusion medicine at the Universitätsklinikum Hamburg-Eppendorf (UKE) with their personal consent. Ethics approval for the experiments with human blood samples was granted by the Ethics Committee of the University of Hamburg (202-10067-BO).

Each donor is assigned an individual ID (s. **Table 2-7**), which will be used throughout the thesis for identification. **Figure 2-1** shows the age distribution of donors.

Table 2-7: Overview of male and female blood donors with their individual ID, year of birth and age.

	Individual ID	Year of birth	Age
male	m1	1997	25
	m2	1998	24
	m3	1987	35
	m4	1980	42
	m5	1994	28
	m6	1963	59
	m7	1956	66
	m8	1993	29
	m9	1980	42
	m10	1964	58
female	f1	1991	31
	f2	1990	32
	f3	1969	53
	f4	1969	53
	f5	1981	41
	f6	1965	57
	f7	1996	26
	f8	1971	51
	f9	1969	53

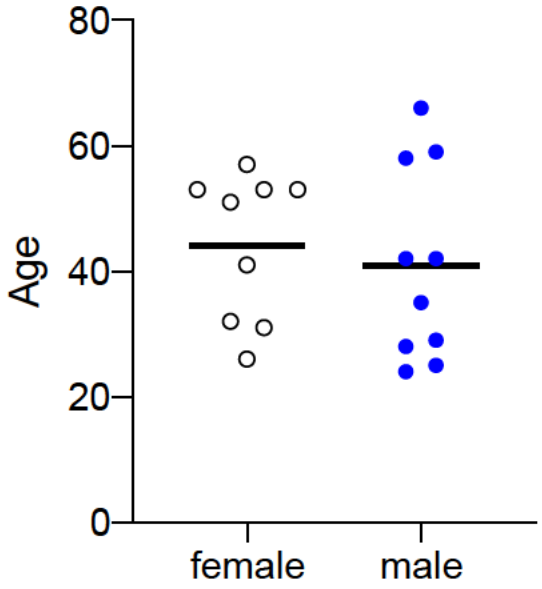

Figure 2-1: Age distribution of donors. The age distribution of donors is displayed graphically with the black line representing the median of age for female and male donors, respectively.

2.1.5 Antibodies

Table 2-8: List of antibodies

Fluorochrome	Antigen	Host Species	Supplier/Manufacturer	Identification Nr.
-	α-HSP90	Mouse	BNITM, RG Molecular Infection Immunology	-

Alexa Fluor 647	goat-α-mouse	Goat	InvitroGen	A32728
BV510	α-CD14	Mouse	Biolegend	301842
BUV395	α-HLA-DR	Mouse	Biolegend	564040
PerCP	α-CD16	Mouse	Biolegend	302030

2.1.6 Technical Devices and Software

Table 2-9: List of technical devices

Device	Supplier	Identification Nr.
Water Bath VWB 6	VWR	462-0258
Incubation/Inactivation Water Bath	GFL	1002
Centrifuge 5810 R	Eppendorf	EP5811000620
Centrifuge 2-16KL	Sigma	-
Class II Safety Cabinet MSC Advantage	Thermo Scientific	51028226
Class II Safety Cabinet NUNC MICROFLOW M51426/5	NUNC	-
Cell Incubator Galaxy 170 S	Eppendorf	EPCO17014005
Cell Incubator CB 170	BINDER	-
CO_2 Cell Incubator HeraCell 150i	Thermo Scientific	50116048
Orbital Shaker (3mm shaking stroke)	IKA	0003208000
FACS LSR II Cytometer	BD Biosciences	-
FACS Aurora	Cytek	-
Ultrasonic Bath SONOREX SUPER	BANDELIN	RK 100 H
Microscope AMG EVOS XL	Thermo Scientific	12-563-452
Microscope NIKON ECLIPSE TS100	NIKON	-
Opera Phenix HCS System	Perkin Elmer	HH14001000
Cell counter Multisizer 3 Coulter Counter	Beckman Coulter	-

Table 2-10: List of software

Software	Supplier	Identification Nr.	Version
Image Analysis Software “Harmony”	Perkin Elmer	HH17000010	4.6
Statistics and Graph Design Software “PRISM”	GraphPad	-	9.0.1
Flow Cytometry Analysis Software “FlowJo”	BD	-	v10
LEGENDplex Evaluation Software “Qognit”	Biolegend	-	2022-07-15
BD FACSDiva Flow Cytometry Software	BD	23-17415-01	6.1.3

2.1.7 Laboratory Supplies

Table 2-11: List of laboratory supplies utilized during the experiments

Material	Supplier	Identification Nr.
PhenoPlate 96-well plates made from cyclic olefin	Perkin Elmer	6055300
V-bottom plates	Biolegend	740379
Neubauer Counting Chamber	MARIENFELD	0640130
Cell Separation Magnet	BD Biosciences	552311
12-channel pipette	Mettler Toledo	17013811
Digital 1-channel multi step pipette	Mettler Toledo	17014489
Digital 1-channel multi step pipette	Eppendorf	4987000010

2.2 Methods

Since experiments included potentially infectious solutions, all work prior to fixation was carried out in class II biosafety cabinets inside a S2 safety level laboratory. All materials used during this period were either packaged under sterile conditions or sterilized before use to minimize contamination.

Several biochemical and biophysical methods were used for the generation of human primary macrophages from buffy coat samples, their infection with *Leishmania* parasites and subsequent treatment with different Leishmaniasis drugs or hormones. Various analysis methods were deployed to gain information about the state of the biological samples. A scheme of the general experiment workflow is displayed in **Figure *2-2***.

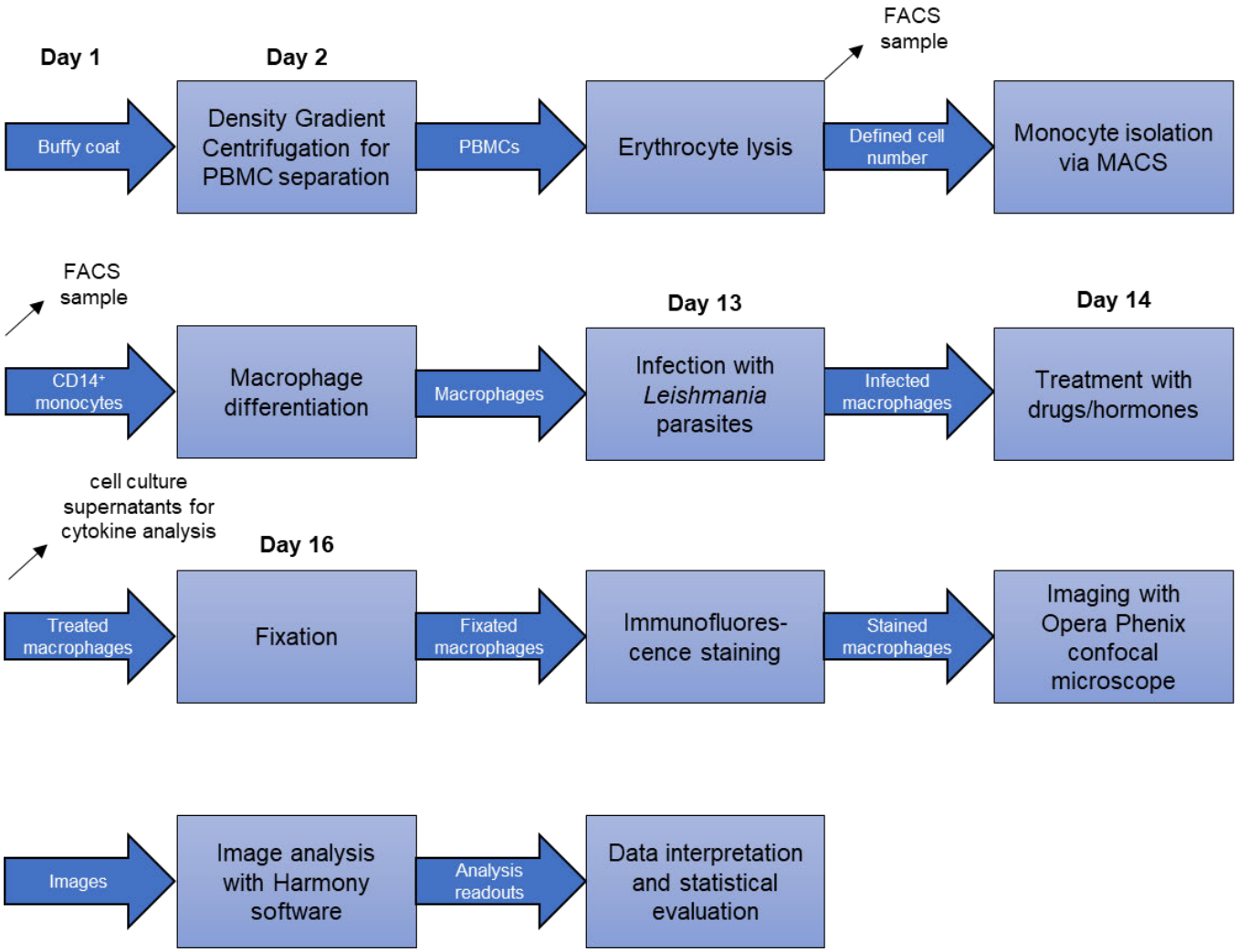

Figure 2-2: Schematic representation of experiment workflow. Methods used are shown in boxes in chronological order. Analysis methods are indicated by small black arrows. Cells in buffy coat samples were separated by density gradient centrifugation and peripheral blood mononuclear cells (PBMCs) were further purified by erythrocyte lysis. Cells were counted and a sample for FACS was taken. Depending on the requirement for the respective experiment, a defined cell number was used for

monocyte isolation via CD14⁺ MACS. Subsequently another FACS sample was taken and CD14⁺ monocytes were cultured for 11 days during macrophage differentiation. Macrophages were then infected with *Leishmania* parasites on day 13 and treated 24 hours post infection (hpi) with drugs or hormones. Two days after treatment cells were fixed for subsequent immunofluorescent staining. Before fixation the supernatants were aspirated and stored at -20°C until cytokine analysis. Following the staining process, cells were imaged with the confocal microscope of the Opera Phenix™ system and the images generated were analyzed with Harmony™ to generate various analysis readouts for interpretation and statistical evaluation.

2.2.1 Parasite cell culture

Leishmania promastigotes were kept in solution in M199+ Medium at 25 °C and pH = 7,4 in anaerobe condition in T25 flasks without filter cap and were split weekly (1:1000 one a week for *L. major*, 1:300 twice a week for *L. infantum*) at a confluence of approximately 80 % to ensure a representative, living and active parasite state. For infection experiments, stationary phase promastigotes were used. These were generated by splitting the 80 % confluent culture at a ratio of 1:10 four days before infection. Active parasite state was confirmed phenotypically by checking parasite motility at the day of infection at 20x magnification under a microscope.

2.2.2 Generation of human primary macrophages from buffy coat samples

To generate an adherent *in vitro* culture of human peripheral blood monocyte derived macrophages (hMDMs), it is necessary to separate monocytes from any remaining cells inside the buffy coat sample (**Figure 2-3**) and cultivate them in the presence of M-CSF to differentiate them into macrophages.

Monocytes can be identified and purified by their characteristic high expression of CD14 on the cells surface. This is done by using CD14 magnetic beads in magnetic activated cell separation (MACS). Since buffy coats contain a heterogenous mixture of different hematopoietic cells that interfere with separation in a magnetic field, it is necessary to purify the mixture before MACS to ensure successful monocyte isolation. This is achieved by density gradient centrifugation and subsequent erythrocyte lysis.

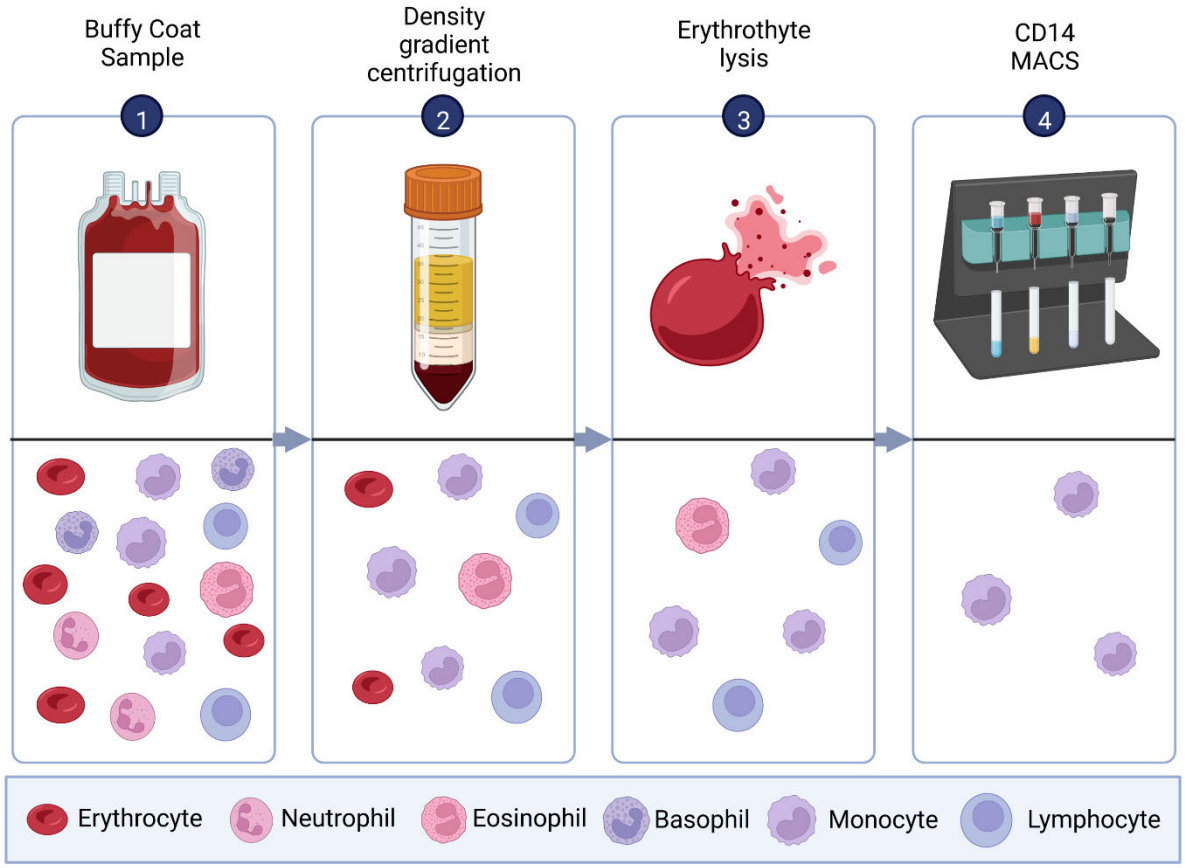

Figure 2-3: Schematic representation of monocyte purification process. Buffy coats from healthy donors are used a starting material (1). Density gradient centrifugation is used to separate PBMCs from neutrophils, basophils and most erythrocytes (2). To further minimize erythrocyte contamination, erythrocyte lysis is carried out (3). Monocytes are then separated by CD14 MACS (4). Source: (Created with BioRender)

2.2.2.1 Density gradient centrifugation

In a first step PBMCs are separated from polymorphonuclear leukocytes and erythrocytes in a density gradient. For this, Biocoll with a density of 1.077 g/ml is used (**Figure 2-4**). Monocytes and platelets have a lower density than Biocoll and can be found in the supernatant, while granulocytes and erythrocytes can be found at the bottom of the tube separated by the Biocoll layer. For this separation step, SepMate tubes are used to minimize contamination with the lower layer and to speed up the separation process.

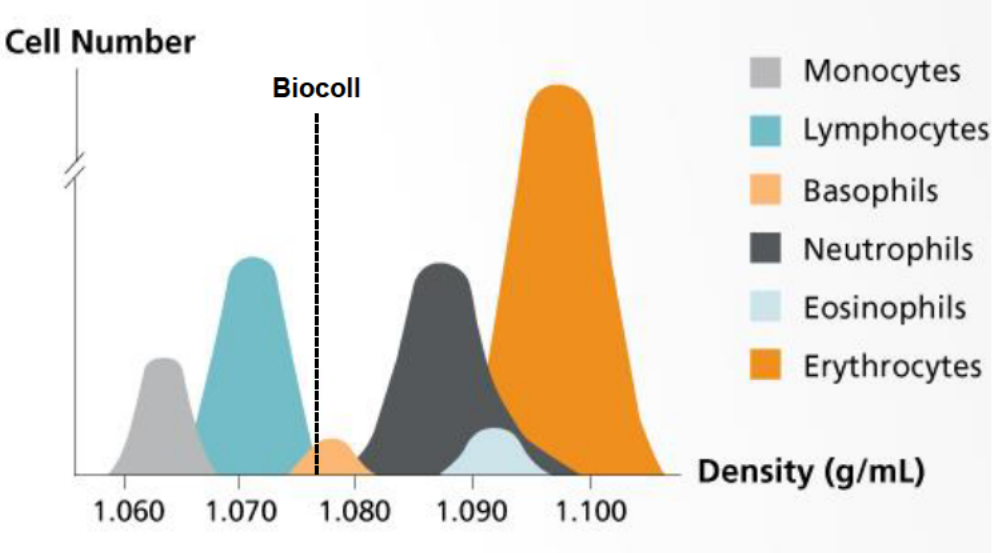

Figure 2-4: Density distribution of human blood cell populations. The dotted line represents the density of Biocoll, above which all cells (neutrophils, eosinophils, erythrocytes, basophils) will be found below the Biocoll layer. All cells with a lower density (mainly monocytes and lymphocytes) will be found above and can be used for further processing. Source: (STEMCELL 2022), edited

Removal of platelets from PCMCs is also achieved by density driven separation. Platelets have a slightly lower density than PBMCs and can be washed out via centrifugation at low speed (around 120 g) in DPBS. Since the centrifugation force is low, the centrifugation is carried out without brakes to ensure minimal disturbance of pellet.

For each experiment, around 60 ml of buffy coat from one individual were used for separation. For the isolation of PBMCs, 10 ml of human buffy coat samples were diluted with 20 ml of DPBS. The mixture was then slowly added to 15 ml of Biocoll in SepMate Tubes and centrifuged at 1200 g, room temperature (RT) for 10 min. To remove platelets, the supernatant was diluted ad 50 ml with DPBS and centrifuged a second time at 120 g, RT for 10 min with the brakes turned off. Cell pellets were resuspended and pooled in 50 ml DPBS and centrifuged for 8 min at 300 g, RT.

2.2.2.2 Erythrocyte lysis

Erythrocytes can be selectively removed from a cell mixture by ammonium chloride lysis. This utilizes osmotic pressure, that is generated by influx of ammonium chloride (NH_4^+/Cl^-) into erythrocytes. Trans-membrane ion exchanger channels of erythrocytes exchange extracellular Cl^- ions and HCO_3^- ions generated inside the cells after NH_3

influx (s. **Figure 2-5**). This accumulation of intracellular NH_4Cl leads to osmotic pressure, swelling and rupture of erythrocytes. (Hemker, Cheroutre et al. 2003, Le P. Ngo 2016)

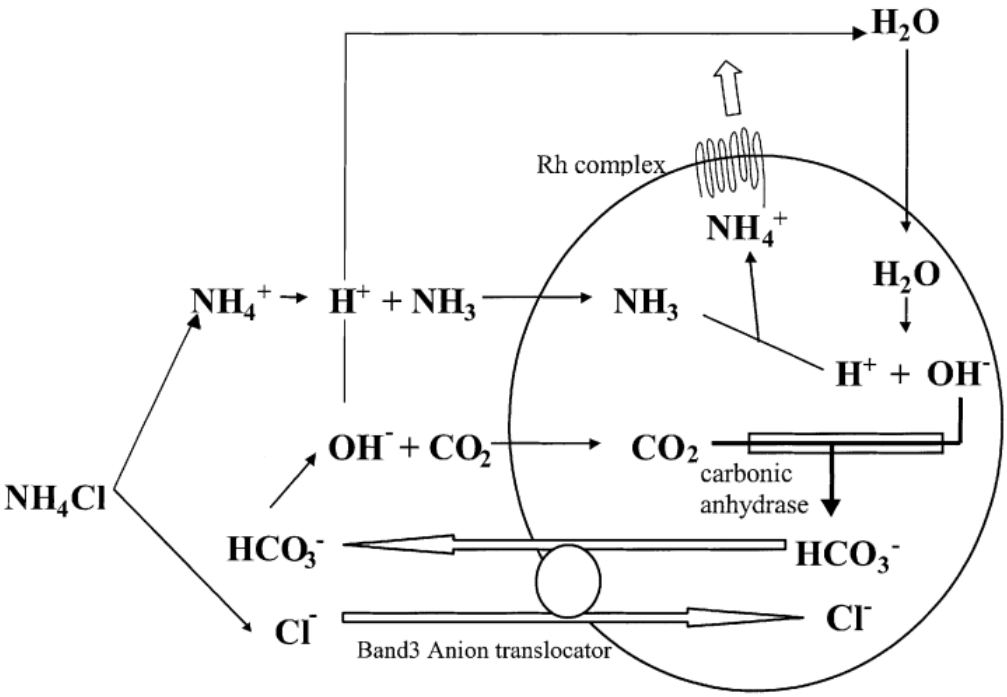

Figure 2-5: Schematic representation of the molecular basis of erythrocyte lysis. NH_4Cl inside lysis buffer can disassociate into NH_3 that diffuses through the cell membrane to react with H_2O forming OH^- and NH_4^+. The enzyme carbonic anhydrase then catalyzes the formation of HCO_3^- with CO_2, which is exchanged with extracellular Cl^- via Band3 anion translocator leading to accumulation of NH_4Cl inside erythrocytes. Source: (Hemker, Cheroutre et al. 2003)

For removal of any remaining erythrocytes, the cells were resuspended thoroughly in 5 ml erythrocyte lysis buffer and incubated for 5 min at RT. After adding 5 ml of DPBS, cells were centrifuged again for 5 min at 1300 rpm, 4 °C. The cell pellet was resuspended in 5 ml DPBS and centrifuged for 5 min at 1300 rpm, 4 °C to further remove any remaining traces of erythrocyte lysis buffer. After resuspending the cell pellet in 10 ml DPBS, cells were counted in 0,04 % Trypan Blue using a Neubauer counting chamber (s. **2.2.2.3**) to adjust the cell number for the following MACS step and a sample of $1x10^6$ PBMCs was taken for FACS analysis.

2.2.2.3 Determination of cell concentration using a Neubauer counting chamber

Cell concentrations in a sample can be determined by a Neubauer counting chamber, which utilizes the distribution of a specific volume in a known depth and area of a glass slide. Prior to counting, cells are stained with the live/dead staining dye Trypan Blue, which colors cells with compromised membranes. Counting a specific area delineated by squares impregnated on the chamber slide allows for the determination of cell concentration in the solution by the following formula:

Equation 1: Formula for the calculation of living cell concentration from cells counted in a Neubauer chamber. The arithmetic mean of unstained cell number counted in four separate squares of the chamber is multiplied by the dilution factor and the chamber correction factor.

$$c = \bar{n} \cdot F \cdot 10000 \ \frac{cells}{ml}$$

$$with\ c = cell\ concentration\ in\ the\ sample, n = cell\ count\ in\ a\ square, F = dilution\ factor$$

2.2.2.4 Determination of cell concentration using a CASY cell counter

Determination of cell concentration by a CASY counter is enabled by the measurement of electric current between two electrodes in a flow cell with defined pore size. As single cells with intact membranes pass through the flow cell, their membrane barrier interrupts current flow between the electrodes generating a pulse signal proportional to their volume and diameter. Dead cells with compromised membranes yield a much smaller signal and are excluded. It is important to note, that for counting, cell samples must be dissolved in CASYton buffer, a specific electrolyte solution for cell counting, in a dilution of 1:1000.

2.2.2.5 Isolation of $CD14^+$ monocytes

To isolate monocytes from any remaining cells, magnetic activated cell separation with anti-human CD14 magnetic beads was used. These magnetic nanoparticles have a monoclonal antibody directed against human CD14 cell surface receptor conjugated to their surface. After incubation with beads, monocytes can be positively selected via

immobilization of beads in a magnetic field, while the supernatant containing $CD14^-$ cells is removed. Since beads have a specific binding capacity, the cell number for bead incubation was adjusted according to manufacturer specifications.

For the isolation of $CD14^+$ cells, the pellet was resuspended in 2 ml MACS buffer after centrifugation for 5 min at 1300 rpm & 4 °C. Subsequently, 50 µl of human anti CD14 antibody-coated magnetic beads were added for every 10^7 cells and the mix was incubated for 30 min at RT. Then the respective volume of MACS buffer was added to generate a cell concentration of 1-8x10^7 cells per ml. The bead-cell suspension was transferred into FACS tubes and separated for 10 min at a cell separation magnet. Negative fractions of the separation were subsequently pooled and separated again. After a second separation step, the tubes were washed to collect any remaining beads and positive fractions were collected in ≈ 3 ml DPBS. To test for monocyte purity by FACS, a sample of 1x10^6 cells was taken from the CD14 positive fraction after separation. The CD14 negative fraction was discarded. $CD14^+$ monocytes were used for the generation of macrophages (**2.2.2.6**).

2.2.2.6 Generation of hMDMs *in vitro*

Macrophages can be generated from peripheral blood monocytes *in vitro* by stimulation with M-CSF in the culture medium. Activated monocytes become adhesive as macrophages at the culture dish surface, while non-activated monocytes stay in solution. Thus, frequent medium changes are deployed as a mechanism for macrophage selection.

It is important to note, that the cRPMI medium used was completed with M-CSF, and heat-inactivated, active carbon filtered fetal calf serum (FCS) to deplete any hormones. After dissolving the CD14 positive fraction in cRPMI medium, 1x10^5 $CD14^+$ monocytes were seeded in PhenoPlate 96-well plates with a film bottom made from cyclic olefin in 200 µl per well. Cyclic olefin provides a glass-like, optically clear surface, that allows for high quality microscopic imaging. The medium was exchanged for fresh cRPMI at day 4 (half medium change), 6 (half medium change) and 8 (full medium change) after seeding.

2.2.3 Infection and treatment of hMDMs

2.2.3.1 Infection of hMDMs with *Leishmania* parasites

Leishmania infection of human macrophages *in vitro* was done at day 11 after seeding with stationary phase promastigotes as it has been reported previously in literature (von Stebut and Udey 2004, Fehling, Choy et al. 2020, Zheng, Chen et al. 2020, Fehling, Niss et al. 2021). Previous experiments have shown that a time span of 4 h allows for efficient phagocytosis of *Leishmania* by macrophages (Dissertation Hanno Niss, BNITM 2020; Master Thesis Fahten Habib, BNITM 2021) and that *L. major* parasites show better infection characteristics when incubated at a temperature of 34 °C, similar to the temperature of human skin (Sacks, Barral et al. 1983), compared to incubation at 37 °C, which is used for infections with the *L. infantum.*

On day 11 after seeding, cells were infected with stationary phase *Leishmania* promastigotes (either *L. infantum* or *L. major*) in a MOI of 15:1. For this, parasites were counted on a Beckman Coulter/CASY cell counter and the respective amount for a MOI of 15:1 was centrifuged at 2500 rpm and 4 °C for 10 min. Subsequently the supernatant was discarded, and the parasite solution was adjusted to a parasite concentration of 1,5 x 10^7 cells/ml with cRPMI medium. After removal of the medium with a vacuum pump, immediately 100 µl of parasite solution was added to the infection wells. Uninfected wells were given 100 µl of cRPMI medium without parasites. Cells infected with *Leishmania infantum* were incubated at 37 °C, 5 % CO_2 and cells infected with *Leishmania major* at 34 °C, 5 % CO_2. After 4 h of incubation, cells were washed twice with 150 µl of warm DPBS to remove remaining extracellular parasites. Subsequently 200 µl of cRPMI Medium were added and cells were further incubated at the temperature of the respective parasite (34 °C / 37 °C).

2.2.3.2 Treatment with different drug combinations

Different reference drugs were used for the treatment of *Leishmania*-infected hMDMs. Amphotericin B and Miltefosine were used as leishmanicidal drugs, while Imiquimod and Eh-1 represent immune response modifiers. Two therapeutic strategies were used: mono treatment and combination treatment.

Drugs were administered as mono treatment in the following concentrations:

Amphotericin B: 0,01 μM, 0,1 μM, 0,5 μM and 1 μM

Miltefosine: 1 μM, 5 μM, 10 μM and 15 μM

Imiquimod: 1 μM, 5 μM and 10 μM

Eh-1: 1 μM, 5 μM and 10 μM

For combination treatments each concentration of the leishmanicidal drugs (AmpB/Mil) was tested with each concentration of the immune response modifiers (Imi/Eh-1):

Amphotericin B + Imiquimod:

0,01 μM AmpB + 1 μM Imi, + 5 μM Imi, + 10 μM Imi

0,1 μM AmpB + 1 μM Imi, + 5 μM Imi, + 10 μM Imi

0,5 μM AmpB + 1 μM Imi, + 5 μM Imi, + 10 μM Imi

1 μM AmpB + 1 μM Imi, + 5 μM Imi, + 10 μM Imi

Amphotericin B + Eh-1:

0,01 μM AmpB + 1 μM Eh-1 + 5 μM Eh-1, + 10 μM Eh-1

0,1 μM AmpB + 1 μM Eh-1, + 5 μM Eh-1, + 10 μM Eh-1

0,5 μM AmpB + 1 μM Eh-1, + 5 μM Eh-1, + 10 μM Eh-1

1 μM AmpB + 1 μM Eh-1, + 5 μM Eh-1, + 10 μM Eh-1

Miltefosine + Imiquimod:

1 μM Mil + 1 μM Imi, 5 μM Imi, + 10 μM Imi

5 μM Mil + 1 μM Imi, + 5 μM Imi, + 10 μM Imi

10 μM Mil + 1 μM Imi, + 5 μM Imi, + 10 μM Imi

15 μM Mil + 1 μM Imi, + 5 μM Imi, + 10 μM Imi

Miltefosine + Eh-1:

1 μM Mil + 1 μM Eh-1 + 5 μM Eh-1, + 10 μM Eh-1

5 µM Mil + 1 µM Eh-1, + 5 µM Eh-1, + 10 µM Eh-1

10 µM Mil + 1 µM Eh-1, + 5 µM Eh-1, + 10 µM Eh-1

15 µM Mil + 1 µM Eh-1, + 5 µM Eh-1, + 10 µM Eh-1

Each drug treatment was tested in four technical replicates, while uninfected and infected untreated controls were carried out in eight technical replicates.

24 h post infection medium of the wells was discarded and immediately replaced with 100 µl of fresh cRPMI Medium. Drug combinations were prepared in cRPMI Medium and 100 µl of each drug combination was added to the cells.

Because of its amphiphilic nature, Eh-1 forms micelles at RT. Therefore, Eh-1 vials were sonicated for 10 min at 37 °C and vortexed thoroughly before use.

Cells were incubated for 48 h at 34 °C / 37 °C, 5 % CO_2 with the respective drugs. Subsequently, supernatants were collected and frozen at -20 °C for further analysis. After that, cells were fixed as described in **2.2.3.3.**

2.2.3.3 Cell fixation

Cell fixation is a method, that is deployed to preserve the given state of a cell. Chemical fixatives like paraformaldehyde (PFA) covalently cross-link all proteins in the cell stopping all biological processes while improving mechanical stability.

Cells were washed twice with 200 µl of warm DPBS. Subsequently, 150 µl of 4 % PFA in PBS were added and incubated for 20 min to fixate cells. Finally, cells were washed again with 200 µl DPBS and stored at 4 °C in 200 µl DPBS until immunofluorescence staining (s. **2.2.4.3**).

2.2.3.4 Stimulation of hMDMs with different sex hormones during *Leishmania* infection

To test the influence of human sex hormones on the infection of hMDMs with *Leishmania infantum*, Dihydrotestosterone (DHT) and 17β-Estradiol (E2) were added to the medium in different concentrations.

DHT reaches concentrations of up to 3 nM in the blood of human adult males (Swerdloff, Dudley et al. 2017). Typical concentrations for *in vitro* DHT stimulation range from 1 - 100 nM in literature (Guth, Bohm et al. 2004, Cai, Hong et al. 2011, Lee, Kim et al. 2019). After an initial experiment in this range had shown no effect (data not shown), the following concentrations were used for DHT:

DHT: 10 nM, 50 nM, 100 nM, 500 nM, 1 µM, 5 µM

E2 blood levels range from 0,1 nM - 1,5 nM in human adult females (Laboratories 2022). For Estradiol, concentrations of 0,1 nM - 10 µM can be found in literature (Behl, Widmann et al. 1995, Pentikainen, Erkkila et al. 2000, Rogers and Eastell 2001). Thus, the following concentrations were used during the experiments:

E2: 10 nM, 100 nM, 500 nM, 1 µM, 2 µM, 5 µM

Importantly, for these experiments cRPMI medium without phenol red was used since it has been shown to be a weak estrogen receptor antagonist (Berthois, Katzenellenbogen et al. 1986).

Buffy coat samples were purified and monocytes differentiated into macrophages (in cRPMI without phenol red) as described in **2.2.2**. Before infection, medium was discarded and replaced with 200 µl of cRPMI containing the respective sex hormone concentration. After incubation for 30 min, the medium was removed, and infection with *L. infantum* (MOI 15:1) was carried out as described in **2.2.3.1**. Cells were fixated 24 h.p.i. as described in **2.2.3.2** until immunofluorescence staining (s. **2.2.4.3**).

2.2.4 Analysis methods

2.2.4.1 Surface marker staining and fluorescence activated cell sorting (FACS) of monocytes0

FACS is a technique based on the analysis of fluorescent signals inside a flowing sample. It can be used to detect and count the number of fluorescent signals in a sample. Inside the cytometer a point laser is placed next to a flow cell. As the sample is pumped through the flow cell, the laser induces fluorescence of the analyte, which will be converted into digital information by several photodetectors. These detect forward scatter, side scatter and fluorescence signals. Based on these signals, analytes inside the sample can also be sorted (BosterBIO 2022). In this case FACS is

used to count the number of monocytes inside samples before and after MACS to ensure successful purification.

FACS samples of $1x10^6$ cells were taken before (PBMCs) and after MACS ($CD14^+$ fraction). An unstained control of $1x10^6$ PBMCs was used to get information about any fluorescent background signals. The cross talk of fluorescent signals in the panel has been previously compensated in the flow cytometry software by our research group. Samples were purified, stained, and analyzed on the same day and kept on ice during the purification and staining process until fixated.

Samples were stained with fluorescent antibodies for the surface markers CD14, HLA-DR, CD16 and the live/dead marker zombie UV (**Table 2-12**).

Samples were collected and dissolved in 1 ml DPBS in FACS tubes on ice. In a first step, cell pellets were washed in FACS buffer. This was achieved by centrifugation at 1400 rpm and 4 °C for 5 min, removal of the supernatant, addition of 1 ml FACS buffer and another centrifugation step at 1500 rpm and 4 °C for 5 min. After that, the supernatant was discarded, and cells were incubated with the surface marker staining panel (**Table 2-12**) for 30 min at 4 °C in the dark. The antibody mixture was prepared with the respective volumes in **Table 2-12** and filled ad 50 µl with FACS buffer. For live/dead staining, a control sample was incubated with 50 µl Zombie UV in a dilution of 1:4000 in PBS. Subsequently, 1 ml of FACS buffer was added to wash off remaining unbound antibodies and cells were centrifuged at 1500 rpm and 4 °C for 5 min. After removal of the supernatant, cells were resuspended in 100 µl of FIX solution and incubated for 30 min at 4 °C in the dark to fixate the antibody staining. The fixation process was stopped by addition of 1 ml PermWash solution. After centrifugation at 1500 rpm and 4 °C for 5 min, discarding of the supernatant and another washing step with 1 ml PermWash solution followed by centrifugation at 1500 rpm and 4 °C for 5 min and removal of the supernatant, cells were resuspended in 150 µl of PermWash solution and measured at a Cytek FACS Aurora cytometer. This device is equipped with four lasers (405, 488, 561 and 640 nm) for the excitation of fluorescence and can detect fluorescence in 48 channels. For each sample, $5x10^5$ events were recorded.

Table 2-12: Antibody panel used for FACS analysis of purification efficiency and identification of CD14+ monocytes

Antigen	Fluorochrome	Description/Function	(mainly) Expressed on	Exc_{max}	Emi_{max}	Volume (µl)
CD14	BV510	Co-receptor for TLR mediated LPS binding (Zanoni and Granucci 2013)	Monocytes/Macrophages (Ong, Teng et al. 2019)	405	510	3,5
HLA-DR	BUV395	MHC class II receptor involved in antigen presentation (Murphy and Weaver 2016)	Monocytes/Macrophages, DCs, activated B-cells (Murphy and Weaver 2016)	348	395	4,5
CD16	PerCP	Part of IgG Fc binding receptor (Murphy and Weaver 2016)	Monocytes/Macrophages, Neutrophils (Murphy and Weaver 2016)	480	675	3
live/dead	Zombie UV	staining of cells with non-intact membranes (Biolegend 2019)	-	360	455	1,25 (1:100)

2.2.4.2 Cytokine analysis using immunoassays

To investigate the cytokine profiles of *Leishmania*-infected and treated human macrophages, a LEGENDplex immunoassay by Biolegend was used to allow for quantification of extracellular cytokine/chemokine concentrations. In cooperation with Biolegend a custom cytokine panel was designed containing the following analytes:

IL-12p70, TNF-α, IL-6, IL-10, IL-1β, Arginase, CCL17, IL-23, IFN-γ, CXCL10, IL-18, CCL2

The assay uses cytokine specific beads labeled with fluorochromes. Allophycocyanin (APC) labeling of different intensity and varying bead size allow for distinction between analytes during analysis in a flow cytometer. Analytes bind to specific antibodies on bead surface and staining is achieved using biotinylated secondary antibodies. Biotin residues are then labeled by binding of Phycoerythrin (PE) conjugated streptavidin. Quantification of analyte concentration is achieved by using a standard for calibration. A schematic overview of LEGENDplex principle can be found in **Figure 2-6**. Flow cytometry data were evaluated for analyte concentrations using Biolegend's Qognit Cloud-Based Data Analysis Software.

LEGENDplex assays were performed in a 96-well V-bottom plate. Standard calibration was done according to manufacturer specifications.

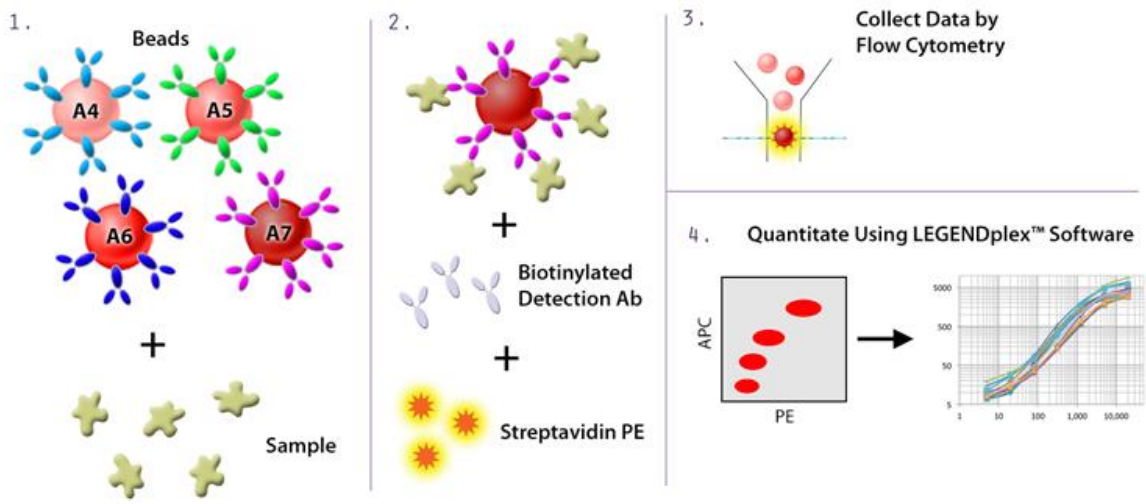

Figure 2-6: Schematic representation of LEGENDplex assay principle. Analytes are bound to antibody coated beads (1.), which are then labeled with biotinylated detection antibodies allowing for streptavidin-PE mediated fluorescent signaling proportional to the respective analyte concentration (2.). Fluorescent signals can be measured in a flow cytometer (3.) and assigned to the respective analyte via distinction in APC signal and bead size (4.). (Biolegend 2022)

For the reaction, 10 µl of cell culture supernatant or standard were mixed with 10 µl of assay buffer and 10 µl of pre-mixed beads. To avoid aggregation, beads were sonicated for 1 min and vortexed thoroughly before use. The mixture was incubated for 2 h at 800 rpm and RT on an orbital laboratory shaker in the dark. After sample binding, plates were centrifuged at 1050 rpm and RT for 5 min. The supernatant was discarded and beads were washed in 200 µl of washing buffer at 800 rpm for 1 min to get rid of remaining unbound sample before being centrifuged at 1050 rpm and RT for 5 min. Subsequently, 10 µl of detection antibody were added and the mixture was incubated for 1 h at 800 rpm and RT on an orbital laboratory shaker in the dark. After that, 10 µl of PE conjugated streptavidin were added without washing and the mixture was incubated for another 30 min at 800 rpm and RT on an orbital laboratory shaker in the dark. In a final washing step 200 µl of washing buffer were added and the plate was centrifuged at 1050 rpm and RT for 5 min after being shook for 1 min at 800 rpm. Supernatants were discarded and the bead mixture was dissolved in 150 µl of washing buffer before flow cytometry analysis at the LSR II. For each sample 3600 counting events were recorded.

2.2.4.3 Immunofluorescence staining

Immunofluorescence staining was used for visualization of macrophages and *Leishmania* parasites in preparation for subsequent confocal imaging and image analysis with Harmony™ software. Specific binding of analytes with monoclonal antibodies and subsequent binding of fluorophore coupled secondary antibody, as well as the use of fluorescent DNA binding dye allows for detection and localization of cells and parasites during fluorescence microscopy.

For staining of *Leishmania* and macrophage cytoplasm, an antibody directed against 90 kDa heat shock protein (Hsp90) was used. 4',6-Diamidino-2-phenylindol (DAPI) was used for staining of nuclei. Alexa 647 was used as fluorochrome for the secondary antibody.

First, cells were washed twice with 200 µl of washing buffer containing Triton X-100 for 5 min at 300 rpm, RT on an orbital laboratory shaker. To permeabilize the cell membrane, cells were incubated with 150 µl of permeabilization buffer containing Triton X-100 and NH_4Cl for 15 min at 300 rpm, RT. To minimize unspecific binding, 150 µl of blocking solution containing bovine serum albumin (BSA) were added and incubated for 30 min at 300 rpm, RT. Subsequently 60 µl of α-HSP90 primary antibody (mouse) in blocking solution were added in a dilution of 1:4000 and incubated for 1,5 h at 300 rpm, RT. After that, cells were washed three times with 200 µl of washing buffer for 5 min at 300 rpm, RT. For incubation of the secondary antibody (Alexa Fluor 647 goat-α-mouse) the 96-well plates were covered with aluminum foil to ensure proper function of the fluorescent dye. The secondary antibody was diluted 1:8000 in blocking buffer with 36 µM DAPI. Then, 60 µl of this solution were added to the cells and incubated for 1h at 300 rpm, RT. To complete the staining procedure, cells were washed twice with 200 µl of washing buffer and subsequently with 200 µl of PBS. Cells were then stored in 200 µl of PBS in the dark at 4 °C until measurement.

2.3 High content screening using automated confocal microscopy

High content screening analyses are a common tool for rapid *in vitro* drug screenings. Combining high content screening with automated confocal microscopy and image analysis allows for rapid evaluation of drug screening experiments. In a first step images are generated by automated, confocal fluorescence microscopy, which are subsequently analyzed with a custom-made image analysis sequence for phenotypic screening of parasite infection by a drug screening image analysis software. For imaging, the confocal microscope of the Opera Phenix™ high content screening unit was used and the respective Harmony™ software by Perkin Elmer allowed for subsequent image analysis.

2.3.1 Confocal microscopy with the Opera Phenix™ unit & Harmony™ image analysis software

With its spinning disc confocal microscope, the Opera Phenix™ unit is capable of imaging fluorescent signals on different wavelengths. During the experiments, images were made in confocal mode, which is often used in fluorescent imaging to increase resolution (Alberts 2008). Moreover, spinning disc synchrony optics allowed for the efficient reduction of emission cross talk (s. **Figure 2-7**) (Angelika Foitzik 2015).

During the experiments excitation of fluorescent Alexa Fluor 647 and DAPI was achieved with the 640 nm and 405 nm laser of the Opera Phenix™. Alexa Fluor 647 was exposed to the 640 nm laser for 500 ms at 100 % power, while DAPI was exposed to the 405 nm laser for 400 ms at 100 % power. Images were generated with large-format sCMOS cameras (16-bit, 4.4 megapixels, 2100 x 2100 resolution, 6.5 µm pixel size). Images were taken at 15 different positions in each well in image stacks ranging from -11 µm to 1 µm as seen in **Figure 2-8**. Stack images were layered to increase resolution allowing for generation of representative, high resolution pictures for subsequent evaluation with Harmony™.

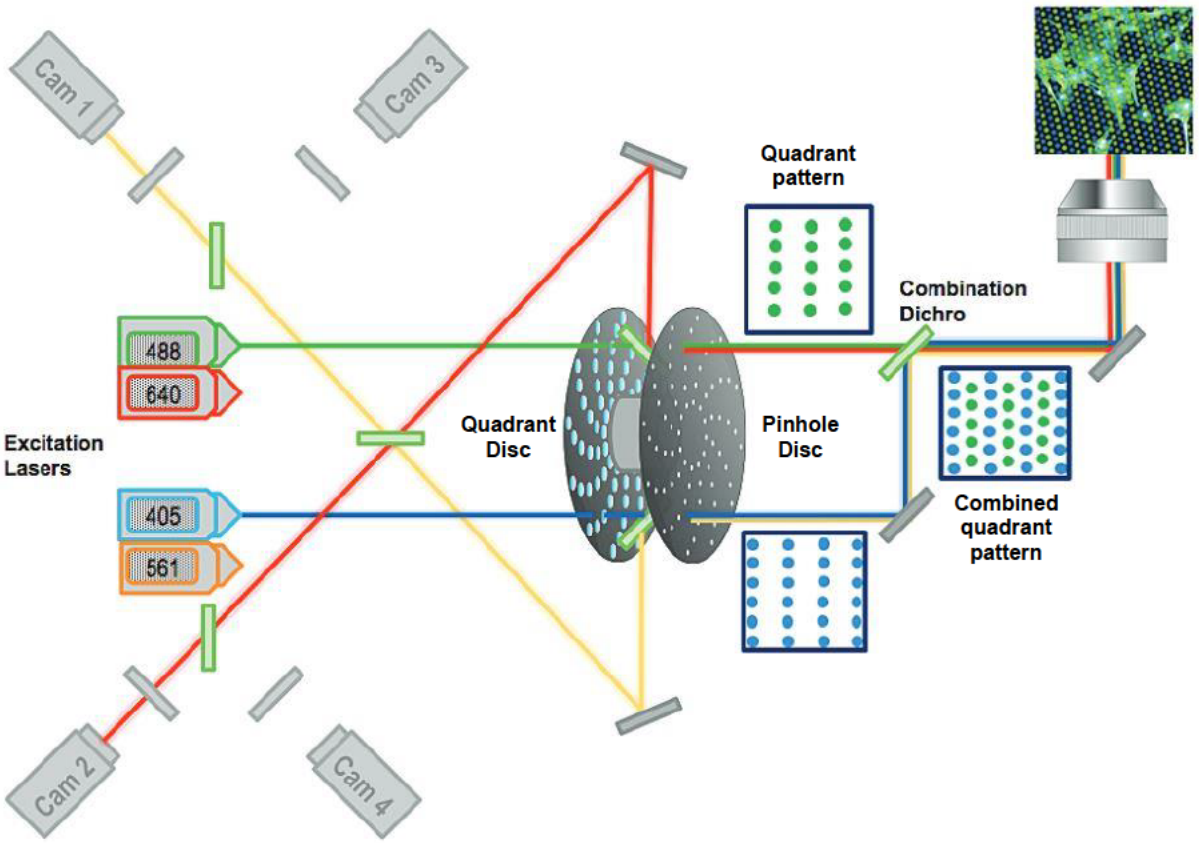

Figure 2-7: Schematic representation of synchrony optics and confocal imaging inside the Opera Phenix unit. Light from wavelength specific excitation lasers is passed through two spinning discs (quadrant disc and pinhole disc) to generate light of a specific quadrant pattern that is used to excite the sample. Lasers of similar wavelengths are spatially separated for minimal crosstalk. After being focused on the sample via the objective lens, emitted light of combined quadrant pattern passes through a dichroic mirror broadly separating emission signals by their wavelength. Further wavelength selection is achieved by the pinhole disc, which reflects any light, that is not in the phase of the spinning disc. These wavelength specific, focused emission light beams pass onto the detector allowing for minimal crosstalk and increased resolution compared to conventional confocal microscopy. (Angelika Foitzik 2015)

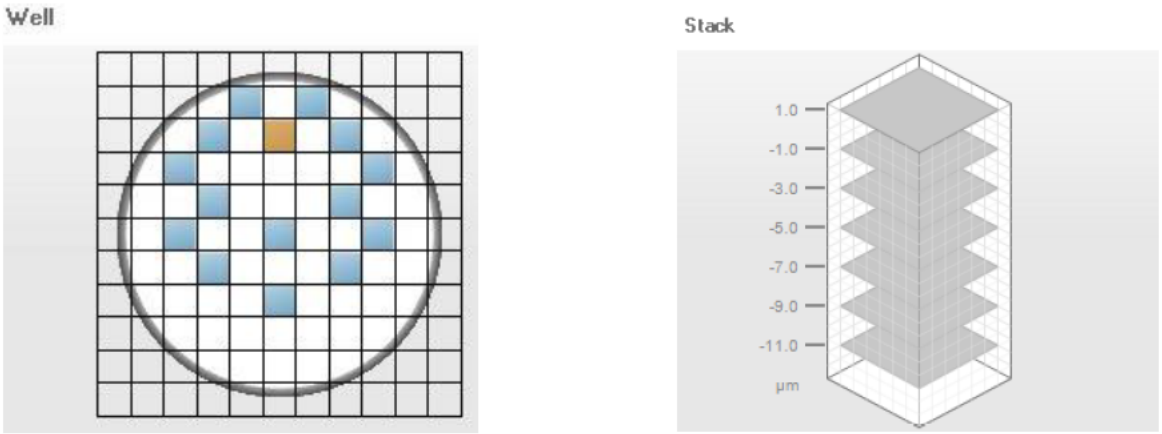

Figure 2-8: Schematic overview of imaging positions and planes during the imaging process inside a 96-plate well. Per well, 15 different positions were analyzed in stacks from -11 to 1 µm. In total roughly 3000-6000 macrophages were imaged and analyzed per well. Source: Screenshots Harmony™ Software

The high content screening analysis software Harmony™ can be used for phenotypical analysis of fluorescence microscopy images according to different criteria like shape and size of fluorescent signals. Subsequently, these data can be related to certain evaluation parameters like cell morphology or intracellular/extracellular pathogens. Fluorescent signals were generated in two channels following excitation with the 640 nm laser and excitation with the 405 nm laser. The evaluation process is divided into separate image processing steps that each segmentize the image depending on signals of the fluorescent channels, define regions of interest, quantify signals in these regions, define subpopulations and generate a readout value.

Utilizing various processing steps and the software's training mechanism, an image analysis sequence for the identification of hMDMs, *Leishmania* parasites and polarization status of macrophages has been set-up in previous work (Dissertation Hanno Niss, BNITM 2020; Master Thesis Fahten Habib, BNITM 2021).

First, the analysis sequence detects nuclei and cytoplasm based on intensity and morphology properties of Alexa 647 and DAPI signal. Subsequently, the cytoplasm is defined as the region of interest, where spots are identified (again by intensity and morphology). These spots are then analyzed for their properties and classified based on highly selective criteria for the identification of *Leishmania*. Like this, infection of macrophages with *Leishmania* parasites can be automatically evaluated.

Some exemplary images of the most important steps of the analysis sequence can be found in **Figure 3-3**. For a more details of image analysis parameters see **6.1** in the appendix.

The custom-made analysis sequence generates several readouts. The following were used for subsequent data analysis: total macrophages per well, total leishmania per well, infected macrophages per well, percent % M1 shaped macrophages of total macrophages, percent % M2 shaped macrophages of total macrophages

2.3.2 Drug screening parameters and quality control for high content screening

2.3.2.1 Introduction of drug screening readout parameters

In drug screening experiments, not all parameters can be kept exactly reproducible like e.g. number of macrophages or *Leishmania*. Thus, for comparability, it is important to generate relative evaluation parameters. Important evaluation factors of parasite drug screenings are cell viability (gives information about the toxicity of a drug), infection rate and parasite burden. These parameters can be calculated by normalization of the data sets total macrophages, % infected macrophages and total leishmania of each well to the mean value of the infected untreated control yielding a value in percent of the control ("POC"). This leads to the following equations for the respective readout parameters:

Viability:

Equation 2: Calculation of the viability as the total macrophages of a well normalized to the mean of the infected untreated control yielding the percentage of control "POC"

$$\%\,POC = \frac{total\ macrophages\ of\ well\ X}{mean\ of\ total\ macrophages\ of\ infected\ untreated\ control}$$

Infection Rate:

Equation 3: Calculation of the infection rate as the % infected macrophages of a well normalized to the mean of the infected untreated control yielding the percentage of control "POC"

$$\%\,POC = \frac{\%\ infected\ macrophages\ of\ well\ X}{mean\ of\ \%\ infected\ macrophages\ of\ infected\ untreated\ control}$$

Parasite Burden:

Equation 4: Calculation of the parasite burden as the total leishmania of a well normalized to the mean of the infected untreated control yielding the percentage of control "POC"

$$\%\,POC = \frac{total\ leishmania\ of\ well\ X}{mean\ of\ total\ leishmania\ of\ infected\ untreated\ control}$$

These parameters allow for comparison of treatment between the two *Leishmania* strains since they do not show the same infection characteristics *in vitro*.

2.3.2.2 Quality control for high content screenings

Since high content drug screenings have a high requirement of measurement precision, assay quality control can be done by calculation of the Z'-Factor (Birmingham, Selfors et al. 2009). It compares deviations of positive and negative controls and gives a statistical tool for the evaluation of assay performance.

Z'-Factor:

Equation 5: Calculation of the Z'-factor. Assuming a Gaussian distribution of sample data, the Z'-Factor gives information about assay precision by comparison of standard deviations and means of positive and negative control.

$$Z' = 1 - \frac{3 \cdot (\sigma_{pos} - \sigma_{neg})}{|\overline{x_{pos}} - \overline{x_{neg}}|} \; with$$

$$\sigma_{\frac{pos}{neg}} = standard\ deviation\ of\ positive\ or\ negative\ control\ \&$$

$$\overline{x_{\frac{pos}{neg}}} = mean\ of\ positive\ or\ negative\ control$$

2.4 Statistical analysis methods

All data was generated in at least three replicates and compared between independent sample groups (e.g. untreated cell and treated cells). For statistical comparison unpaired two tailed t-tests are used, which assume a Gaussian distribution of data (Motulsky 2016, Frost 2018). Student's t-statistic gives information about the probability of a difference between two data sets considering the mean, sample size and variance of each data set (Motulsky 2016, Frost 2018) The probability of difference between the data sets is represented by the p-value. Unpaired, two-tailed t-tests were carried out using the software GraphPad PRISM (version 8).

Significances are displayed by the software PRISM as follows:

ns p ≥ 0,05 (not significant)

*	$p \leq 0{,}05$
**	$p \leq 0{,}01$
***	$p \leq 0{,}001$
****	$p \leq 0{,}0001$

3 Results

3.1 FACS analysis of monocyte purity before and after MACS separation

In blood samples, usually three monocyte populations with different degrees of CD14/CD16 expression can be detected by fluorescence activated cell sorting (FACS) (Yang, Zhang et al. 2014). Because of their high degree of CD14 expression, monocytes for *in vitro* studies are often purified via CD14 positive selection in magnetic activated cell separation (MACS). This method shows high monocyte yields and high degrees of purity compared to other methods (Nielsen, Andersen et al. 2020). After density gradient centrifugation and erythrocyte lysis, monocytes were purified with MACS separation using CD14 magnetic beads. This step is crucial for minimizing contamination with other cell types, which could heavily influence experiment outcomes. After HLA-DR, CD14 and CD16 surface marker staining, FACS analysis was used for determination of monocyte purity.

For the analysis of flow cytometry data, the gating scheme shown in **Figure 3-1** was used. In a first step lymphocytes are separated from any cell debris according to size and granularity by forward and side scatter area signals (FSC-A & SSC-A), respectively. Subsequently single cells are selected by their difference in size compared to doublets or aggregates via forward scatter area and height (FSC-A & FSC-H). Zombie-UV dye cannot access alive cells with intact membranes but will color dead cells with compromised membranes allowing for gating of living cells, which do not show any Zombie-UV signal. In a next step, HLA-DR is used to separate monocytes from neutrophils and NK cells. Subsequently monocytes and monocyte subsets can be identified by their degree of CD14/CD16 expression. Non-classical monocytes are characterized by high CD16 expression, intermediate monocytes show both CD14 and CD16 expression and classical monocytes are characterized by high CD14 expression.

Compared to the sample before MACS (**Figure 3-1 A**), after purification, cells showed a higher degree of SSC-A in the first gating step (**Figure 3-1 B**). Both samples consisted mostly of single cells, but after purification a bigger portion of cells showed a Zombie UV signal (7,2 % less cells in “alive” gate). The degree of HLA-DR signal in

the sample was elevated greatly after purification (58,4 % more cells in “HLA-DR+” gate). Compared to 54,2 % in PBMCs, 95,7 % monocytes could be found in the sample after MACS. The percentage of non-classical monocytes was reduced by 11,0 % and intermediate monocytes by 4,55 %, while classical monocyte percentage was increased by 15,6 % after purification. Generally, yields after MACS were around 10-25 % of PBMCs.

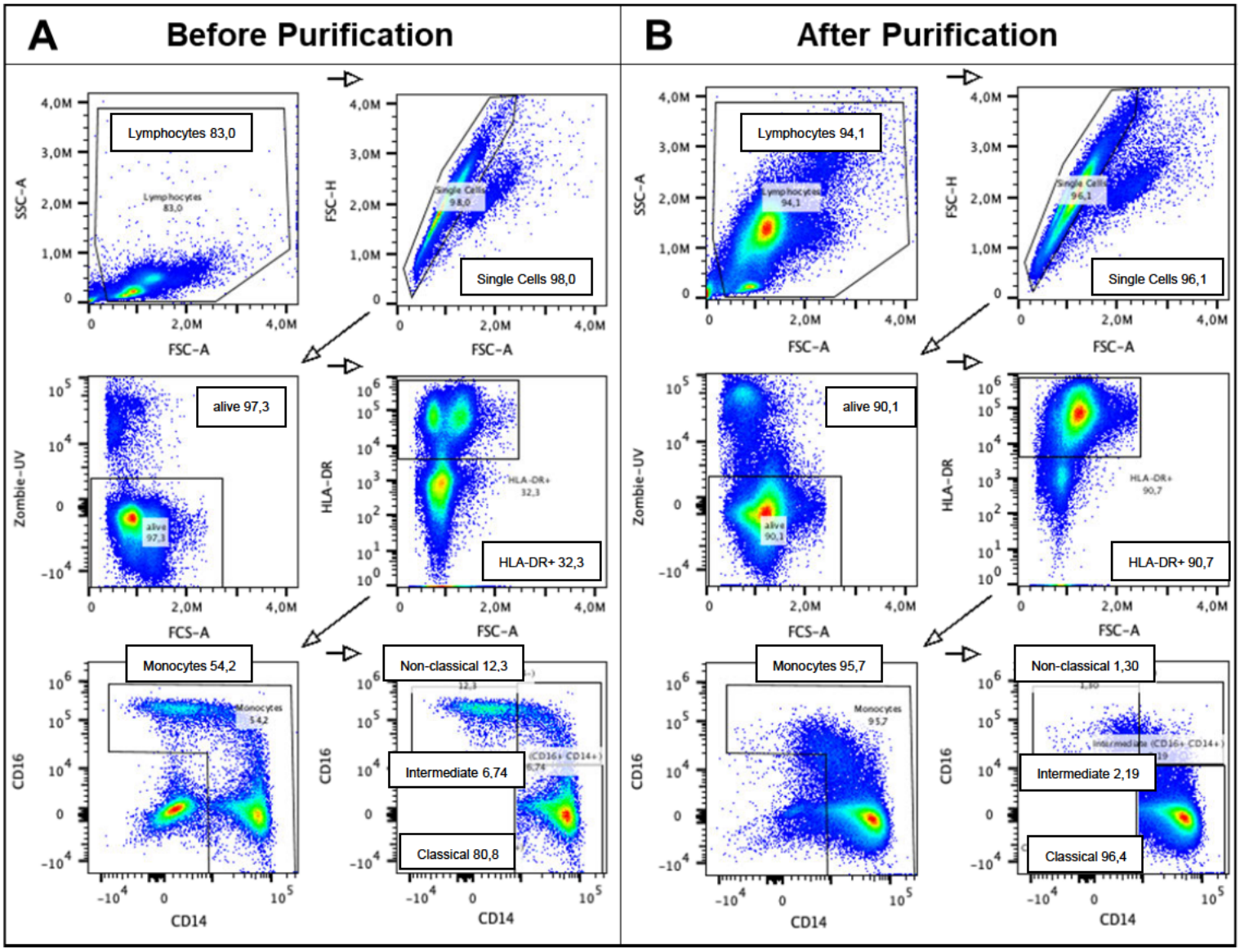

Figure 3-1: Representative flow cytometry analysis of monocyte purification for a blood sample from a male individual (*1994, age 28) with sequential gating strategy for the identification of monocyte subsets. Samples were obtained before (A) and after (B) MACS. Surface marker staining with fluorescent antibodies allows for the gating of different cell populations. Lymphocytes are separated from debris by forward and side scatter area (FSC-A & SSC-A) representing cell size and granularity, respectively. Doublets and aggregates are identified and excluded via side scatter height (SSC-H). Subsequently, alive cells are selected via Zombie-UV signal. HLA-DR gating excludes neutrophils and NK cells. Non-classical, intermediate, and classical monocytes are then identified via CD14/CD16 expression profiles. All gating values are shown in percentage of cells from the previous gating step.

3.2 HCS assay for the infection of human primary macrophages with *Leishmania* ssp.

3.2.1 Confocal imaging of hMDMs infected with *L. infantum* and *L. major*

After differentiation of monocytes to macrophages using M-CSF, hMDMs were infected with *Leishmania infantum* and *Leishmania major*. Infections were carried out in a MOI of 15:1. After immunofluorescence staining of HSP-90 and DNA, with the help of the Opera Phenix confocal microscope the following images were created in infected untreated cells:

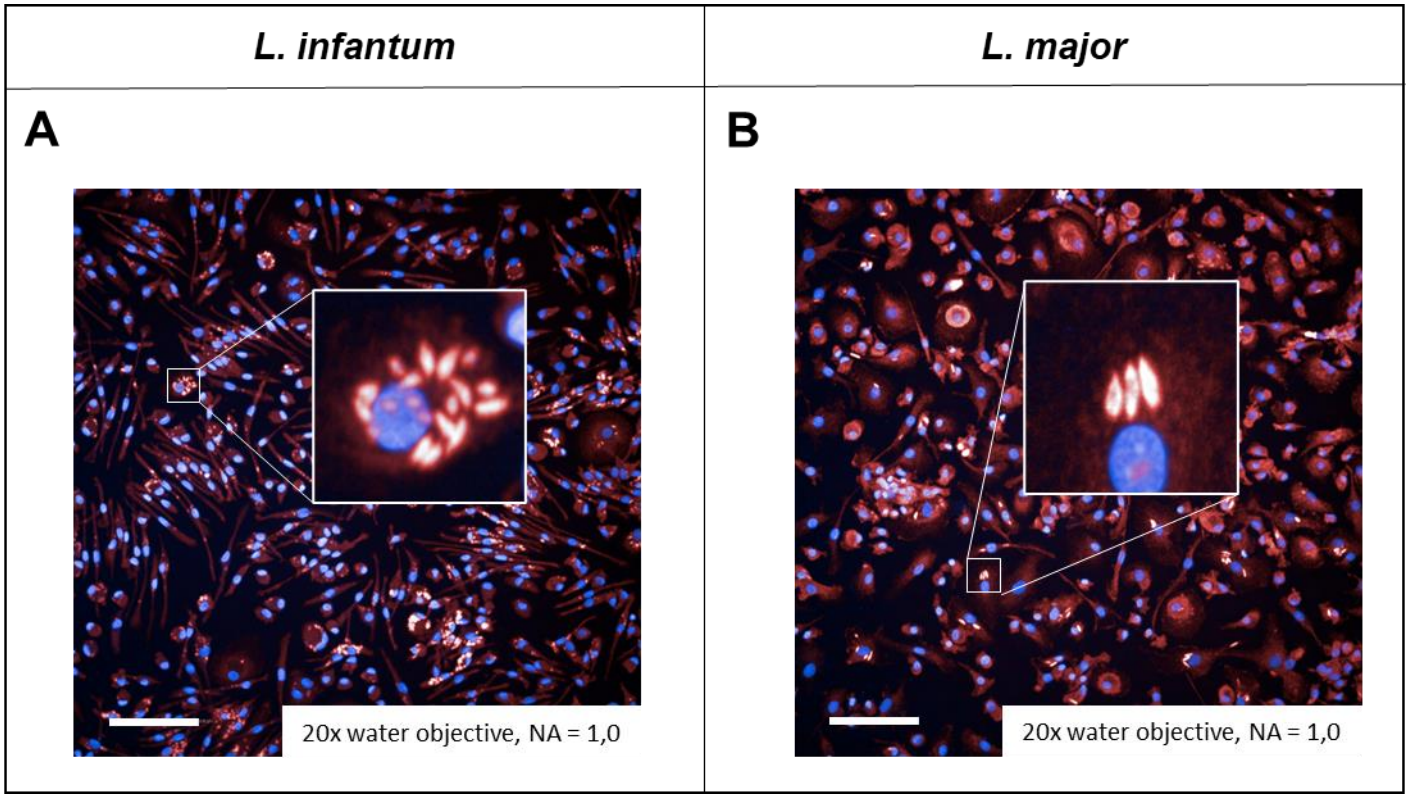

Figure 3-2: Confocal microscopy images of *L. infantum* (A) and *L. major* (B) in infected macrophages (MOI 15:1). Shown here are macrophages from a male individual (m3) that were infected with *L. infantum* (A) and another male individual (m7) that were infected with *L. major* (B). Fluorescence signals of Alexa647 (red) and DAPI (blue) were detected and visualized with the confocal microscopy unit of the Opera Phenix system as described in **2.3.1**. Scale bar = 100 μm

Figure 3-2 shows that staining of HSP-90 in *Leishmania* and macrophages and DNA in macrophage nuclei, *Leishmania* nuclei and *Leishmania* kinetoplast (very small DAPI spot inside *Leishmania* lumen, not visible in the images) could be achieved with Alexa

Fluor 647 and DAPI, respectively. *Leishmania* parasites could be found in cell cytoplasm primarily in their amastigote form, which is characterized by their oval shape and small size of around 2 µm in diameter.

3.2.2 Using Harmony™ analysis sequence for high content drug screening of *Leishmania* infected hMDMs

Confocal images created with the Opera Phenix™ were evaluated using the high content screening analysis software Harmony™. An analysis sequence for the identification of *Leishmania* parasites and macrophage polarization states was used to generate different analysis readouts. **Figure 3-3** shows some exemplary outputs of processing steps inside the used analysis sequence.

Leishmania can be identified by their abundant Hsp90 expression, which is a protein conveying temperature and pH resistance highly expressed in *Leishmania* parasites (2,8 % of total protein) (Brandau, Dresel et al. 1995). In human cells HSP90 is expressed in the cytoplasm to a much lesser extent (1-2 % of total protein) allowing for differentiation between human cells and parasites while staining hMDM cytoplasm for morphology investigation (Chen, Piel et al. 2005).

Leishmania parasites and infected macrophages could be reliably detected in their image analysis building blocks of the analysis sequence. Macrophages were counted by the signals of their nuclei and could be successfully classified into M1/M2 state by evaluation of their phenotype.

Generally, *L. major* parasites showed much higher numbers in macrophage samples upon infection compared to *L. infantum*. For *L. major* around 15 000 parasites were found in a well, while during *L. infantum* infection only around 4000 parasites could be detected.

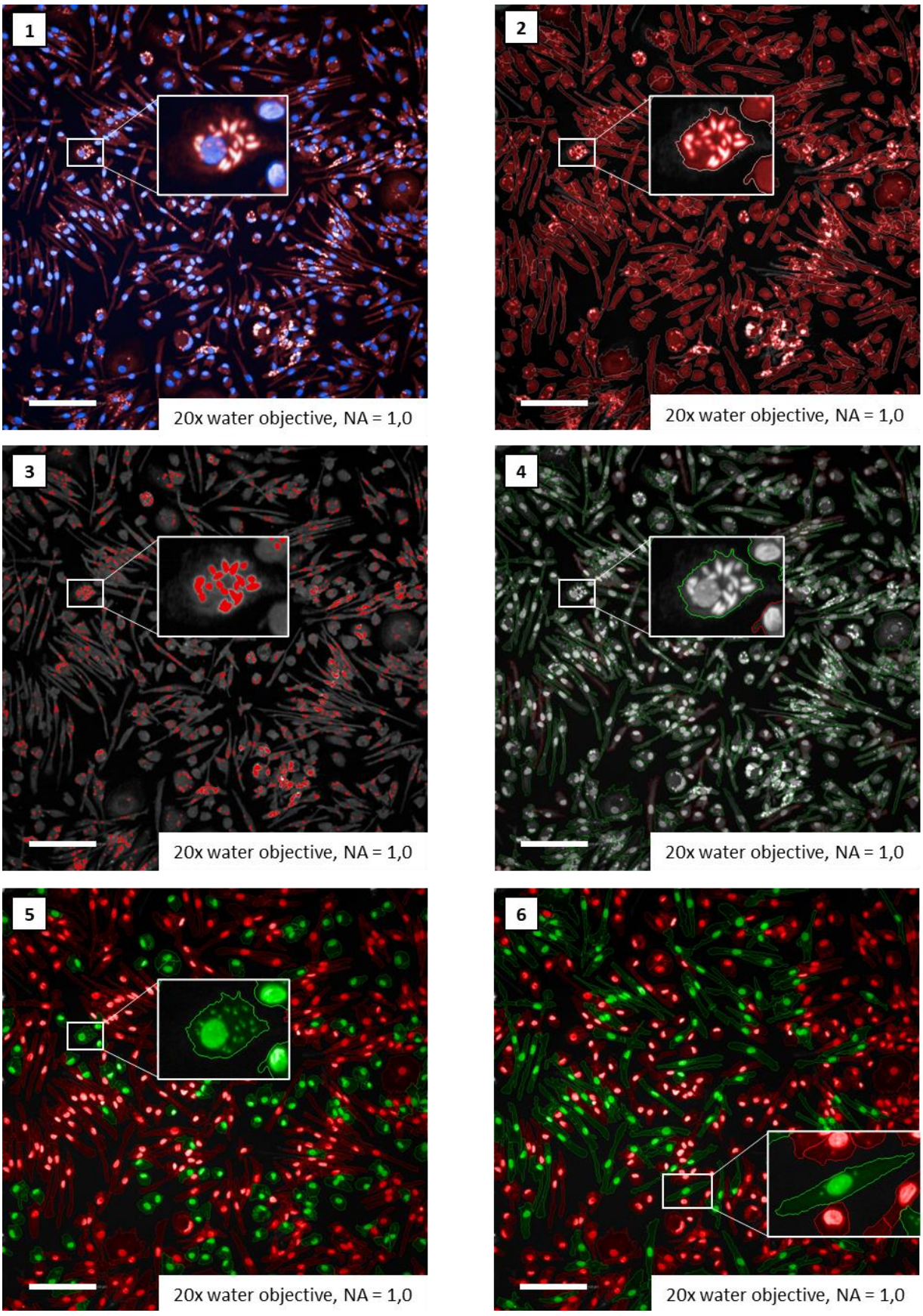

Figure 3-3: Exemplary images of hMDMs infected with *L. infantum* parasites (MOI 15:1) after immunofluorescent staining as described in 2.2.4.3 made with the 20x water objective (NA = 1,0) of the Opera Phenix™ confocal microscope. Macrophages were generated from a blood sample of a male individual (m3). Shown here are Harmony™ software outputs at different steps of the analysis

sequence. The input image (**1**) shows fluorescence of DAPI (blue) and Alexa Fluor 647 (red). These fluorescent signals are used to generate the outputs "cytoplasm" (**2**, red), "*Leishmania*" (**3**, red), "infected macrophages" (**4**, green border), "M1 macrophages" (**5**, green) and "M2 macrophages" (**6**, green) of different processing steps. Scale bar = 100 μm

3.3 Analyzation of sex differences in infection characteristics

It has been shown that parasite induced diseases show an infection bias toward male gender (Sellau, Groneberg et al. 2019). They show a higher susceptibility and higher parasite load during *Leishmania* infection (de Araujo Albuquerque, da Silva et al. 2021). Moreover, macrophage polarization and cytokine response play important roles during disease development, as they regulate Th1 and Th2 responses (Italiani and Boraschi 2014).

During the work for this thesis, multiple infections of male and female macrophages with both *L. infantum* and *L. major* were carried out (MOI 15:1) generating data from five male and five female individuals for *L. infantum* infection and three male and two female individuals for *L. major* infection. For each experiment, eight technical replicates of infected untreated control give information about general infection behavior, which can be compared to eight technical replicates of uninfected control cells. Each replicate well contained $1x10^5$ of isolated monocytes. During image analysis around 3000-6000 macrophages were analyzed per well.

In the analysis sequence used, macrophage polarization status is analyzed according to morphology. It has been shown in previous experiments, that surface marker signature from M1 or M2 polarized hMDMs correlates with their morphology. Macrophages polarized into M1 state by stimulation with GM-CSF and IFN-γ show a round morphology and are generally smaller compared to macrophages polarized into M2 state by stimulation with M-CSF and IL-4, that show an elongated, spindle-like morphology. Based on this, morphology parameters in the analysis sequence (cell roundness, cell width, cell length and width to length ration) were adjusted to identify M1 and M2 phenotype in previous work (Master Thesis Fahten Habib, BNITM 2021). Generally, M1/M2 state evaluation must be handled with care since cell morphology can vary extensively. For trustable results, an additional FACS analysis with M1/M2 state markers or a transcriptome analysis should always be carried out.

For the M1/M2 analysis in this thesis I rely on the confirmation of phenotypical M1/M2 state analysis of hMDMs by FASC of previously generated results (BNITM, Fehling et al., unpublished). During the study “M1-like macrophages” were generated by stimulation with GM-CSF and IFN-γ, and “”M2-like macrophages” were generated by stimulation with M-CSF and IL-4. Both macrophage populations were analyzed regarding M1 and M2 phenotype with the analysis sequence used during my experiments and compared by FACS analysis of the M1 surface markers CD86, CD64, CD68 and HLA-DR and M2 surface markers CD163, CD200R and CD206. The results in **Figure 3-4** show, that M1-like macrophages are recognized by the analysis sequence as M1 macrophages, while M2-like macrophages are predominantly recognized as M2 macrophages.

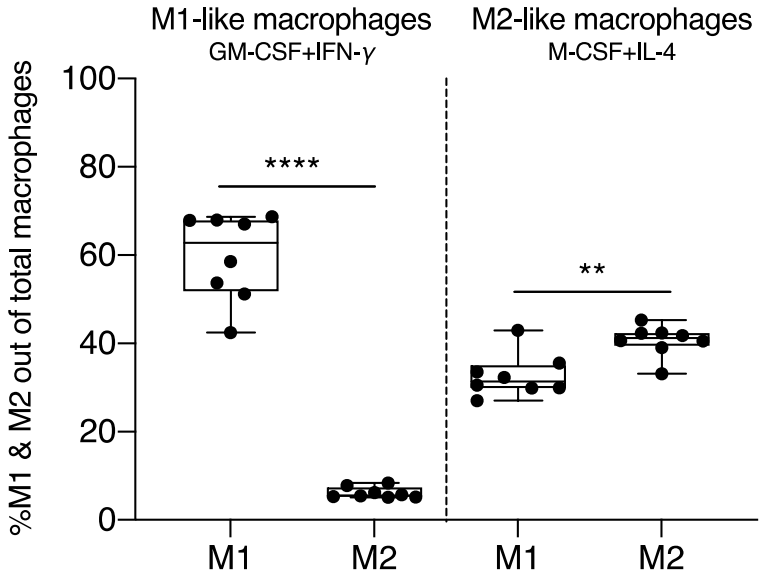

Figure 3-4: Percentage of M1- and M2-like macrophages in samples stimulated with GM-CSF and IFN-γ (M1-like macrophages), and M-CSF and IL-4 (M2-like macrophages) as classified by the Harmony™ analysis sequence used during the experiments. Macrophages stimulated with GM-CSF and IFN-γ are recognized by the analysis sequence as M1 macrophages, while macrophages stimulated with M-CSF and IL-4 are predominantly declared as M2 macrophages. Source: (BNITM, Fehling et al., unpublished)

Figure 3-5 shows, that M1 markers are significantly upregulated in M1-like macrophages compared to M2-like macrophages, which show significantly higher expression of M2 markers.

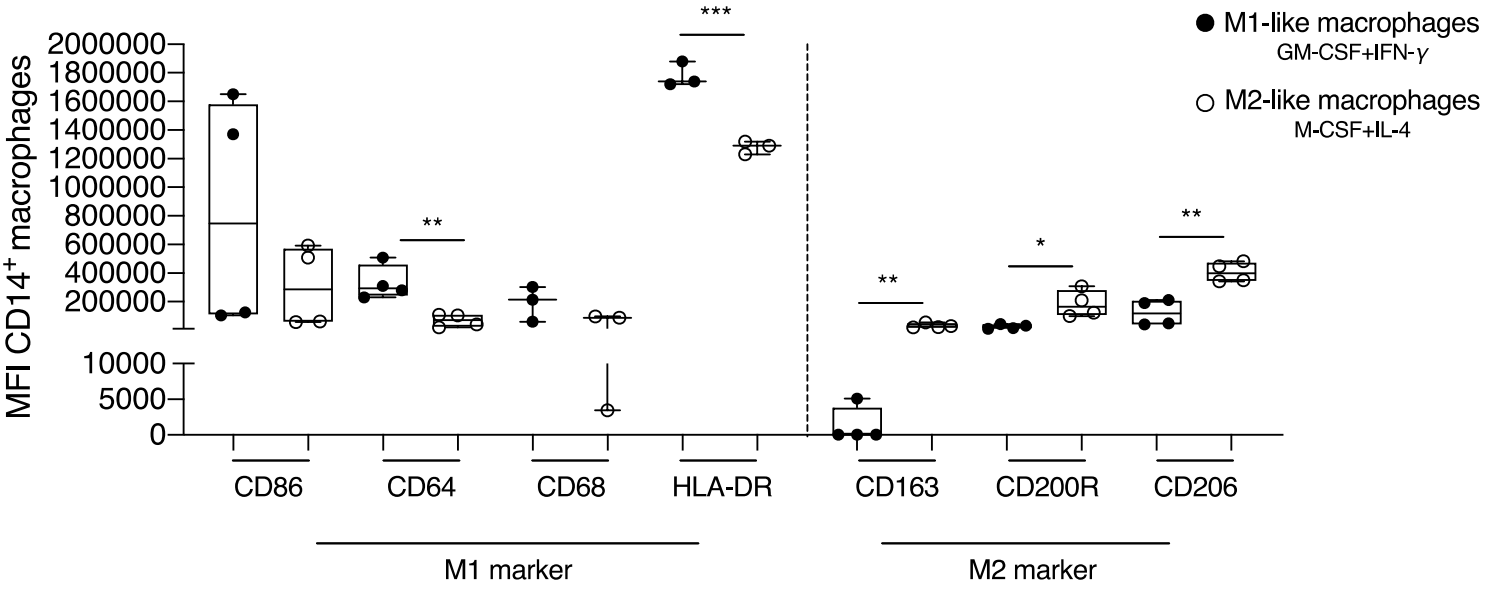

Figure 3-5: FACS analysis of M1 and M2 surface marker expression of M1- and M2-like macrophages. After surface marker staining of M1 markers (CD86, CD64, CD68 and HLA-DR) and M2 markers (CD163, CD200R and CD206) for M1-like and M2-like macrophages, M1-like macrophages show significantly higher mean fluorescence intensities (MFIs) for M1 markers compared to M2-like macrophages, while M2-like macrophages show higher MFIs for M2 markers. Source: (BNITM, Fehling et al., unpublished)

To see if there are differences in gender specific infection intensity, the percentage of infected macrophages from infected untreated controls of all male and female individuals were analyzed for both parasites (**Figure 3-6 A & B**).

Since Leishmaniasis disease is driven by differences in Th1 and Th2 responses, analyzation of changes in M1/M2 state following *Leishmania* infection are compared for each macrophage activation state and gender respectively (**Figure 3-6 C – F)**.

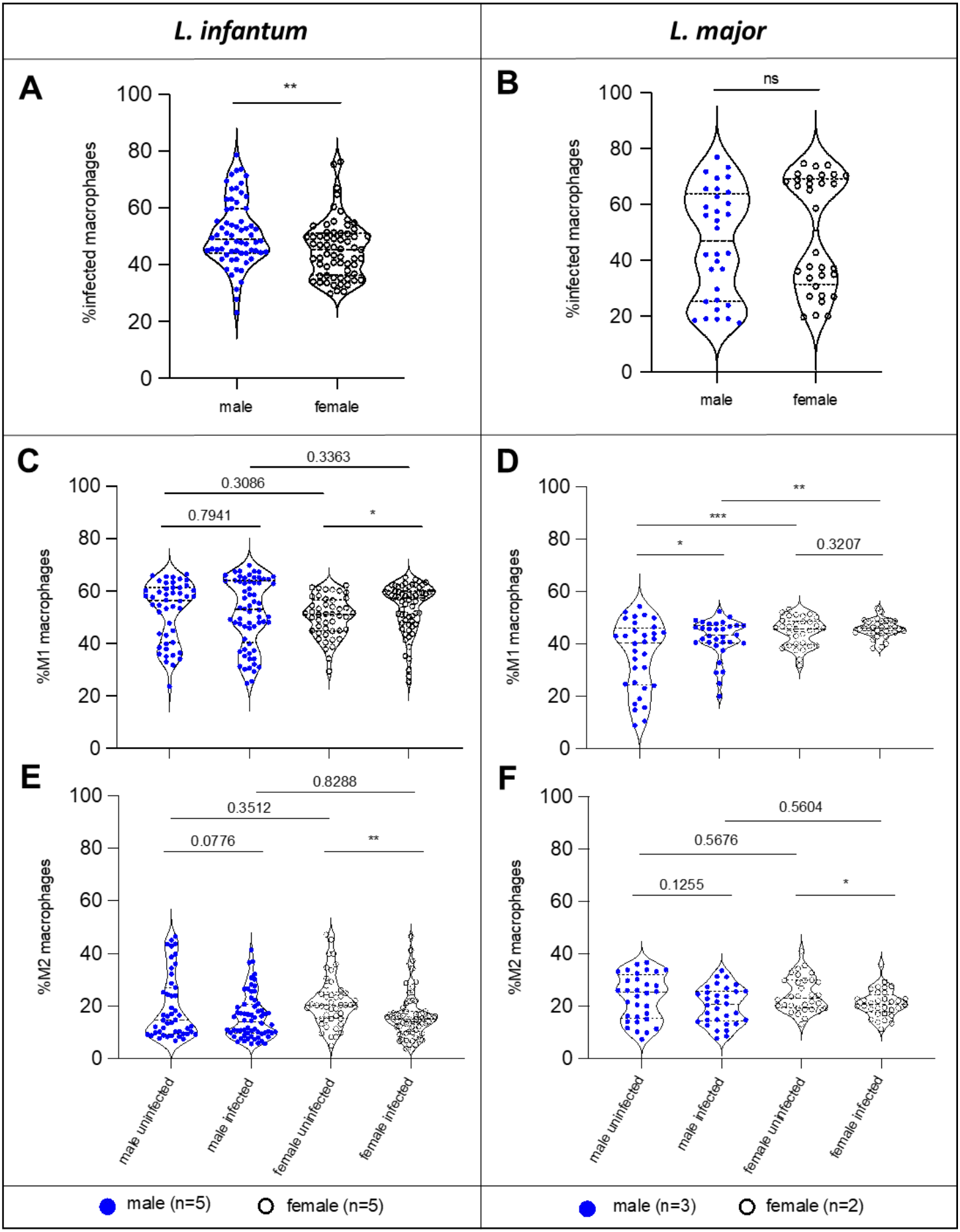
L. infantum
L. major
A
%infected macrophages
100
80
60
40
20
0
**
male
female
B
ns
male
female
C
%M1 macrophages
0.3363
0.3086
0.7941
*
D
**
***
*
0.3207
E
%M2 macrophages
0.8288
0.3512
0.0776
**
male uninfected
male infected
female uninfected
female infected
F
0.5604
0.5676
0.1255
*
male (n=5)
female (n=5)
male (n=3)
female (n=2)

Figure 3-6: Differences observed 72 h after *L. major* (left) and *L. infantum* (right) infection (MOI 15:1) of macrophages from seven male (L. infantum: m1, m2, m3, m4 & m5; L. major: m5, m6 & m7) and six female (L. infantum: f1, f2, f3, f4 & f5; L. major: f5 & f6) individuals. Immunofluorescent staining and image analysis with Harmony™ allowed for the evaluation of infected macrophages and macrophage phenotype as described in **2.3.1** and **2.3.2.1**. Shown here are the difference in infected macrophages (in %) of male and female individuals for *L. infantum* (A) and *L. major* (B) infection as well as the difference in M1 (C & D) and M2 (E & F) phenotype (in % of total macrophages) between uninfected and infected macrophages of male and female individuals in violin plots. Distribution of data points is represented by the body width of the violin plot. Median and standard deviation are represented by the centered and outer lines inside the violin body, respectively.

In *L. infantum* infection experiments significantly higher percentages of male macrophages were infected compared to female macrophages (**, p = 0,0044), while in *L. major* infection no significant difference was observed (ns, p = 0,4488). In *L. infantum* infection, both genders showed a rather stable infection of around 30-60 % of macrophages. In *L. major* infection a much higher scattering of the percent of infected macrophages could be observed. Around half of the infection experiments showed infection of around 20-40 % of macrophages, while the other half showed infection of around 60-80 %.

Following *L. infantum* infection, females showed a significant increase in macrophages with M1 phenotype (*, p = 0,0465) and a significant decrease in macrophages with M2 phenotype (**, p = 0,0032), while for males no significant differences in M1/M2 phenotype were observed, although a tendency toward reduction of M2 phenotype could be seen (**Figure 3-6 E**, p = 0,0776). In *L. major* infection, male macrophages showed a significant increase in M1 phenotype (*, p = 0,0237), but no difference in M2 phenotype (ns, p = 0,1255). Female macrophages showed no significant difference in M1 phenotype (ns, p = 0,3207) but a significant decrease in M2 phenotype (*, p = 0,0308).

When comparing male and female macrophage polarization response to *L. infantum* infection, no significant differences in M1/M2 state could be observed between the sexes. In *L. major* infection however, females showed significantly more macrophages with M1 phenotype in both uninfected and infected cells (uninfected: ***, p = 0,0008; infected: **, p = 0,0098).

3.3.1 Comparison of drug mono treatment strategies for Leishmania *infantum* and *Leishmania major* infection of hMDMs

To compare drug treatment efficiencies, *in vitro* cultures of hMDMs were infected with *Leishmania infantum* and *Leishmania major* in a MOI of 15:1 and treated with different concentrations of Amphotericin B, Miltefosine, Imiquimod and Eh-1 24 h.p.i. for a duration of 48 h. Amphotericin and Miltefosine are FDA approved leishmanicidal drugs for the treatment of human visceral Leishmaniasis (FDA 2014, FDA 2022). Imiquimod is an immune stimulant, that has shown effectiveness in topical application in cutaneous Leishmaniasis (Fuentes-Nava, Tirado-Sanchez et al. 2021). These drugs are used as references. Eh-1 is a promising drug candidate for immune stimulation therapy in Leishmaniasis, that is compared to its commercial counterparts ´(Fehling, Choy et al. 2020). Treatment effects were analyzed after immunofluorescence staining by confocal imaging with the Opera Phenix and subsequent image analysis with Harmony™ allowing for the visualization of cells and parasites. With the help of an analysis sequence, readouts were generated that allowed for the calculation of normalized drug screening parameters viability, infection rate and parasite burden.

To evaluate beneficial and cytotoxic treatment effects, viability, infection rate and parasite burden are compared between the different drugs and concentrations. Uninfected and infected untreated controls are used as references. The drug screening parameter viability is used to test for drug toxicity. It gives information about the number of alive macrophages compared to the negative control (infected untreated). A drug is considered toxic when it yields a viability of ≤ 50 POC. Leishmanicidal drug effects can be evaluated with infection rate and parasite burden. The infection rate compares the percentage of infected macrophages of wells with drug treatment with the infected untreated control. Drug efficacy on *Leishmania* infection can be seen by reduction in infection rate, while direct killing effects on *Leishmania* are displayed by the parasite burden, which represents the total number of *Leishmania* in a treated well compared to the infected untreated control. Analysis of infection rate and parasite burden of uninfected cells can give valuable information about image quality and success of image analysis sequence.

3.3.1.1 *L. infantum* infection

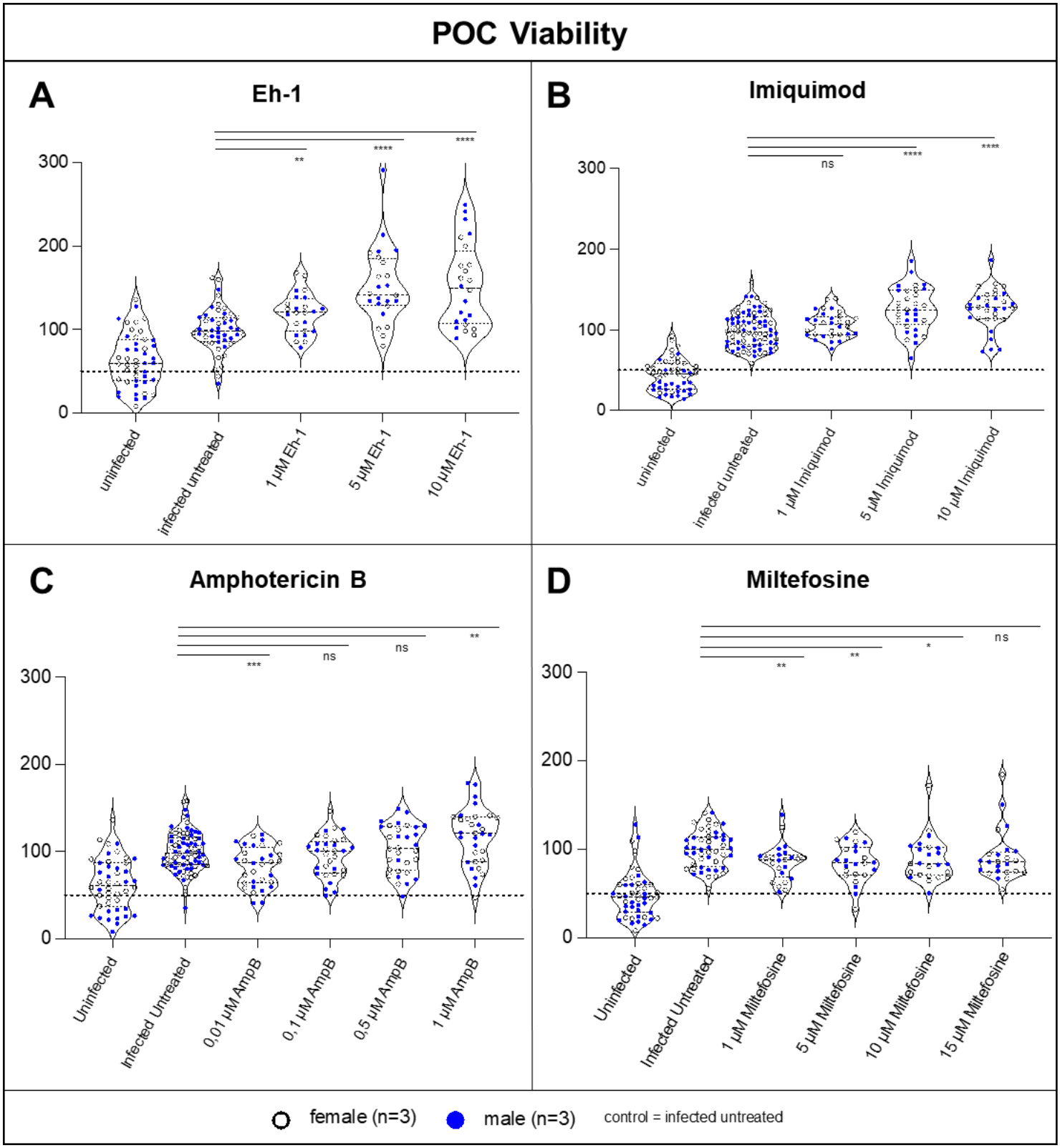

Figure 3-7: Viability of male and female macrophages 72 h after *L. infantum* infection and 48 h of mono-treatment with different drugs in percentage of infected untreated control (POC). 24 h after infection (MOI 15:1), Eh-1 (A), Imiquimod (B), Amphotericin B (C) and Miltefosine (D) were administered in the given concentrations in four technical replicates each. Immunofluorescent staining and image analysis with Harmony™ allowed for the evaluation of macrophage viability as explained in **2.3.1** and **2.3.2.1**. Macrophages were obtained from three male and three female individuals (Eh-1: m3, m4, m5, f3, f4, f5; Imiquimod: m1, m2, m5 (x2), f1, f2, f5 (x2); Amphotericin B: m1, m3, m5 (x2), f1, f3, f5 (x2);

Miltefosine: m2, m4, m5, f2, f4, f5) yielding a total biological sample size of n = 6. The dotted line represents 50 % of infected untreated cell viability, which is used as a threshold for drug toxicity. Drugs yielding a viability of ≤ 50 % are considered toxic. Shown here are uninfected control, infected untreated control (both with eight technical replicates per individual) and respective concentrations of immune stimulants (Eh-1, Imiquimod) or leishmanicidal drugs (Amphotericin B, Miltefosine) in violin plots. Distribution of data points is represented by the body width of the violin plot. Median and standard deviation are represented by the centered and outer lines inside the violin body, respectively.

Figure 3-7 A shows, that macrophages treated with Eh-1 had significantly higher viability compared to infected untreated cells (1 μM: **, p = 0,0035; 5 μM: ****, p < 0,0001; 10 μM: ****, p < 0,0001) in *L. infantum* infection. This effect increased with Eh-1 concentration.

Imiquimod treatment in a concentration of 5 μM or 10 μM also yielded a significantly higher viability compared to infected untreated cells (5 μM: ****, p < 0,0001; 10 μM: ****, p < 0,0001) as seen in **Figure 3-7 B**, while a concentration of 1 μM showed no effect (ns, p = 0,1496).

Amphotericin B treatment showed significant impairment of macrophage viability in a concentration of 0,01 μM (***, p = 0,0006), whereas a concentration of 1 μM increased macrophage viability significantly (**, p = 0,0026) (**Figure 3-7 C**). Concentrations of 0,1 μM and 0,5 μM showed no effect on viability (0,1 μM: ns, p = 0,3323; 0,5 μM: ns, p = 0,5581).

Application of Miltefosine in the concentrations of 1 μM, 5 μM and 10 μM showed a significant decrease in macrophage viability (1 μM: **, p = 0,0057; 5 μM: **, p = 0,0042; 10 μM: *, p = 0,0499), while 15 μM Miltefosine did not have the same effect (ns, p = 0,1719) (**Figure 3-7 D**).

Interestingly, uninfected macrophages generally showed a lower viability compared to infected macrophages with a high degree of variance. Single replicates of some drug concentrations crossed the toxicity threshold, but no drug showed a median that is lower than 50 POC.

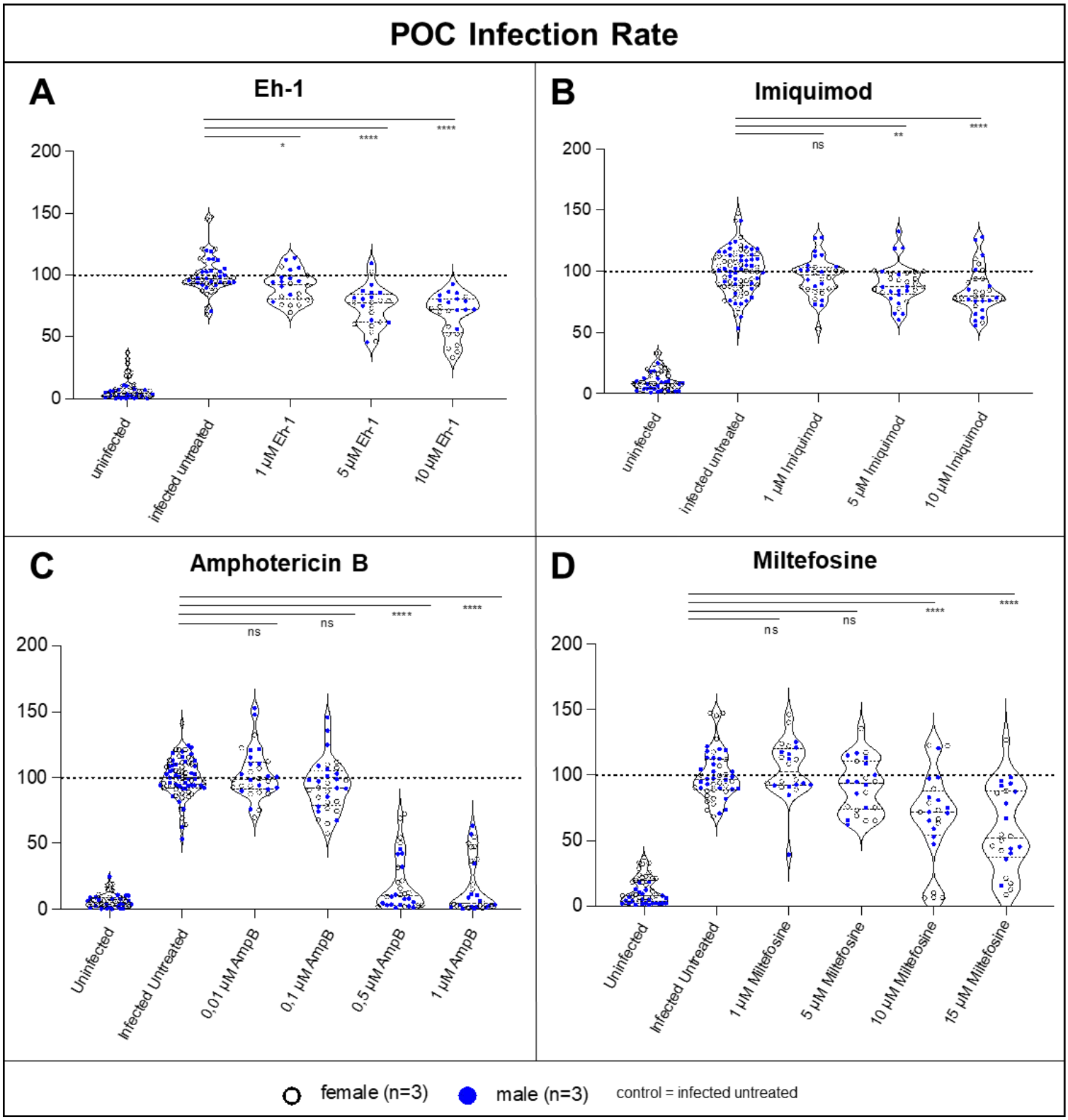

Figure 3-8: Infection rate of male and female macrophages 72 h after *L. infantum* infection and 48 h of drug mono-treatment in percentage of infected untreated control (POC). 24 h after infection (MOI 15:1), Eh-1 (A), Imiquimod (B), Amphotericin B (C) and Miltefosine (D) were administered in the given concentrations in four technical replicates each. Immunofluorescent staining and image analysis with Harmony™ allowed for the evaluation of macrophage infection rate as explained in **2.3.1** and **2.3.2.1**. Macrophages were obtained from three male and three female individuals (Eh-1: m3, m4, m5, f3, f4, f5; Imiquimod: m1, m2, m5 (x2), f1, f2, f5 (x2); Amphotericin B: m1, m3, m5 (x2), f1, f3, f5 (x2); Miltefosine: m2, m4, m5, f2, f4, f5) yielding a total biological sample size of n = 6. The dotted line represents the mean of infected untreated infection rate. Shown here are uninfected control, infected

untreated control (both with eight technical replicates per individual) and respective concentrations of immune stimulants (Eh-1, Imiquimod) or leishmanicidal drugs (Amphotericin B, Miltefosine) in violin plots. Distribution of data points is represented by the body width of the violin plot. Median and standard deviation are represented by the centered and outer lines inside the violin body, respectively.

In *L. infantum* infection, Eh-1 showed increasing reduction of macrophage infection rate with increasing concentration (1 μM: *, p = 0,0169; 5 μM: ****, p < 0,0001; 10 μM: ****, p < 0,0001) as seen in **Figure 3-8 A**. The infection rate was moderately decreased to a median of around 70 POC in the highest concentration. In female macrophages higher reduction of infection rate could be observed compared to male macrophages.

A significant, dose-dependent reduction of infection rate in Imiquimod treatment could only be observed in concentrations of 5 μM and 10 μM (5 μM: **, p = 0,0040; 10 μM: ****, p < 0,0001), while treatment with 1 μM Imiquimod had no effect on infection rate (ns, p = 0,1536) (**Figure 3-8 B**). The infection rate dropped to a similar median value of around 70 POC in the highest Imiquimod concentration as observed in Eh-1 treatment.

For Amphotericin B treatment, a sudden drop of infection rate could be observed at the concentration of 0,5 μM (**Figure 3-8 C**). This and the higher concentration of 1 μM showed very low infection rates around 5 - 20 POC in their median (0,5 μM: ****, p < 0,0001; 1 μM: ****, p < 0,0001).

Miltefosine treatment showed a dose-depended decrease of infection rate with high amount of variation in the data. A significant decrease was observed for concentrations of 10 μM and 15 μM (10 μM: ****, p < 0,0001; 15 μM: ****, p < 0,0001) with medians of around 60 POC and 50 POC, respectively (**Figure 3-8 D**). Interestingly, a tendency towards stronger reduction of infection rate could be observed for female macrophages compared to male macrophages.

Uninfected cells generally showed very low infection rates (around 0 - 15 POC), but still some instances of POC around 30-40 could be found. Interestingly, treatments showed varying efficacy depending on drug and individual. For example, in Miltefosine treatment a female individual showed reduction up to around 10 POC, while a male individual showed only a minor reduction to around 90 POC.

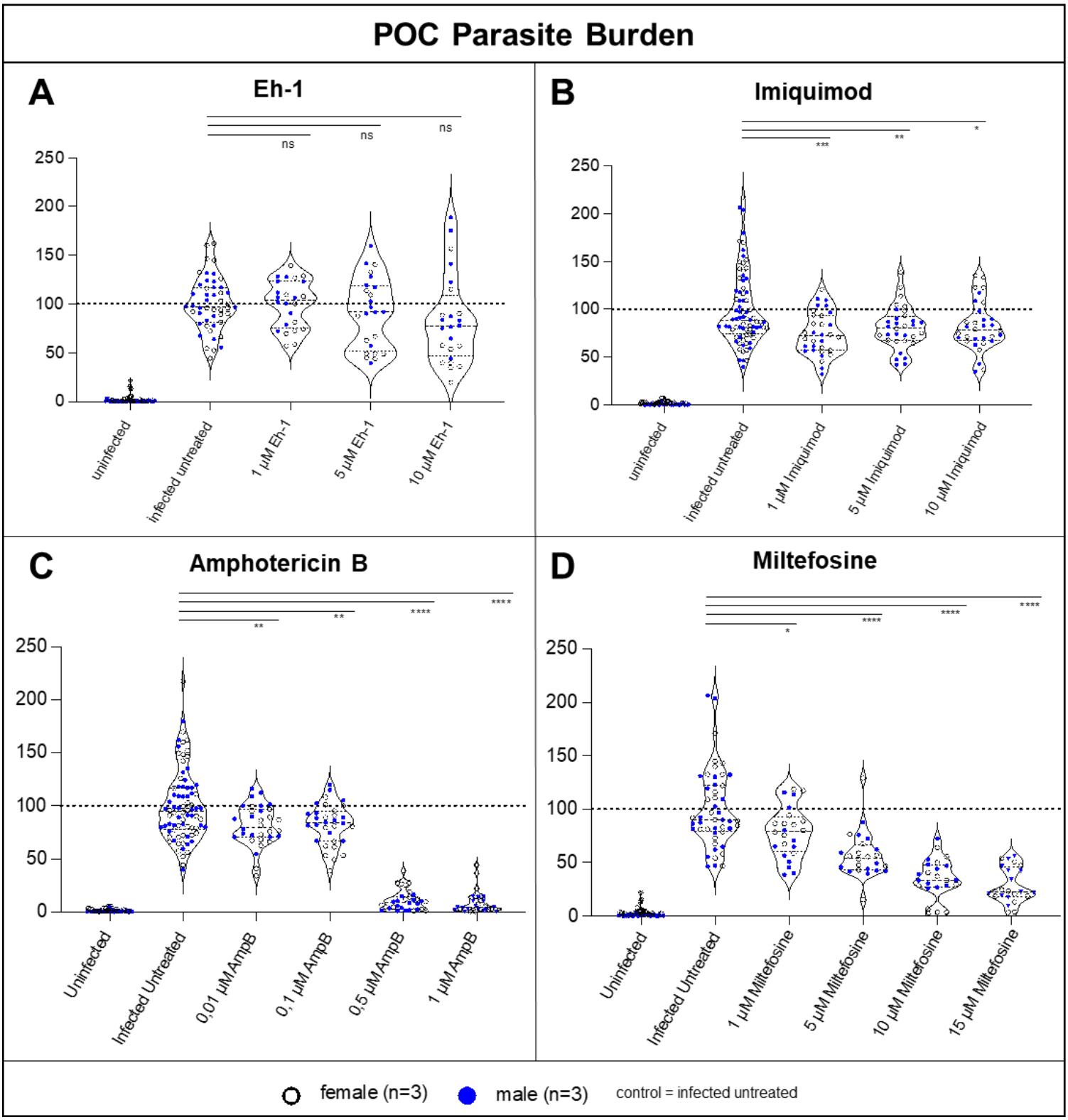

Figure 3-9: Parasite burden of male and female macrophages 72 h after *L. infantum* infection and 48 h of drug mono-treatment in percentage of infected untreated control (POC). 24 h after infection (MOI 15:1), Eh-1 (A), Imiquimod (B), Amphotericin B (C) and Miltefosine (D) were administered in the given concentrations in four technical replicates each. Immunofluorescent staining and image analysis with Harmony™ allowed for the evaluation of macrophage parasite burden as explained in **2.3.1** and **2.3.2.1**. Macrophages were obtained from three male and three female individuals (Eh-1: m3, m4, m5, f3, f4, f5; Imiquimod: m1, m2, m5 (x2), f1, f2, f5 (x2); Amphotericin B: m1, m3, m5 (x2), f1, f3, f5 (x2); Miltefosine: m2, m4, m5, f2, f4, f5) yielding a total biological sample size of n = 6. The dotted line represents the mean of infected untreated parasite burden. Shown here are uninfected control, infected

untreated control (both with eight technical replicates per individual) and respective concentrations of immune stimulants (Eh-1, Imiquimod) or leishmanicidal drugs (Amphotericin B, Miltefosine) in violin plots. Distribution of data points is represented by the body width of the violin plot. Median and standard deviation are represented by the centered and outer lines inside the violin body, respectively.

Eh-1 treatment of *L. infantum* infection showed indistinct effects on the parasite burden. In some instances, Eh-1 increased parasite burden and in others a reduction of parasite burden was observed (**Figure 3-9 A**). It is important to note, that next to Eh-1 treated macrophages also infected untreated cells showed a high variance of parasite burden. In a concentration of 10 μM, parasite burden was reduced to a mean of around 80 POC without statistical significance (ns, p = 0,0625).

Treatment with Imiquimod led to significant reduction of parasite burden (**Figure 3-9 B**). For 1 μM Imiquimod, parasite burden was decreased to around 70 POC (***, p = 0,0007). Both 5 μM and 10 μM Imiquimod showed a parasite burden of around 80 POC with lower statistical significance (5 μM: **, p = 0,0091; 10 μM: *, p = 0,0193).

Amphotericin B treatment showed similar results in parasite burden as in infection rate. Both are reduced significantly to around 0 - 20 POC in a concentration of 0,5 μM and 1 μM (0,5 μM: ****, p < 0,0001; 1 μM: ****, p < 0,0001), but also in concentrations of 0,01 μM and 0,1 μM a reduction of parasite burden to around 70 - 80 POC could be observed (0,01 μM: **, p = 0,0038; 0,1 μM: **, p = 0,0067 (**Figure 3-9 C**).

Upon treatment with Miltefosine a significant, dose-depended decrease of parasite burden could be observed. It dropped to around 80 POC with 1 μM, around 55 POC with 5 μM, 35 POC with 10 μM and 20 POC with 15 μM Miltefosine addition (1 μM: *, p = 0,0106; 5 μM: ****, p < 0,0001; 10 μM: ****, p < 0,0001; 15 μM: ****, p < 0,0001) (**Figure 3-9 D**).

Generally, uninfected cells showed little to no parasite burden.

3.3.1.2 *L. major* infection

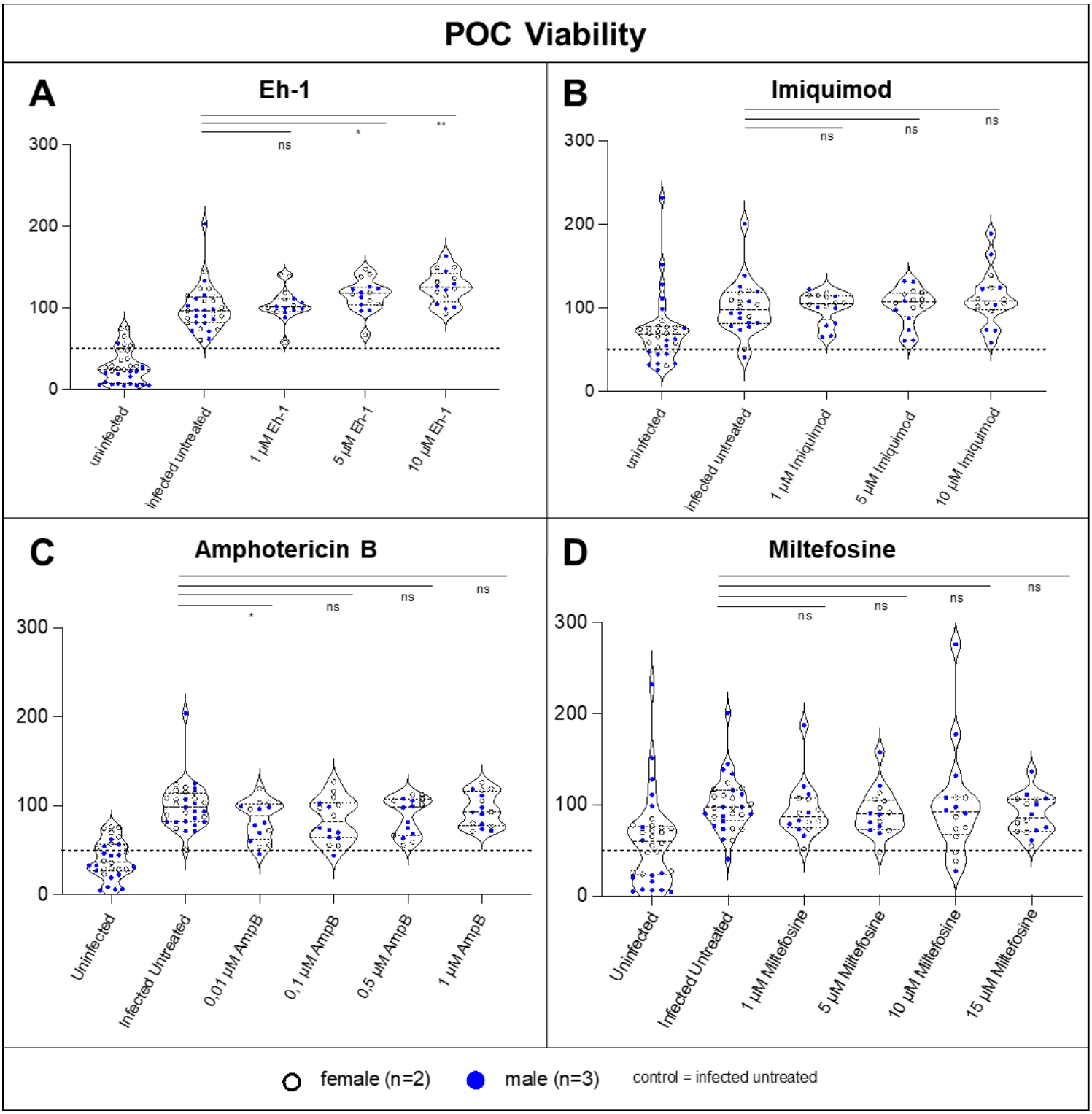

Figure 3-10: Viability of male and female macrophages 72 h after *L. major* infection and 48 h of drug mono-treatment in percentage of infected untreated control (POC). 24 h after infection (MOI 15:1), Eh-1 (A), Imiquimod (B), Amphotericin B (C) and Miltefosine (D) were administered in the given concentrations in four technical replicates each. Immunofluorescent staining and image analysis with Harmony™ allowed for the evaluation of macrophage viability as explained in **2.3.1** and **2.3.2.1**. Macrophages were obtained from three male and two female individuals (Eh-1: m5 (x2), f5 (x2); Imiquimod: m6, m7, f6 (x2); Amphotericin B: m5, m7, f5, f6; Miltefosine: m5, m6, f5, f6) yielding a total biological sample size of n = 5. The dotted line represents 50 % of infected untreated cell viability, which is used as a threshold for drug toxicity. Drugs yielding a viability of ≤ 50 % are considered toxic. Shown here are uninfected control, infected untreated control (both with eight technical replicates per individual)

and respective concentrations of immune stimulants (Eh-1, Imiquimod) or leishmanicidal drugs (Amphotericin B, Miltefosine) in violin plots. Distribution of data points is represented by the body width of the violin plot. Median and standard deviation are represented by the centered and outer lines inside the violin body, respectively.

Similar to the observations during treatment of *L. infantum* infection, during *L. major* infection Eh-1 significantly enhanced cell viability to around 120 POC in concentrations of 5 μM and 10 μM (5 μM: *, p = 0,0485; 10 μM: **, p = 0,0017), although no significant increase of viability could be seen for 1 μM Eh-1 (**Figure 3-10 A**).

Imiquimod treatment yielded no significant increase in macrophage viability, although small increases of viability median could be observed in all concentrations (**Figure 3-10 B**).

Compared to infected untreated macrophages a minor decrease in viability could be observed during treatment with 0,01 μM Amphotericin B (*, p = 0,0409) as seen in **Figure 3-10 C**. In a concentration of 0,1 μM the mean of cell viability was even lower, but without statistical significance (ns, p = 0,0515). This effect could not be observed in Amphotericin B concentrations of 0,5 μM and 1 μM.

Miltefosine treatment in a concentration of 1 μM led to a small decrease of viability median without statistical significance (ns, p = 0,5067) (**Figure 3-10 D**). This could not be found in higher concentrations.

Uninfected cells, as seen in *L. infantum* infection, showed a lower viability than infected cells with a high amount of variance in the data. Generally, single data points crossed the toxicity threshold, but no drug showed a median that is lower than 50 POC.

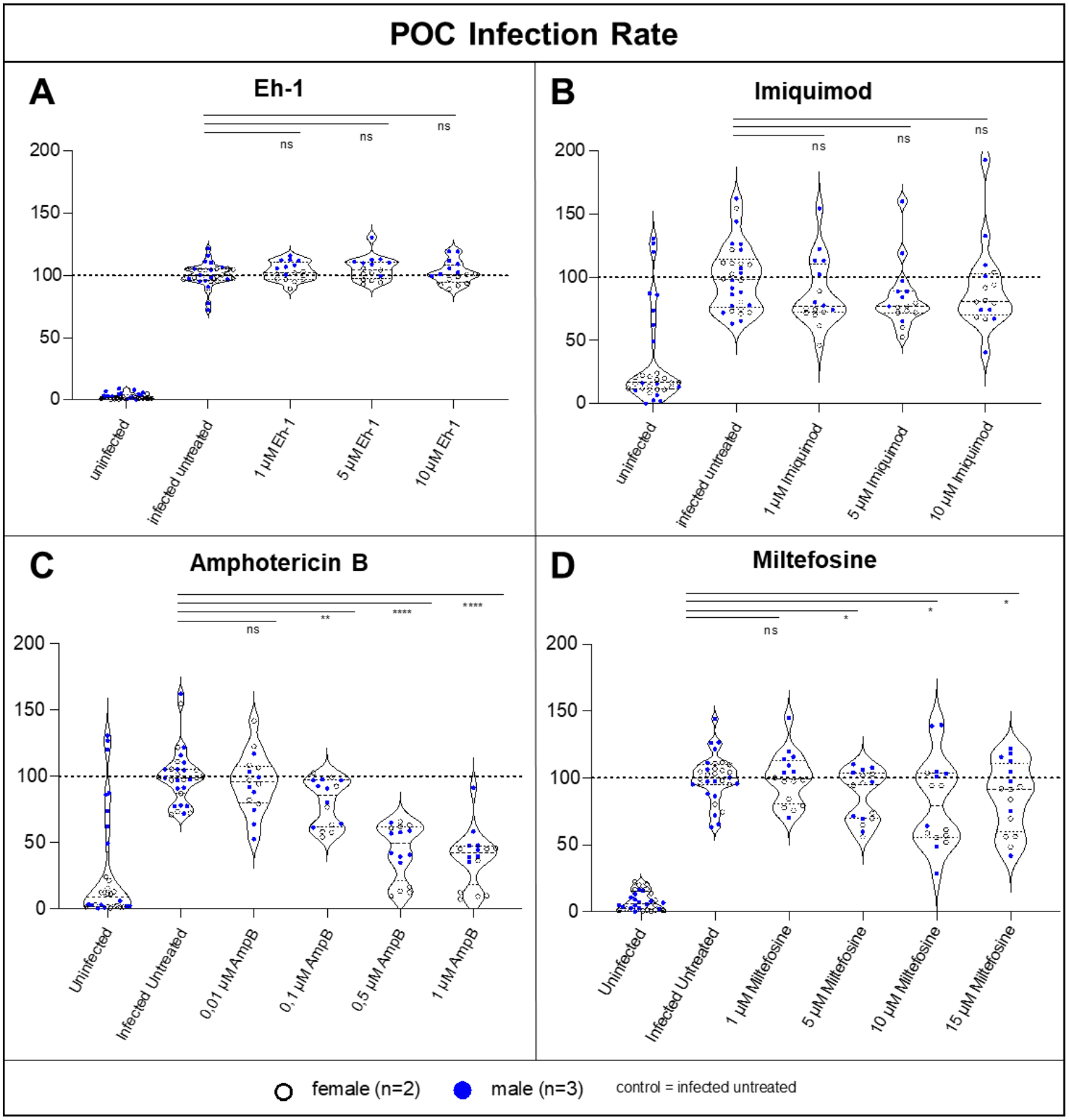

Figure 3-11: Infection rate of male and female macrophages 72 h after *L. major* infection and 48 h of drug mono-treatment in percentage of infected untreated control (POC). 24 h after infection (MOI 15:1), Eh-1 (A), Imiquimod (B), Amphotericin B (C) and Miltefosine (D) were administered in the given concentrations in four technical replicates each. Immunofluorescent staining and image analysis with Harmony™ allowed for the evaluation of macrophage infection rate as explained in **2.3.1** and **2.3.2.1**. Macrophages were obtained from three male and two female individuals (Eh-1: m5 (x2), f5 (x2); Imiquimod: m6, m7, f6 (x2); Amphotericin B: m5, m7, f5, f6; Miltefosine: m5, m6, f5, f6) yielding a total biological sample size of n = 5. The dotted line represents the mean of infected untreated infection rate. Shown here are uninfected control, infected untreated control (both with eight technical replicates per

individual) and respective concentrations of immune stimulants (Eh-1, Imiquimod) or leishmanicidal drugs (Amphotericin B, Miltefosine) in violin plots. Distribution of data points is represented by the body width of the violin plot. Median and standard deviation are represented by the centered and outer lines inside the violin body, respectively.

Conversely to *L. infantum* infection, in *L. major* infection Eh-1 treatment showed no effect on macrophage infection rate (**Figure 3-11 A**).

Imiquimod treatment of *L. major* infection showed a reduction of infection rate median to around 80 POC, but without statistical significance (**Figure 3-11 B**) (1 μM: ns, p = 0,1311;5 μM: ns, p = 0,0515; 10 μM: ns, p = 0,3332). High variance of data points could be observed and uninfected cells showed rather high infection rate (around 20-30 POC) with one male individual (m7) displaying exceptionally high infection rates.

Samples of the same male individual also showed high infection rates in uninfected cells of Amphotericin B treatments (**Figure 3-11 C**). Next to this, most samples of uninfected macrophages showed low infection rates of 0-15 POC. Application of Amphotericin B led to significant decrease of infection rate in the concentrations of 0,1 μM, 0,5 μM and 1 μM (0,1 μM: **, p = 0,0026; 0,5 μM: ****, p < 0,0001; 1 μM: ****, p < 0,0001). For 0,01 μM Amphotericin B only a minor decrease of infection rate median could be observed. The reduction of infection rate to around 45 - 50 POC in high concentrations of Amphotericin B seen in *L. major* infection is less strong than the effect observed in *L. infantum* infection (reduction to around 5 - 20 POC).

Miltefosine treatment leads to significant infection rate for concentrations of 5 μM, 10 μM and 15 μM (5 μM: *, p = 0,0206; 10 μM: *, p = 0,0156; 15 μM: *, p = 0,0359) (**Figure 3-11 D**).

Interestingly, it can be observed that in some individuals high reduction of infection rate to around 50 POC at higher concentrations is achieved, while some individuals show no reduction at all leading to high variance of data.

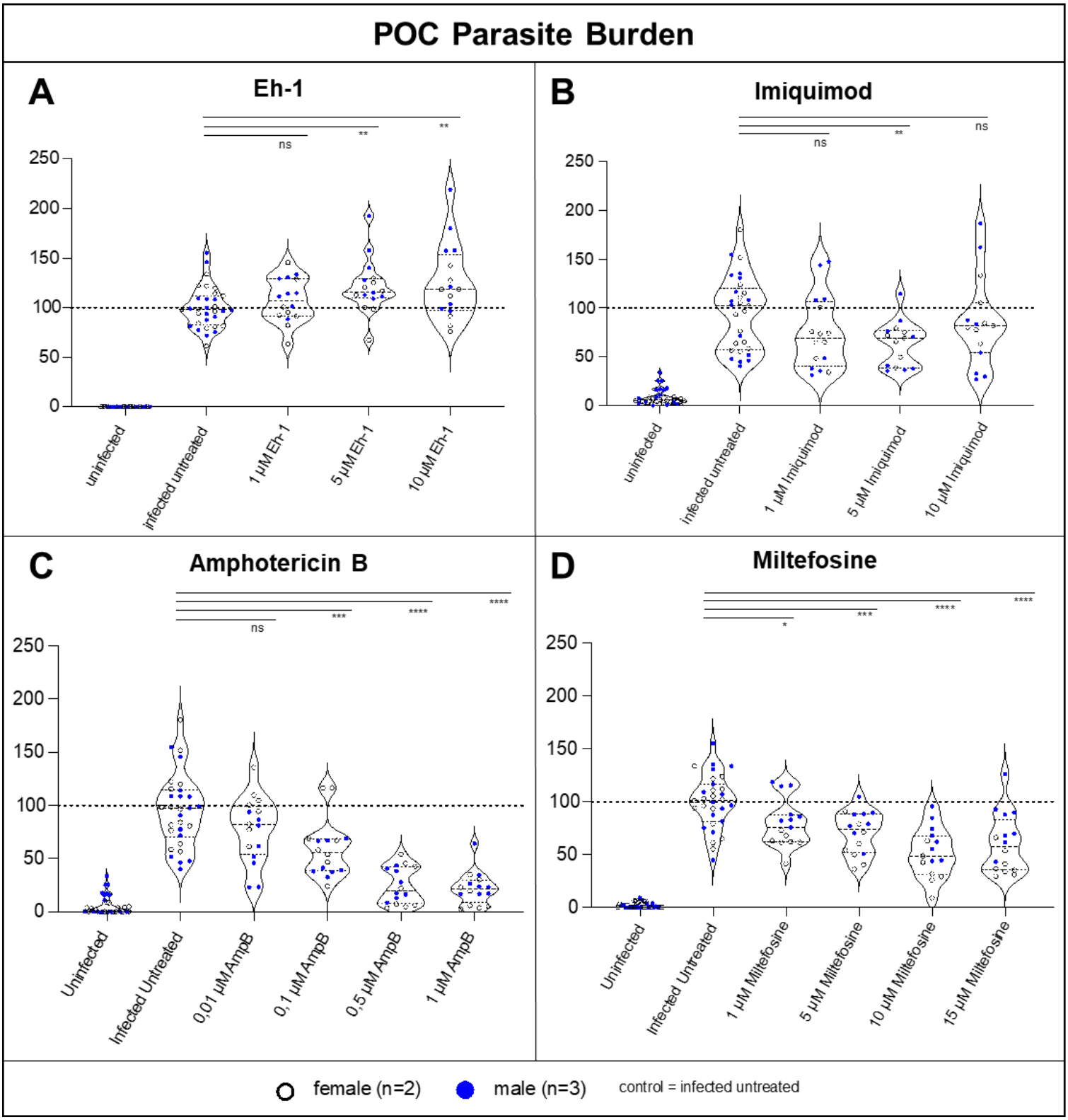

Figure 3-12: Parasite burden of male and female macrophages 72 h after *L. major* infection and 48 h of drug mono-treatment in percentage of infected untreated control (POC). 24 h after infection (MOI 15:1), Eh-1 (A), Imiquimod (B), Amphotericin B (C) and Miltefosine (D) were administered in the given concentrations in four technical replicates each. Immunofluorescent staining and image analysis with Harmony™ allowed for the evaluation of macrophage parasite burden as explained in **2.3.1** and **2.3.2.1**. Macrophages were obtained from three male and two female individuals (Eh-1: m5 (x2), f5 (x2); Imiquimod: m6, m7, f6 (x2); Amphotericin B: m5, m7, f5, f6; Miltefosine: m5, m6, f5, f6) yielding a total biological sample size of n = 5. The dotted line represents the mean of infected untreated parasite burden. Shown here are uninfected control, infected untreated control (both with eight technical replicates per individual) and respective concentrations of immune stimulants (Eh-1, Imiquimod) or

leishmanicidal drugs (Amphotericin B, Miltefosine) in violin plots. Distribution of data points is represented by the body width of the violin plot. Median and standard deviation are represented by the centered and outer lines inside the violin body, respectively.

Treatment of *L. major* infection with Eh-1 showed a significant increase in parasite burden in concentrations of 5 μM and 10 μM (5 μM: **, p = 0,0048; 10 μM: **, p = 0,0049) to around 120 POC (**Figure 3-12 A**).

In experiments with Imiquimod, data shows high variance and *Leishmania* could be detected in some uninfected cells, but especially in those from one male individual (m7). Otherwise, Imiquimod showed reduction of parasite burden to a median of around 70 POC in all concentrations, but only the concentration of 5 μM showed statistical significance (**, p = 0,0053) (**Figure 3-12 B**).

In Amphotericin B treatment, again in uninfected cells, high parasite burden could be detected in samples from male m7, while the other uninfected samples showed little to no parasites. Treatment of *L. major* infection with Amphotericin B showed a significant, dose-depended decrease of parasite burden with a median POC of 20 - 25 in higher concentrations (0,1 μM: ***, p = 0,0007; 0,5 μM: ****, p < 0,0001; 1 μM: ****, p < 0,0001) (**Figure 3-12 C**).

Miltefosine reduced parasite burden significantly in every concentration (1 μM: *, p = 0,0118; 5 μM: ***, p = 0,0002; 10 μM: ****, p < 0,0001; 15 μM: ****, p < 0,0001) up to a median parasite burden of around 50 POC in higher concentrations (**Figure 3-12 D**).

3.3.1.3 Treatment response

During evaluation of drug mono treatments, high variance of treatment efficacy could be observed for different individuals. Thus, treatment response of each individual to the respective drugs was evaluated creating the classifications “Responder” and “Non-Responder” for each parasite and drug. A responder is characterized by a significant reduction ($p \leq 0,05$) in infection rate compared to infected untreated control of the same individual following treatment with any concentration of a drug. In some cases, an individual showed a response to a treatment with minor statistical significance in one experiment, while in another experiment with the same treatment no response was found. These cases were classified as “Weak Responder”.

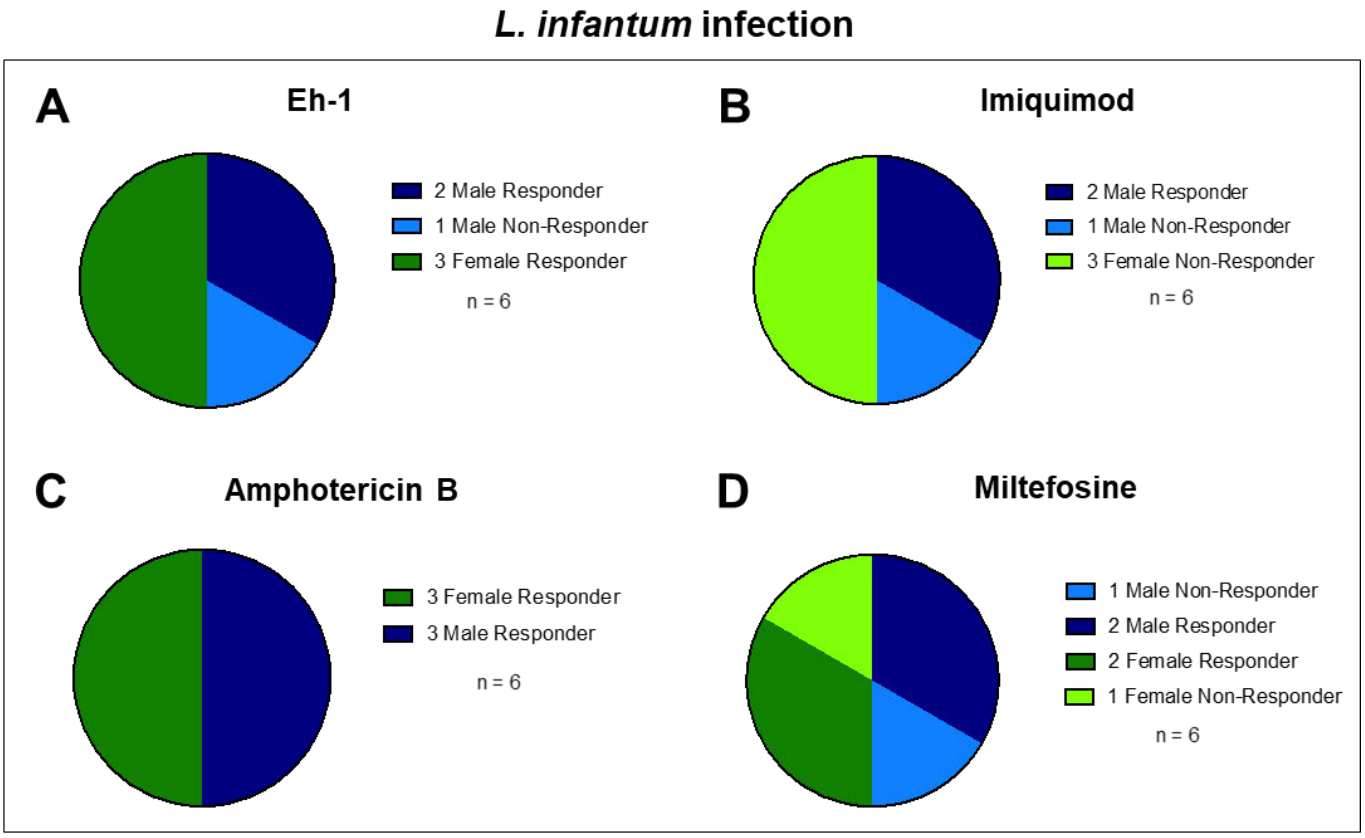

Figure 3-13: Treatment response in in the context of *L. infantum* infection. 24 h after parasite infection (MOI 15:1), macrophages of male and female individuals were treated for 48 h with either Eh-1 (A), Imiquimod (B), Amphotericin B (C) or Miltefosine (D) in the concentrations seen in **Figure 3-8**. Immunofluorescent staining and image analysis with Harmony™ allowed for the evaluation of macrophage infection rate as explained in **2.2.4.3** and **2.3.1**. A treatment response is defined by a significant decrease ($p \leq 0,05$) in macrophage infection rate at any drug concentration compared to infected untreated control of the same individual.

For Eh-1 treatment of *L. infantum* infection, two (m3 & m5) out of three (m3, m4 & m5) males and all three females (f3, f4 & f5) showed a response (**Figure 3-13 A**). Treatment of *L. infantum* infection with Imiquimod yielded a response in two (m2 & m5) out of three (m1, m2 & m5) males and no response in three females (f1, f2 & f5) (**Figure 3-13 B**). All three males (m1, m3 & m5) and females (f1, f3 & f5) responded to Amphotericin B treatment (**Figure 3-13 C**) while only two (m2 & m5, f2 & f4) out of three (m2, m4 & m5, f2, f4 & f5) males and females showed a response to Miltefosine treatment in *L. infantum* infection (**Figure 3-13 D**).

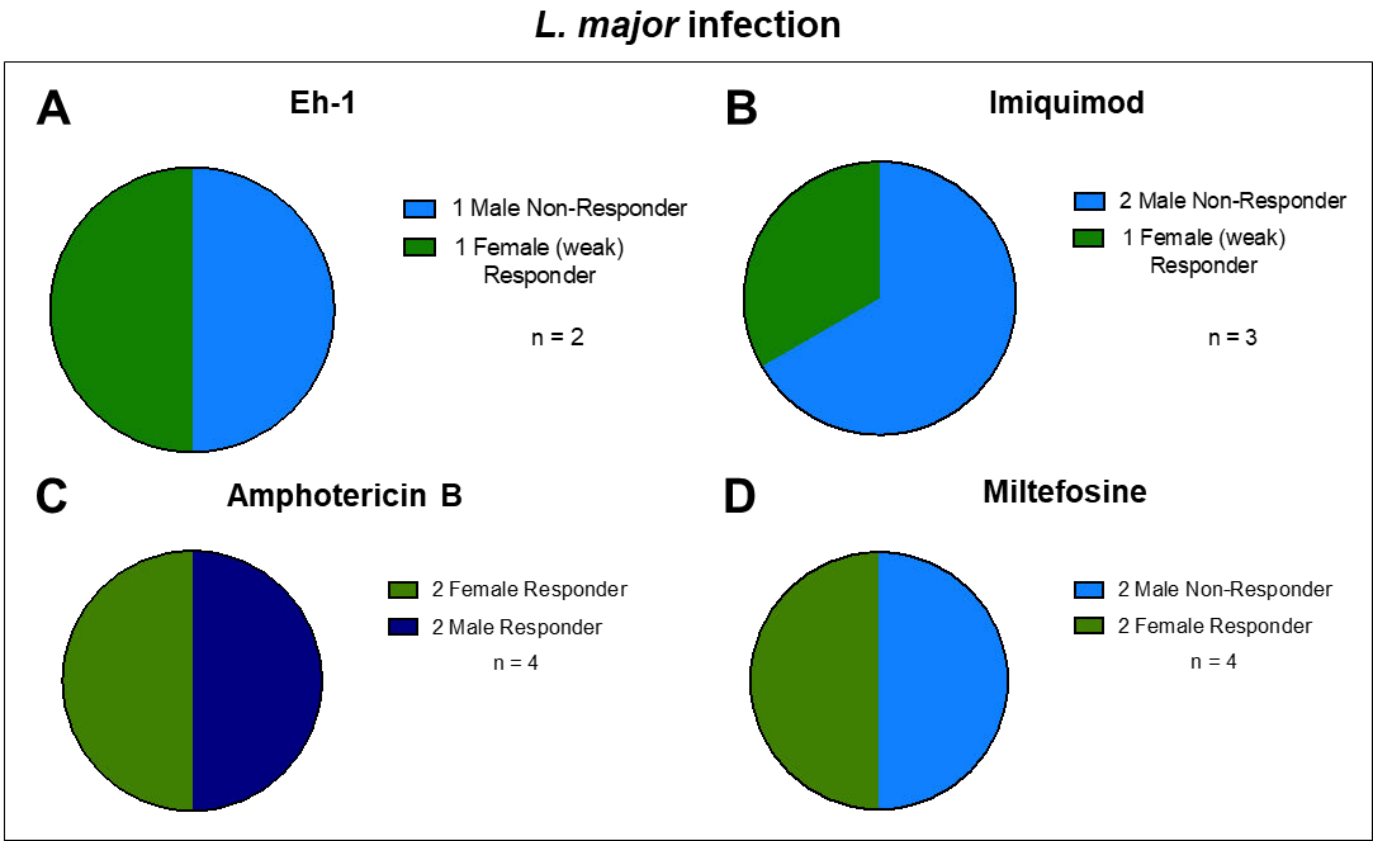

Figure 3-14: Treatment response in in the context of *L. major* infection. 24 h after parasite infection (MOI 15:1), macrophages of male and female individuals were treated for 48 h with either Eh-1 (A), Imiquimod (B), Amphotericin B (C) or Miltefosine (D) in the concentrations seen in **Figure 3-8**. Immunofluorescent staining and image analysis with Harmony™ allowed for the evaluation of macrophage infection rate as explained in **2.2.4.3** and **2.3.1**. A treatment response is defined by a significant decrease ($p \leq 0,05$) in macrophage infection rate at any drug concentration compared to infected untreated control of the same individual.

For Eh-1 treatment of *L. major* infection, one female (f5) showed a weak response while one male individual (m5) showed no response (**Figure 3-14 A**). Treatment of *L. major* infection with Imiquimod yielded a weak response in one female (f6) and no response in two males (m6 & m7) (**Figure 3-14 B**). Both males (m5 & m7) and females

(f5 & f6) responded to Amphotericin B treatment (**Figure 3-14 C**) while only female (f5 & f6) and no male individuals (m5 & m6) showed a response to Miltefosine treatment in *L. major* infection (**Figure 3-14 D**).

3.3.2 Analyzing the potential of drug combination treatment strategies for *L. infantum* and *L. major* infection of hMDMs

In recent years *Leishmania* parasites have become increasingly resistant to common treatment strategies increasing the need for alternative treatment strategies (Mann, Frasca et al. 2021). One possibility is to combine different drug treatments in combination therapy to increase effectiveness and circumvent resistance (Ahmed, Curtis et al. 2020). To investigate if drug combination treatment of *Leishmaniasis* with FDA approved leishmanicidal drugs, and immune stimulatory molecules could be an alternative to mono treatments, their combined effect was tested on hMDMs in an *in vitro* setting. Moreover, results from male and female individuals were compared to investigate sex differences in treatment response and infection.

As described in **3.3.1**, evaluation of the normalized drug screening parameters viability, infection rate and parasite burden allow for the analysis of beneficial or cytotoxic treatment effects. Additionally, M1/M2 macrophage state was assessed phenotypically by image analysis as described in **2.3.1** to characterize treatment effects on macrophage polarization.

3.3.2.1 Assessment of beneficial and cytotoxic effects of drug combination treatment by drug screening parameters

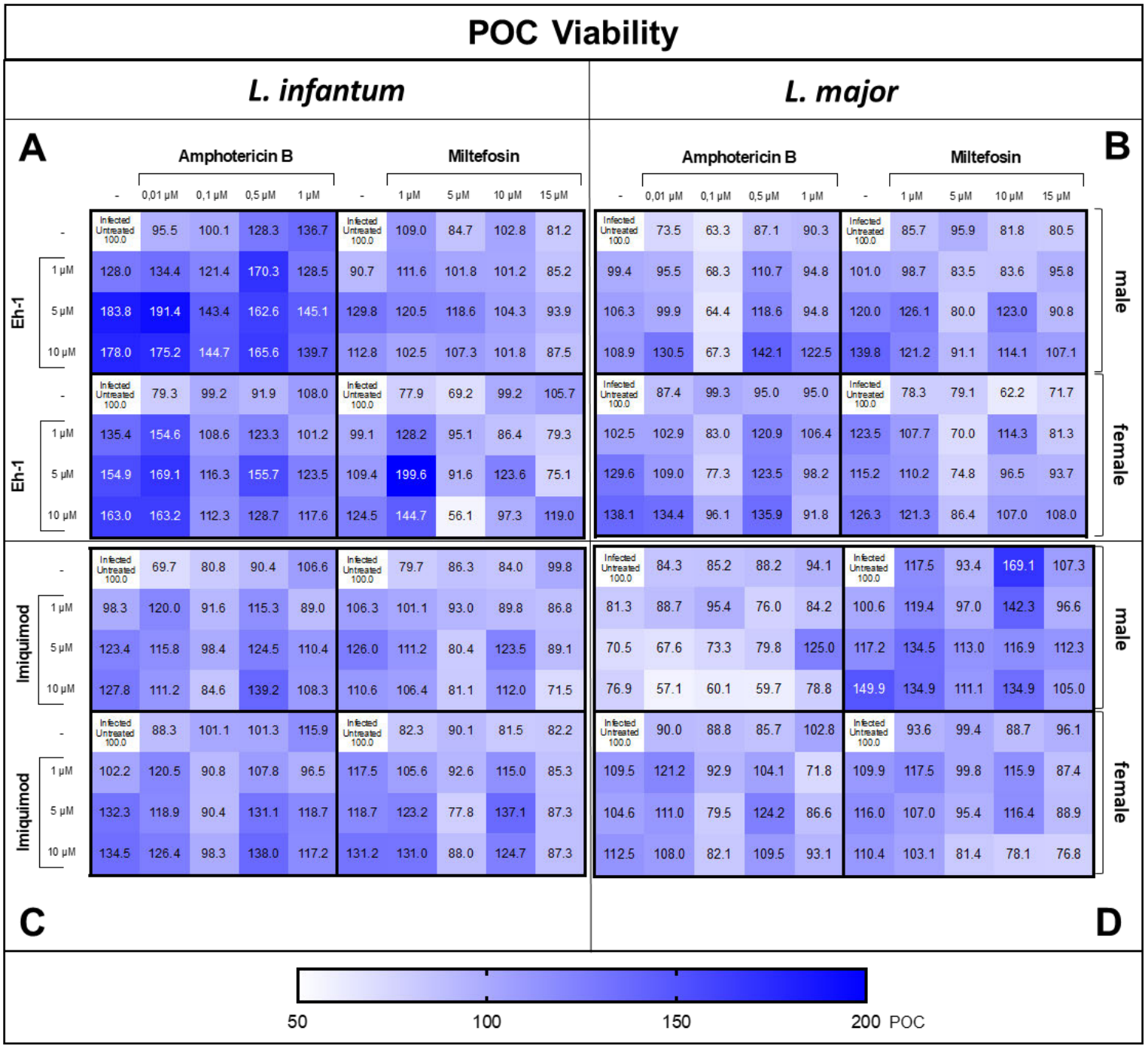

Figure 3-15: Heat map of male and female macrophage viability in percentage of infected untreated control (POC) 72 h after *L. infantum* (A & C) and *L. major* (B & D) infection (MOI 15:1) and treatment with leishmanicidal drugs (Amphotericin B & Miltefosine) in combination with either Eh-1 (A & B) or Imiquimod (C & D). Drug combinations were administered 24 h after parasite infection in the given concentrations for 48 h in four technical replicates. Here the mean is shown. For Amphotericin B + Eh-1, Amphotericin B + Imiquimod and Miltefosine + Imiquimod combinations in *L. infantum* infection, macrophages from two male and two female individuals were used (Amphotericin B + Eh-1: m3 & m5, f3 & f5; Amphotericin B + Imiquimod: m1 & m5, f1 & f5; Miltefosine + Imiquimod: m2 & m5, f2 & f5), while only one individual of each gender was used for Miltefosine + Eh-1 combination (m4 & f4). In *L. major* infection, for each drug combination macrophages from one male and one female

individual were used (Amphotericin B + Eh-1: m5, f5; Amphotericin B + Imiquimod: m7, f6; Miltefosine + Eh-1: m5, f5; Miltefosine + Imiquimod: m6, f6). Immunofluorescent staining and image analysis with Harmony™ allowed for the evaluation of macrophage viability as explained in **2.3.1** and **2.3.2.1**. Drug combinations yielding a viability of ≤ 50 % are considered toxic.

For the statistical analysis during combination treatment, drug mono treatments were taken into consideration. If a drug showed an effect (also non-significant increase/decrease) on infection rate during mono treatment, combination treatment effect was tested against the effect of the respective drug in the respective mono treatment concentration. Results are shown in **Figure 3-16**, **Figure 3-18** and **Figure 3-20**. For an overview of p-values s. **6.2**.

Generally, no drug mono or combination treatment crossed the toxicity threshold of 50 POC.

Amphotericin B mono treatment often showed an impairment of macrophage viability in low concentrations (low statistical significance, **Figure 3-16**), but not in higher concentration for both male and female individuals in *L. infantum* and *L. major* infection (**Figure 3-15**). During Amphotericin B treatment of male macrophages after *L. infantum* infection, for two individuals (m3 and m5) a significant increase in cell viability could be observed in higher concentrations (**Figure 3-15 A**, **Figure 3-16 A**).

As seen in **Figure 3-15**, for Miltefosine mono treatment often a reduced cell viability could be observed (low statistical significance, **Figure 3-16**).

In Imiquimod mono treatment a slight increase in macrophage viability could be observed for male and female individuals in *L. infantum* infection with high statistical significance (**Figure 3-15 left**, **Figure 3-16 left**). In *L. major* infection, this effect could also be observed, but with low statistical significance (**Figure 3-16**). In one individual (m7) Imiquimod treatment of *L. major* infection led to significant impairment of cell viability.

Eh-1 mono treatment shows an increase in viability for both female and male individuals in *L. infantum* and *L. major* infection with high statistical significance (**Figure 3-15**, **Figure 3-16**).

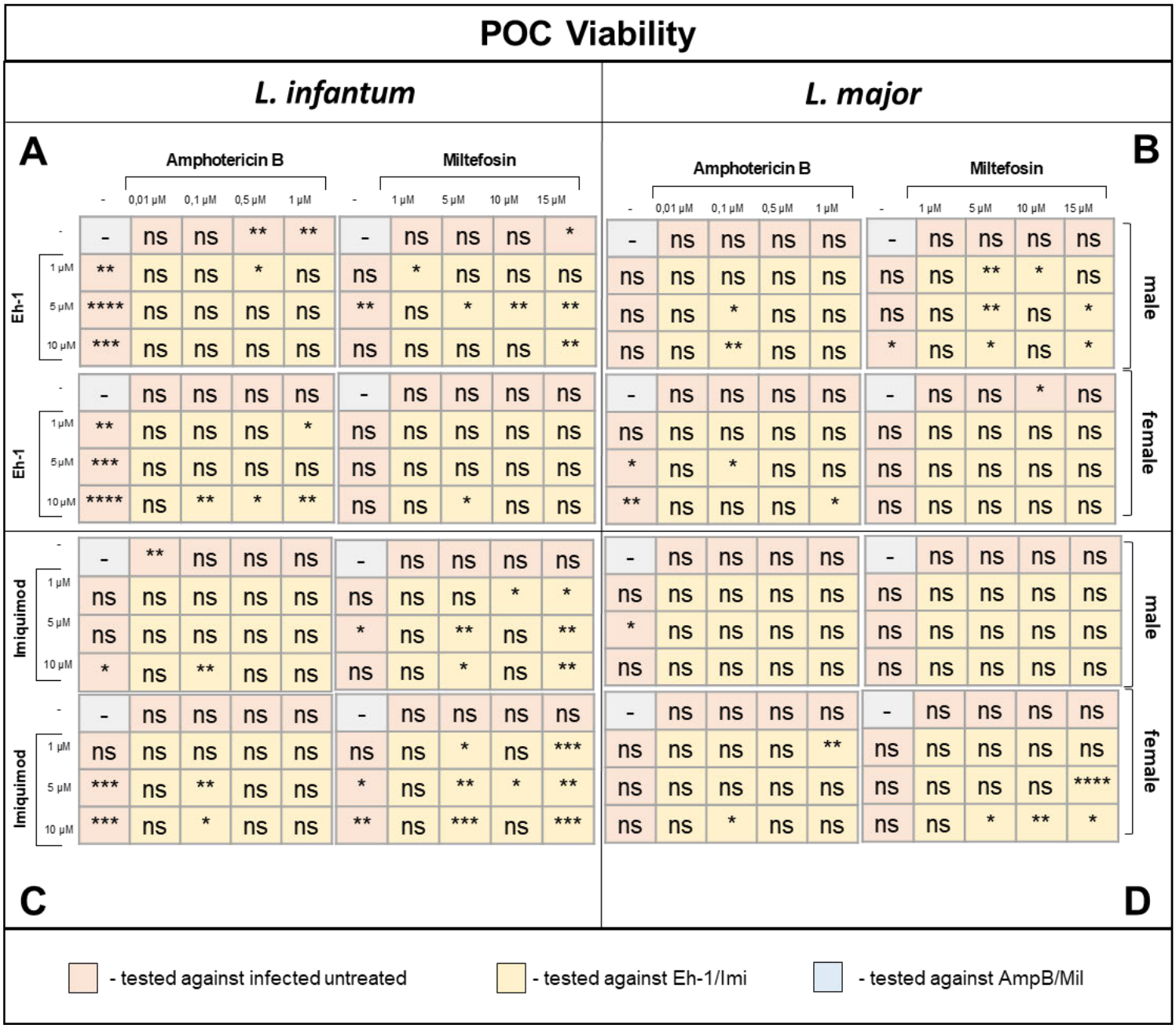

Figure 3-16: Overview of statistical significances of differences in viability after *L. infantum* (A & C) and *L. major* (B & D) infection (MOI 15:1) and treatment with leishmanicidal drugs (Amphotericin B & Miltefosine) in combination with either Eh-1 (A & B) or Imiquimod (C & D). Statistical significance was tested against either infected untreated cells, cells treated with only Eh-1 in the respective concentration or cells treated with only AmpB in the respective concentration with unpaired two-tailed t-tests. Significances are displayed as stars (ns: $p \geq 0,05$; *: $p \leq 0,05$; **: $p \leq 0,01$; ***: $p \leq 0,001$; ****: $p \leq 0,0001$)

Combination treatment of Amphotericin B or Miltefosine with Eh-1 or Imiquimod generally led to a decrease of the positive effect of immune response modifiers on viability observed during mono treatment (**Figure 3-15**), often with high statistical significance (**Figure 3-16**). This reduction was stronger for Miltefosine treatment than

for Amphotericin B treatment. No significant increase in viability could be seen compared to mono treatment with Eh-1 or Imiquimod.

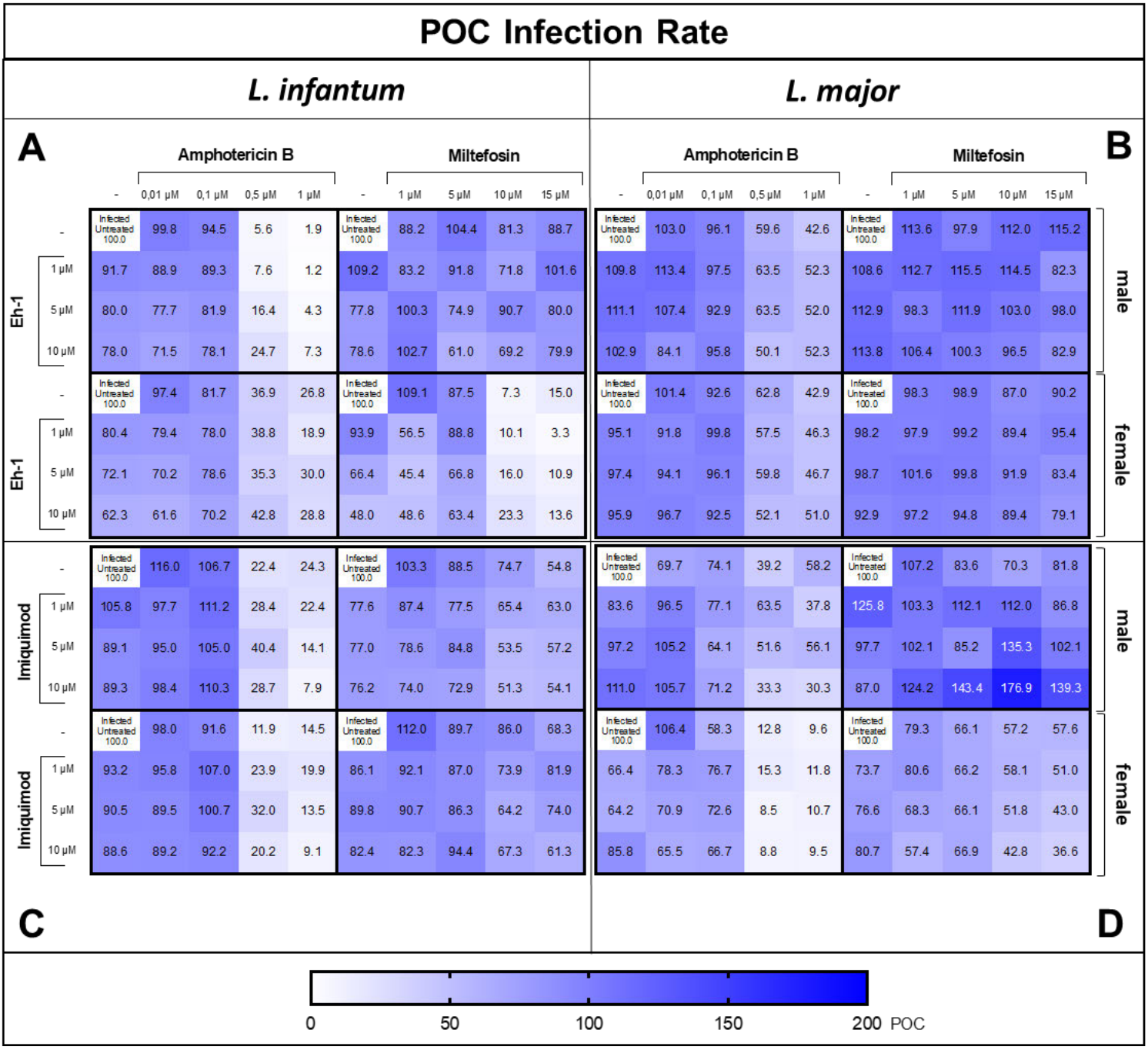

Figure 3-17: Heat map of male and female macrophage infection rate in percentage of infected untreated control (POC) 72 h after *L. infantum* (A & C) and *L. major* (B & D) infection (MOI 15:1) and treatment with leishmanicidal drugs (Amphotericin B & Miltefosine) in combination with either Eh-1 (A & B) or Imiquimod (C & D). Drug combinations were administered 24 h after parasite infection in the given concentrations for 48 h in four technical replicates. For Amphotericin B & Eh-1, Amphotericin B & Imiquimod and Miltefosine & Imiquimod combinations in *L. infantum* infection, macrophages from two male and two female individuals were used (Amphotericin B + Eh-1: m3 & m5, f3 & f5; Amphotericin B + Imiquimod: m1 & m5, f1 & f5; Miltefosine + Imiquimod: m2 & m5, f2 & f5), while only one individual of each gender was used for Miltefosine + Eh-1 combination (m4 & f4). In *L. major* infection, for each drug combination macrophages from one male and one female individual were used (Amphotericin B + Eh-1: m5, f5; Amphotericin B + Imiquimod: m7, f6; Miltefosine + Eh-1: m5, f5;

Miltefosine + Imiquimod: m6, f6). Immunofluorescent staining and image analysis with Harmony™ allowed for the evaluation of macrophage infection rate as explained in **2.3.1** and **2.3.2.1**.

Macrophage infection rate was decreased very strongly by Amphotericin B mono treatment in high concentrations (0,5 μM and 1 μM) with high statistical significance in both *L. infantum* and *L. major* infection, while in low Amphotericin B concentrations no significant decrease could be detected (**Figure 3-17**, **Figure 3-18**).

Mono treatment with Eh-1 led to significant reduction of infection rate in *L. infantum* infection in higher concentrations (**Figure 3-17 left, Figure 3-18 left**), while in *L. major* infection no effect of Eh-1 could be observed. The reduction of infection rate was stronger in female individuals compared to male individuals.

Imiquimod also showed significant reduction in infection rate during mono treatment of *L. infantum* infection (**Figure 3-17 left, Figure 3-18**). The effect was weaker than Eh-1 in *L. infantum* infection, but in infection with *L. major* Imiquimod induced a stronger reduction of infection rate than Eh-1 (**Figure 3-17 right**). A similar reduction of infection rate was observed for mono treatment of *L. infantum* and *L. major* infection with Imiquimod. No difference between male and female macrophages was observed.

During Amphotericin B treatment, a drop in infection rate could be observed for concentrations of 0,5 μM and 1 μM in all experiments (**Figure 3-17**). In lower concentration only a mild decrease with low statistical significance was observed (**Figure 3-18**). Efficacy of Amphotericin B treatment was higher in *L. infantum* infection (**Figure 3-17 left**) compared to *L. major* infection (**Figure 3-17 right**), although in one individual (f6) the same strong decrease as in *L. infantum* infection could be seen.

Mono treatment with Miltefosine also showed a decrease in infection rate in higher concentrations with high statistical significance (**Figure 3-17, Figure 3-18**). In contrast to Amphotericin B mono treatment, the reduction was also visible in low concentrations of 5 μM Miltefosine, but with low statistical significance. The reduction of infection rate generally was lower than in Amphotericin B mono treatment, although for one female individual (f4) a similar reduction of infection rate like in Amphotericin B treatment could be observed. Reduction of infection rate was stronger in *L. infection* than in *L. major* infection and female macrophages often showed stronger reduction in infection rate in Miltefosine mono treatment compared to male macrophages.

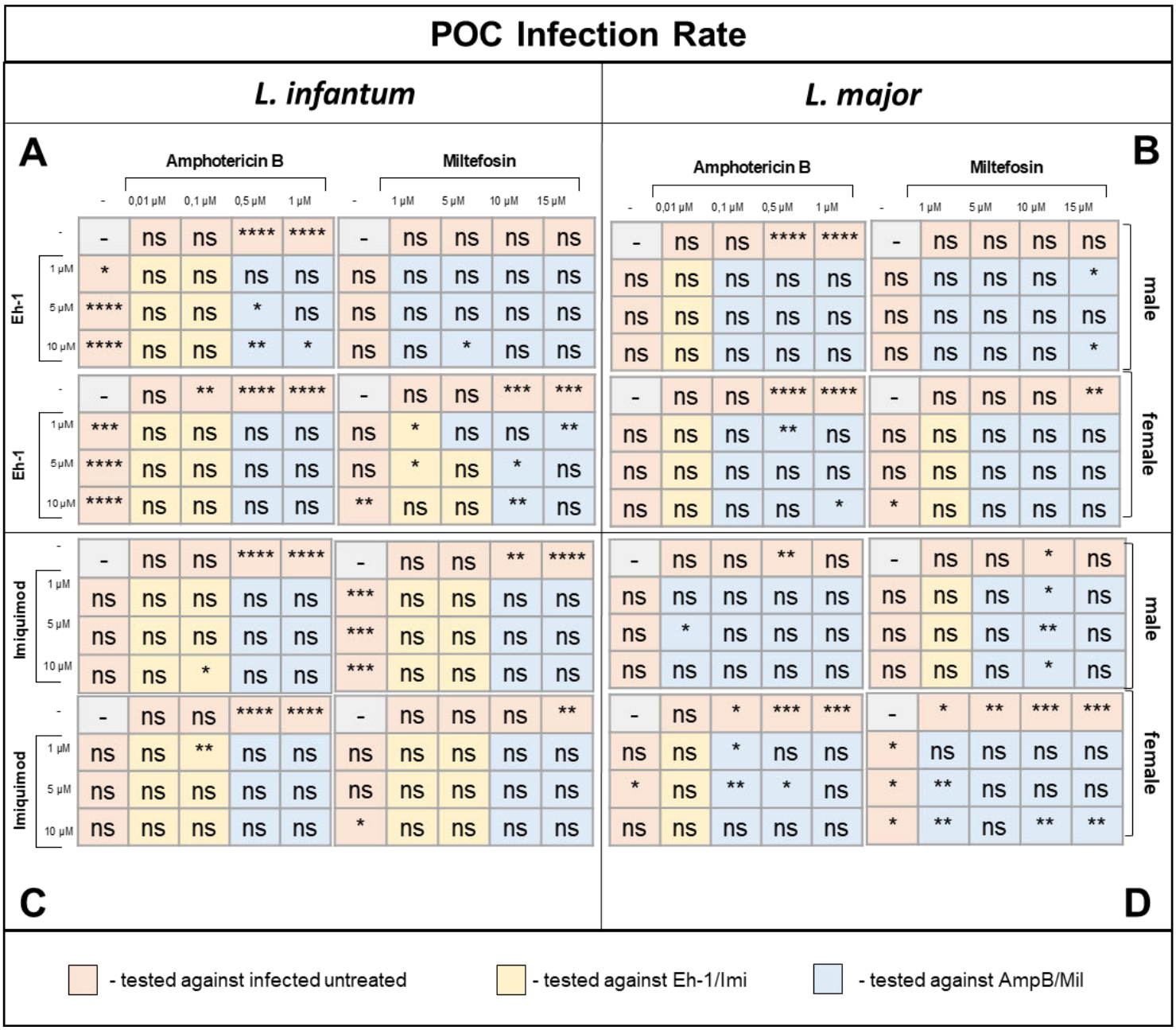

Figure 3-18: Overview of statistical significances of differences in infection rate after *L. infantum* (A & C) and *L. major* (B & D) infection (MOI 15:1) and treatment with leishmanicidal drugs (Amphotericin B & Miltefosine) in combination with either Eh-1 (A & B) or Imiquimod (C & D). Statistical significance was tested against either infected untreated cells, cells treated with only Eh-1 in the respective concentration or cells treated with only AmpB in the respective concentration with unpaired two-tailed t-tests. Significances are displayed as stars (ns: $p \geq 0,05$; *: $p \leq 0,05$; **: $p \leq 0,01$; ***: $p \leq 0,001$; ****: $p \leq 0,0001$)

In *L. infantum* infection both male and female macrophages responded to Amphotericin B and Eh-1 treatment. Combination treatment of *L. infantum* infection of male macrophages with high Amphotericin B concentrations and Eh-1 led to a significant increase in infection rate in high concentrations of Eh-1 (**Figure 3-17 A, Figure 3-18 A**). In low concentrations of Amphotericin B, the effect of Eh-1 dominated, but no

significant reduction could be achieved when combined. In *L. major* infection, where both female and male individuals responded to Amphotericin B, but not Eh-1, combining Amphotericin B with Eh-1 also led to increased infection rate in high concentrations (**Figure 3-17 B, Figure 3-18 B**). Only in one combination (0,5 μM Amphotericin B with 1 μM Eh-1) a statistically significant decrease of around 5 POC could be observed in female macrophages.

When combining Miltefosine and Eh-1 it could be observed that in high Miltefosine concentration Eh-1 could further decrease infection rate for *L. infantum* and *L. major* infection in most cases (**Figure 3-17 A&B, Figure 3-18 A&B**). Interestingly, in *L. infantum* infection, also in low concentrations of both drugs a cooperative reduction in infection rate could be seen.

In contrast to Eh-1, combination of high Amphotericin B concentrations with Imiquimod led to further reduction of infection rate for both male and female macrophages in *L. infantum* and *L. major* infection, although this effect was often not statistically significant (**Figure 3-17 C&D, Figure 3-18 C&D**). All individuals responded to Amphotericin B but only one female individual showed a response in Imiquimod mono treatment. In lower concentrations no positive effects but rather an increase in infection rate could be observed compared to mono treatments.

Administration of 10 μM Miltefosine in combination with Imiquimod showed a reduction of infection rate compared to Miltefosine mono treatment in *L. infantum* infection for both male and female macrophages, but without statistical significance (**Figure 3-17, Figure 3-18**). In *L. major* infection for one male (m6) individual (responded to Miltefosine, but not Imiquimod) the opposite effect could be observed, while one female (f6) individual (responded to both mono treatments) showed significant reduction. In female macrophages during L. major infection significant reduction could also be observed for 15 μM Miltefosine with 10 μM Imiquimod.

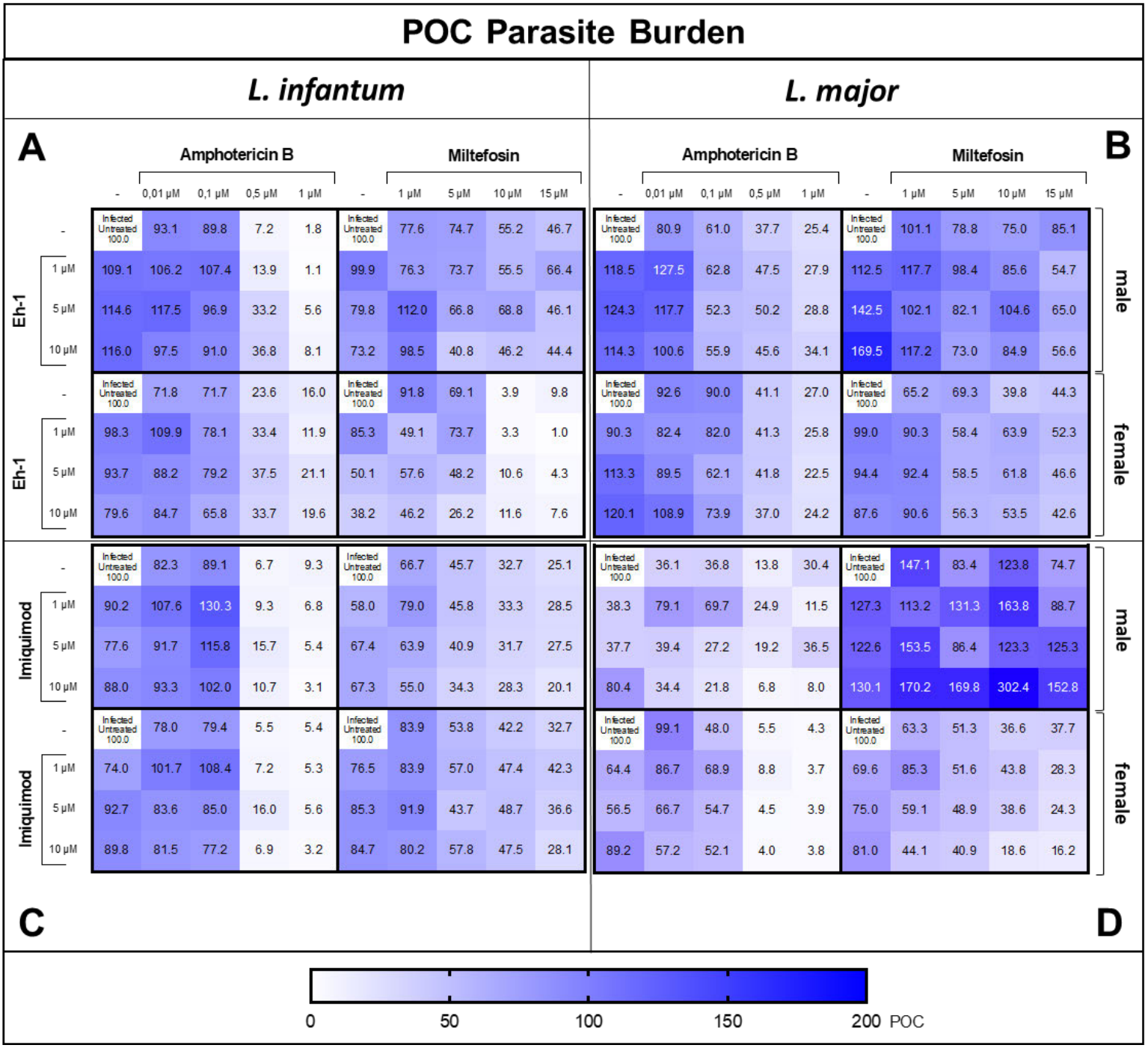

Figure 3-19: Heat map of male and female macrophage parasite burden in percentage of infected untreated control (POC) 72 h after *L. infantum* (A & C) and *L. major* (B & D) infection (MOI 15:1) and treatment with leishmanicidal drugs (Amphotericin B & Miltefosine) in combination with either Eh-1 (A & B) or Imiquimod (C & D). Drug combinations were administered 24 h after parasite infection in the given concentrations for 48 h in four technical replicates. For Amphotericin B & Eh-1, Amphotericin B & Imiquimod and Miltefosine & Imiquimod combinations in *L. infantum* infection, macrophages from two male and two female individuals were used (Amphotericin B + Eh-1: m3 & m5, f3 & f5; Amphotericin B + Imiquimod: m1 & m5, f1 & f5; Miltefosine + Imiquimod: m2 & m5, f2 & f5), while only one individual of each gender was used for Miltefosine + Eh-1 combination (m4 & f4). In *L. major* infection, for each drug combination macrophages from one male and one female individual were used (Amphotericin B + Eh-1: m5, f5; Amphotericin B + Imiquimod: m7, f6; Miltefosine + Eh-1: m5, f5; Miltefosine + Imiquimod: m6, f6). Immunofluorescent staining and image analysis with Harmony™ allowed for the evaluation of macrophage parasite burden as explained in **2.3.1** and **2.3.2.1**.

Similar to the results of infection rate, parasite burden during Amphotericin B mono treatment showed a large drop in concentrations of 0,5 μM and 1 μM with high statistical significance (**Figure 3-19**). This could be observed for all treatments. In some instances, a reduction of parasite burden could be seen in concentrations of 0,01 μM or 0,1 μM but with very low statistical significance.

Mono treatment with Miltefosine led to dose dependent reduction of parasite burden with high statistical significance in most cases (**Figure 3-19**, **Figure 3-20**). But compared to Amphotericin B treatment, parasite burden stayed higher. In *L. major* infection for male individuals a lower reduction was observed compared to female individuals. Generally, parasite burden was higher during Miltefosine mono treatment in *L. major* infection compared to *L. infantum* infection.

When treated with Eh-1, parasite burden in *L. infantum* infection was reduced in all females, but only in one case with statistical significance (**Figure 3-19**, **Figure 3-20**). Here a very strong reduction of parasite burden was observed. Interestingly, in two male individuals (m3 & m5) parasite burden was increased while infection rate was decreased in higher concentrations of Eh-1 (**Figure 3-17**, **Figure 3-19**). For the other male individual, a statistically non-relevant reduction could be seen. In *L. major* infection, for three out of four individuals, treatment with Eh-1 led to increased parasite burden, one of which was statistically significant. For the other, a slight non-significant reduction could be observed.

Imiquimod mono treatment showed minor reduction in parasite burden for almost all individuals with low statistical significance (**Figure 3-19**, **Figure 3-20**). Increasing Imiquimod concentration did not lead to a stronger reduction of parasite burden. Results between *L. infantum* and *L. major*, and male and female individuals were very similar.

Combining Amphotericin B and Eh-1 lead to significantly increased parasite burden in *L. infantum* infection of male and female macrophages. In infection with *L. major* the same effect occurred for male and female cells, although a slight non-significant reduction could be observed for 0,1 μM Amphotericin B combined with 5 μM or 10 μM Eh-1 (**Figure 3-19**, **Figure 3-20**).

In contrast, treatment of 1 μM Amphotericin B in combination with 10 μM Imiquimod was found to significantly reduce parasite burden compared to mono treatment for

L. infantum infection of both, male and female macrophages (**Figure 3-19**, **Figure 3-20**). In lower Amphotericin B concentration Imiquimod showed a tendency to increase parasite burden. In infection with *L. major*, combination of Amphotericin B and Imiquimod in high concentrations generally led to reduction in parasite burden, although in lower concentrations of Imiquimod, increases could also be observed.

When Miltefosine was combined with Eh-1 for the treatment of *L. infantum* infection, for male macrophages no difference in efficacy could be observed in high concentrations (**Figure 3-19**, **Figure 3-20**). For female macrophages in low concentrations of 1 μM Eh-1 and 1 μM Miltefosine significant reduction of parasite burden could be observed and in high a concentration of 15 μM Miltefosine cooperative reduction could be seen but without statistical significance. In *L. major* infection, parasite burden was found to be increased by Eh-1 in low concentration. For one male individual parasite burden was significantly reduced following 15 μM Miltefosine treatment in combination with Eh-1.

Combination treatment of Miltefosine with Imiquimod mostly reduced parasite burden in *L. infantum* and *L. major* infection compared to Miltefosine mono treatment, although in low Imiquimod concentration often a slight increase was observed (**Figure 3-19**, **Figure 3-20**).

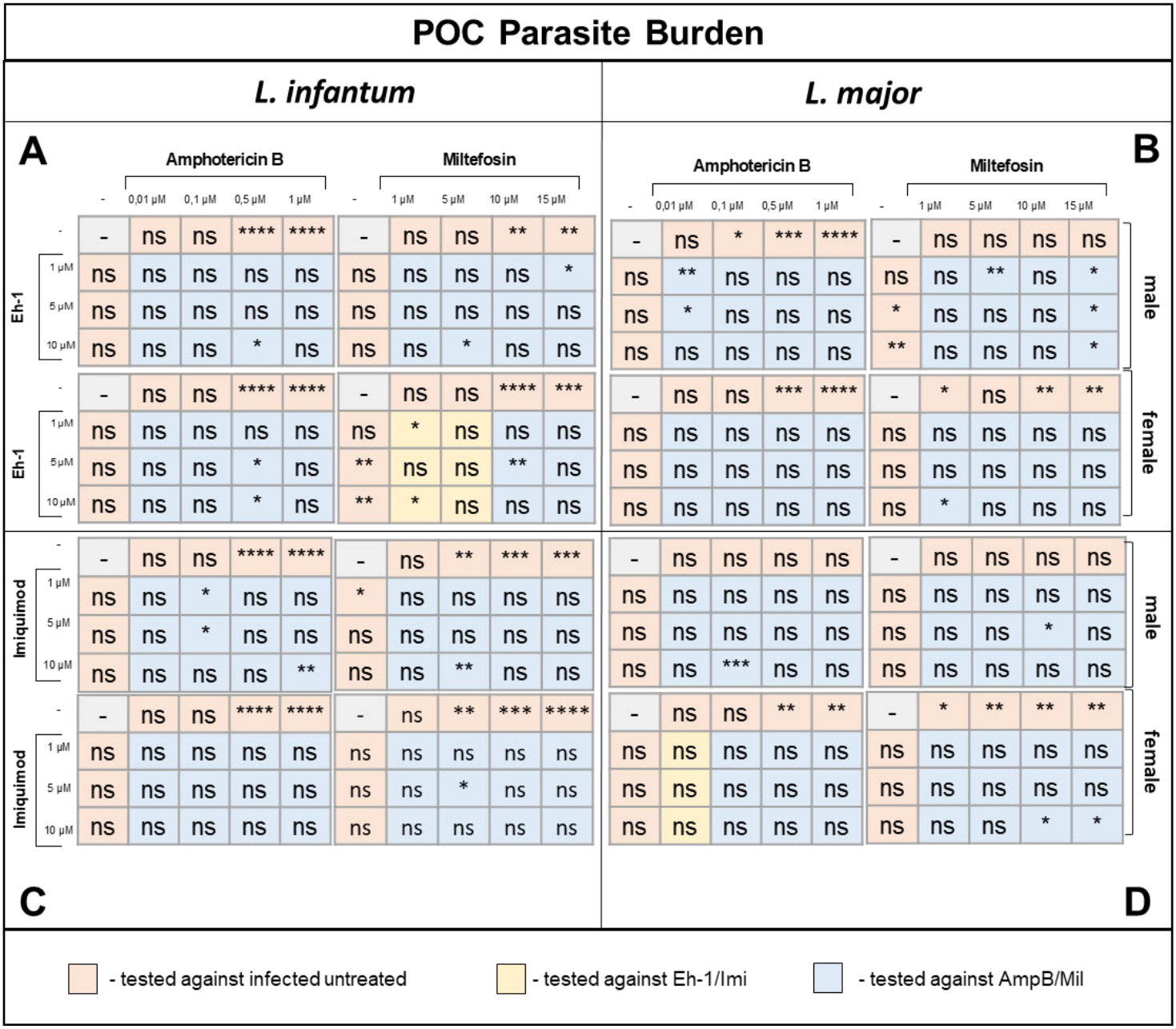

Figure 3-20: Overview of statistical significances of differences in parasite burden after *L. infantum* (A & C) and *L. major* (B & D) infection (MOI 15:1) and treatment with leishmanicidal drugs (Amphotericin B & Miltefosine) in combination with either Eh-1 (A & B) or Imiquimod (C & D). Statistical significance was tested against either infected untreated cells, cells treated with only Eh-1 in the respective concentration or cells treated with only AmpB in the respective concentration with unpaired two-tailed t-tests. Significances are displayed as stars (ns: $p \geq 0,05$; *: $p \leq 0,05$; **: $p \leq 0,01$; ***: $p \leq 0,001$; ****: $p \leq 0,0001$)

3.4 Analysis of extracellular cytokine profiles of hMDMs after *L. infantum* and *L. major* infection and combination treatment with Amphotericin B and Eh-1

The development of Leishmaniasis disease is based on the differential development of immune response of individuals. Immediate Th1 immune responses have been related to parasite control, while Th2 responses are usually associated with exacerbated disease (Mann, Frasca et al. 2021). Macrophages as main replication centers for *Leishmania* are key players in the early control of parasite infection. Diverse cytokines and effector molecules have shown to be involved in parasite clearance and survival.

To investigate parasite-specific macrophage response to drug mono and combination treatments, cytokine profiles of male and female macrophages after *L. infantum* or *L. major* infection and treatment with Amphotericin B and Eh-1 were generated via LEGENDplex assays of cell culture supernatants. Individuals were picked, that showed high reduction of infection rate in combination treatment (s. **Figure 3-21 C & D**). All individuals showed response to Amphotericin B treatment. Except for m5 and m9, all individuals showed response to Eh-1 treatment. For each individual two wells of each mono treatment, combination treatment and infected untreated macrophages were analyzed in technical duplicates. Male and female macrophages were included allowing for the analyzation of sex differences. With this number of replicates no statistical evaluation could be done.

The LEGENDplex cytokine panel was custom made in cooperation with Biolegend and designed to cover macrophage-specific cytokines, that are relevant during *Leishmania* infection. In **Figure 3-22** and **Figure 3-24**, cytokines are grouped depending on their function regarding T-cell activation.

Cytokine concentrations were determined via standard calibration during LEGENDplex assays. Unfortunately, the molecules CCL2, IL-8 and Arginase showed higher fluorescence intensity than the maximum standard. Dilution of cell culture supernatants could not be deployed as a solution to this problem, since many cytokines showed low concentrations, that would not have been detected if diluted. Thus, since concentration values for CCL2, IL-8 and Arginase cannot be trusted, mean fluorescence intensities (MFI) are compared for these cytokines (**Figure 3-23**). It is important to note, that no

comparison of MFI between the cytokines can be done without the standard calibration. Since MFI is directly proportional to the cytokine concentration, still a comparison between treatment effects for individual cytokines is possible.

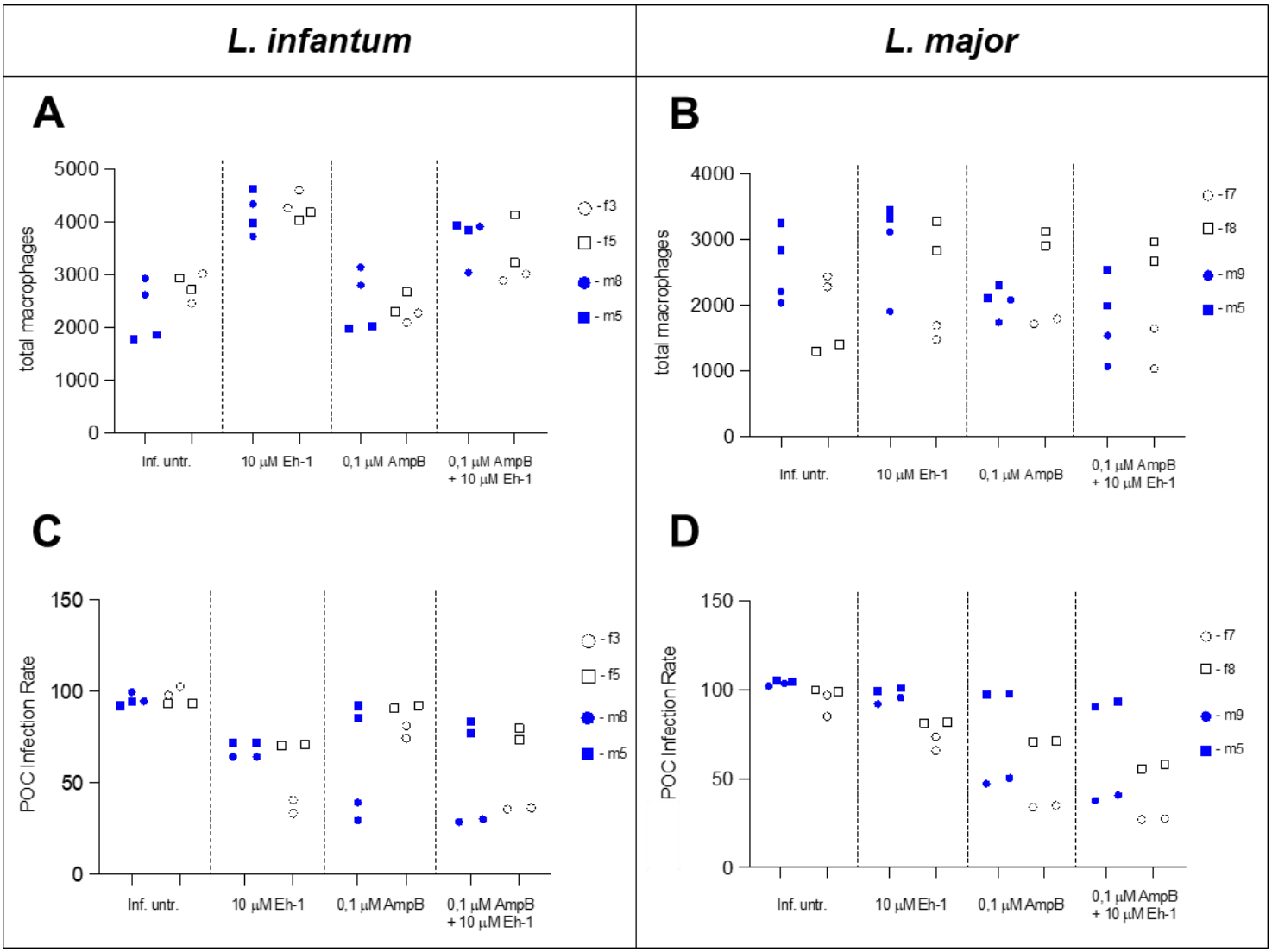

Figure 3-21: Background information on analyzed cell supernatants. Shown here are total macrophages (A & B) and infection rates (C & D, in POC) of analyzed macrophage cultures for *L. infantum* (left) and *L. major* (right) infection generated via image analysis with Harmony™ and subsequent calculation of infection rate as described in **2.3.1** and **2.3.2.1**.

LEGENDplex assays measure cytokine concentrations, which highly depend on the macrophage number that is present in a particular sample. During image analysis, Harmony™ determines the number of total macrophages for each well. As shown in **Figure 3-21 A & B**, macrophage numbers were different in the analyzed wells. Thus, normalization of measured cytokine concentrations to a relative expression of 1000

macrophages was done to improve comparability between wells. It is important to note, that the results regarding macrophage number determined by Harmony™ do not accurately depict the real number of macrophages in the sample, as not the whole area of the culture well is analyzed.

Generally, cytokine concentrations were found to show a high degree of variation between individuals of same gender and infection (**Figure 3-22**, **Figure 3-24**).

L. major infection of female macrophages led to high expression of CCL2, IL-8, CXCL10, IL-18 and Arginase, and low expression of TNF-a, IL-12p70, IL-1β, IL-10, CCL17 in untreated cells (**Figure 3-22 A, Figure 3-23**). In male macrophages in response to *L. major* infection the same cytokines were found, but in lower concentrations for almost all cytokines (**Figure 3-24 A, Figure 3-23**).

Infection with *L. infantum* produced similar cytokine expression as it was seen in *L. major* infection (**Figure 3-22 A**, **Figure 3-24 A, Figure 3-23**). Higher levels of CCL2, CXCL10 and Arginase and no expression of TNF-α, IL-12p70 and IL-1β could be detected. IL-10 expression could only be observed for one individual. Interestingly for f3 and m8 IFN-γ could be detected. Cells from both individuals showed considerably higher cytokine concentrations compared to the respective other individual with same conditions. This was especially evident for CCL2, IL-8 and Arginase. When comparing f5 and m5, that did not show IFN-γ expression, it can be seen, that female macrophages showed higher levels of CCL2, IL-8, IL-18, but lower levels of CXCL10 and Arginase.

For *L. major* infection, in macrophages from f7, treated with 10 μM Eh-1, CXCL10, IL-18 and IL-1β were present in higher concentrations compared to untreated cells, while TNF-α was detected in lower concentration (**Figure 3-22 B**). In macrophages from f8 all cytokines showed lower expression compared to untreated cells, except for IL-18, which showed a slightly higher concentration (**Figure 3-22 B, Figure 3-23**). Macrophages from f3 infected with *L. infantum* showed higher levels of CCL2, CCL17 and Arginase upon treatment with Eh-1. For all other cytokines lower levels were observed and IFN-γ could not be detected. For f5, higher levels of CCL2 and IL-8 and a slight increase in IL-23 could be seen, while all other cytokine concentrations were reduced.

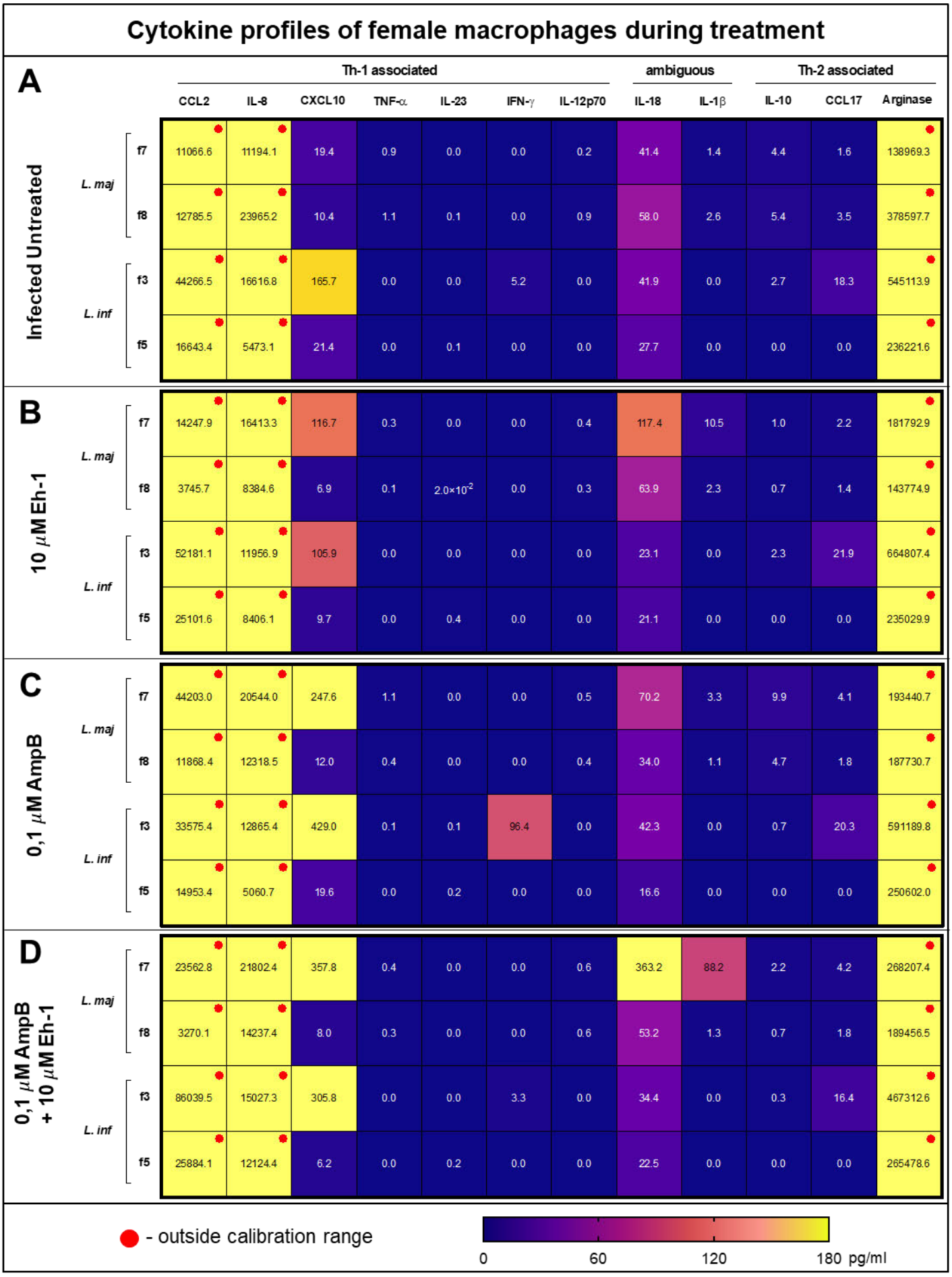
Cytokine profiles of female macrophages during treatment
A
Infected Untreated
B
10 µM Eh-1
C
0,1 µM AmpB
D
0,1 µM AmpB + 10 µM Eh-1
Th-1 associated
ambiguous
Th-2 associated
CCL2
IL-8
CXCL10
TNF-α
IL-23
IFN-γ
IL-12p70
IL-18
IL-1β
IL-10
CCL17
Arginase
L. maj
L. inf
f7
f8
f3
f5
11066.6 11194.1 19.4 0.9 0.0 0.0 0.2 41.4 1.4 4.4 1.6 138969.3
12785.5 23965.2 10.4 1.1 0.1 0.0 0.9 58.0 2.6 5.4 3.5 378597.7
44266.5 16616.8 165.7 0.0 0.0 5.2 0.0 41.9 0.0 2.7 18.3 545113.9
16643.4 5473.1 21.4 0.0 0.1 0.0 0.0 27.7 0.0 0.0 0.0 236221.6
14247.9 16413.3 116.7 0.3 0.0 0.0 0.4 117.4 10.5 1.0 2.2 181792.9
3745.7 8384.6 6.9 0.1 2.0×10-2 0.0 0.3 63.9 2.3 0.7 1.4 143774.9
52181.1 11956.9 105.9 0.0 0.0 0.0 0.0 23.1 0.0 2.3 21.9 664807.4
25101.6 8406.1 9.7 0.0 0.4 0.0 0.0 21.1 0.0 0.0 0.0 235029.9
44203.0 20544.0 247.6 1.1 0.0 0.0 0.5 70.2 3.3 9.9 4.1 193440.7
11868.4 12318.5 12.0 0.4 0.0 0.0 0.4 34.0 1.1 4.7 1.8 187730.7
33575.4 12865.4 429.0 0.1 0.1 96.4 0.0 42.3 0.0 0.7 20.3 591189.8
14953.4 5060.7 19.6 0.0 0.2 0.0 0.0 16.6 0.0 0.0 0.0 250602.0
23562.8 21802.4 357.8 0.4 0.0 0.0 0.6 363.2 88.2 2.2 4.2 268207.4
3270.1 14237.4 8.0 0.3 0.0 0.0 0.6 53.2 1.3 0.7 1.8 189456.5
86039.5 15027.3 305.8 0.0 0.0 3.3 0.0 34.4 0.0 0.3 16.4 467312.6
25884.1 12124.4 6.2 0.0 0.2 0.0 0.0 22.5 0.0 0.0 0.0 265478.6
- outside calibration range
0
60
120
180 pg/ml

Figure 3-22: Cytokine concentrations in pg/ml per 1000 macrophages 72 h after infection of female macrophages with *L. infantum* or *L. major* and treatment with either nothing (A), 10 μM Eh-1 (B), 0,1 μM Amphotericin B (C) or 0,1 μM Amphotericin B + 10 μM Eh-1 (D) for 48 h at 24 h.p.i. Supernatants of macrophages from two female individuals were analyzed for both *Leishmania* ssp. (*L. infantum*: f3 & f5, *L. major*: f7 & f8). Red dots indicate cytokines that showed fluorescence signals higher than the maximum standard. MFIs of cytokines outside calibration range are shown in **Figure 3-23**.

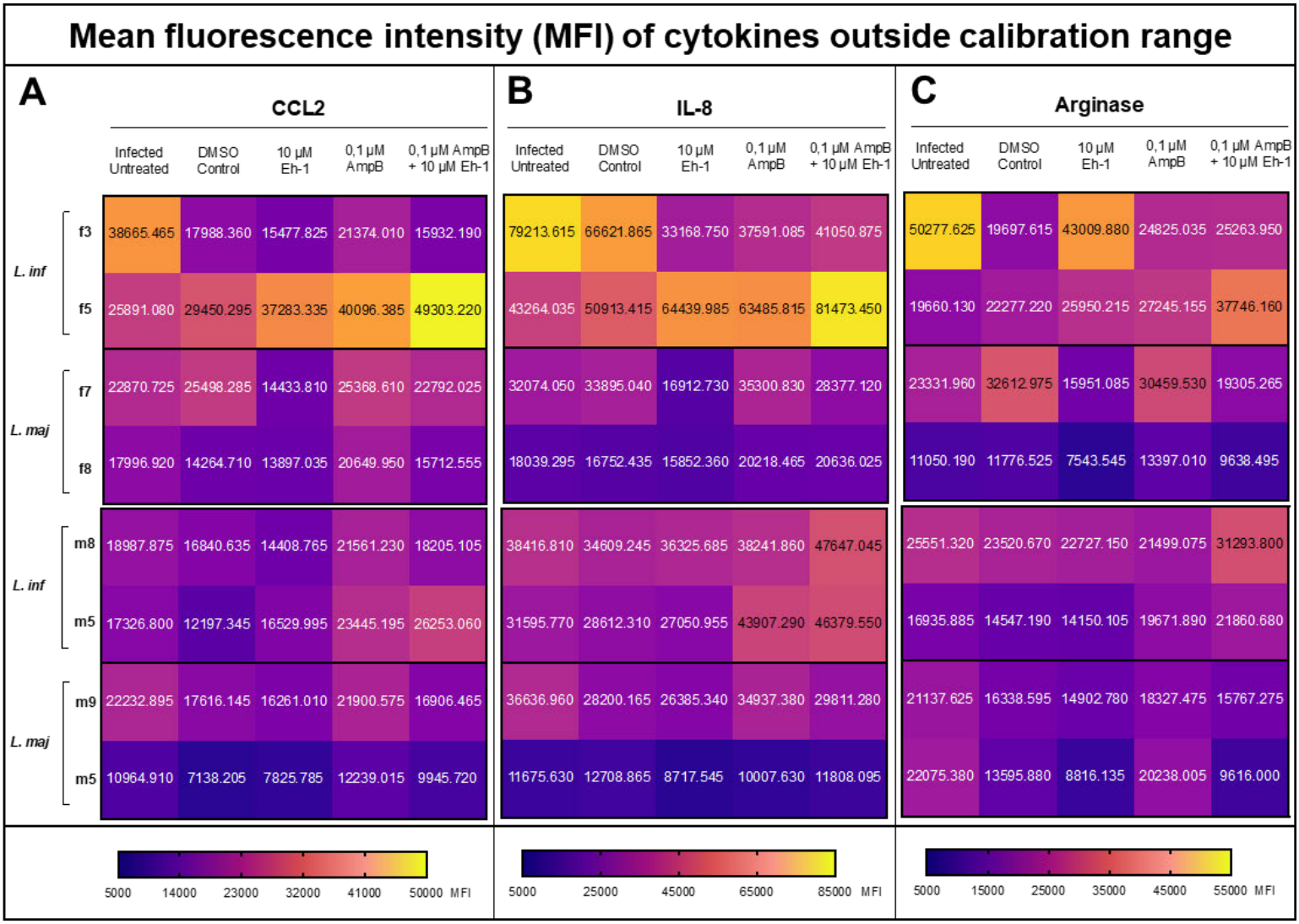

Figure 3-23: Heat maps of mean fluorescence intensity (MFI) of CCL2 (A), IL-8 (B) and Arginase (C) that showed fluorescence outside calibration range. Here, treatment conditions are shown side by side for each individual and an individual legend is shown for each cytokine, because MFIs cannot be compared between different cytokines.

When treated with 0,1 μM Amphotericin B, *L. major* infected macrophages of f7 produced higher levels of CCL2, IL-8, CXCL10, TNF-a, IL-10 and a slightly higher level of Arginase compared to Eh-1 treatment (**Figure 3-22 C, Figure 3-23**). IL-18 showed a lower concentration than during Eh-1 treatment, but higher than untreated cells. For f8, higher levels of CCL2, IL-8, CXCL10, TNF-a, IL-10 and slightly higher levels of

Arginase were observed compared to Eh-1 treatment. Arginase concentration was still considerably lower than in untreated cells. IL-18 and IL-1β concentrations were lower than in Eh-1 treated and uninfected cells, while IL-10 showed a higher concentration without treatment. In *L. infantum* infection, for f3 CXCL10, IFN-γ and IL-18 were increased compared to Eh-1 treatment. Especially CXCL10 and IFN-γ showed a very high increase. CCL2, IL-10 and Arginase showed lower levels, while IL-8 was found in similar concentration. The other female individual (f5) showed lower concentrations of CCL2, IL-8 and IL-18 compared to Eh-1 treatment. CXCL10 and Arginase were found in higher concentration.

During combination treatment of *L. major* infection, for f7 CXCL10, IL-18, Arginase and IL-1β showed much higher concentrations compared to both mono treatments (**Figure 3-22 D, Figure 3-23**). This was accompanied by low IL-10 expression and high IL-8 expression. CCL2 concentration was higher than in Eh-1 treatment, but lower than in Amphotericin B treatment. For f8, CCL2, IL-8, IL-10 and Arginase levels were much lower during combination treatment than in infected untreated cells, similar to what was seen during Eh-1 treatment. In combination however, IL-8, CXCL10 and Arginase show higher levels, while IL-18 and CCL2 show slightly lower concentration compared to Eh-1 treatment. Combination treatment of *L. infantum* infection showed very high concentration of CCL2 for f3. This was higher than in all other treatments. Moreover, a high CXCL10 concentration was observed. IFN-g, IL-18, CCL17 and Arginase were present in lower concentrations than for uninfected cells. For f5 high IL-8, IL-18 and Arginase levels were observed, whereas CCL2 and CXCL10 showed lower concentrations compared to untreated cells and mono treatments.

For male macrophages from individual m9 infected with *L. major*, in Eh-1 mono treatment high levels of IL-18 and IL-1β were found while CCL2, IL-10 and Arginase showed lower concentrations compared to infected untreated cells (**Figure 3-24 B, Figure 3-23**). For m5 all cytokine levels except CCL2, which was slightly increased, were lowered during Eh-1 treatment. In *L. infantum* infection of macrophages from m8, Eh-1 led to increased concentrations of all cytokines except IL-18, which was slightly lower, compared to untreated cells. Interestingly, IFN-γ showed the highest concentration during Eh-1 treatment for m8. During *L. infantum* infection, for m5 higher concentrations of CCL2 and IL-8 were found in Eh-1 treated macrophages compared to untreated cells, while CXCL10, IL-18 and Arginase levels were reduced.

In Amphotericin B treatment m9 showed higher concentrations of CCL2, CXCL10 and IL-10 compared to Eh-1 treatment, but considerably lower levels of IL-8 and IL-18, which were still higher than in untreated cells (**Figure 3-24 C, Figure 3-23**). During Amphotericin B treatment for m9 the lowest Arginase level could be observed compared to other conditions. For m5, almost all cytokines showed higher levels than in untreated cells and Eh-1 mono treatment. Only CXCL10 and CCL17 showed higher concentrations without treatment. Treatment of *L. infantum* infection with Amphotericin B led to lower concentrations of almost all cytokines compared to Eh-1 treatment for m8. Only IL-18 was found in a considerably higher amount compared to both, untreated cells and cells treated with Eh-1. Interestingly, the lowest Arginase concentration could be detected during Amphotericin B treatment compared to other conditions, although for m8 the highest Arginase levels were observed compared to the other male individuals. For m5 Amphotericin B treatment led to lower levels of CCL2 and IL-8, while IL-18 and Arginase were found in higher concentration compared to Eh-1 treatment. CXCL10 was found in comparable levels to untreated cells.

For m9 combination treatment of *L. major* infection with Amphotericin B and Eh-1 led to high levels of CXCL10, IL-18, IL-1β and Arginase (**Figure 3-24 D, Figure 3-23**). CCL2 and IL-10 were found in lower concentration compared to all other conditions. In combination treatment of *L. major* infection, high levels of almost all cytokines were observed for m5. Especially CCL2 and IL-8 were found in very high concentrations, but also Arginase and IL-18 showed increased concentration compared to all other conditions. Combination treatment of *L. infantum* infection led to very low cytokine levels in macrophages from m8. Very low levels were observed for CCL2, CXCL10, while IL-8, IL-18 and Arginase showed only slightly lower levels than during Eh-1 treatment. For m5, combination treatment reduced CXCL10 level compared to all other conditions, while CCL2 and IL-8 were found in very high concentrations. Arginase and IL-18 were found in similar concentrations compared to other conditions.

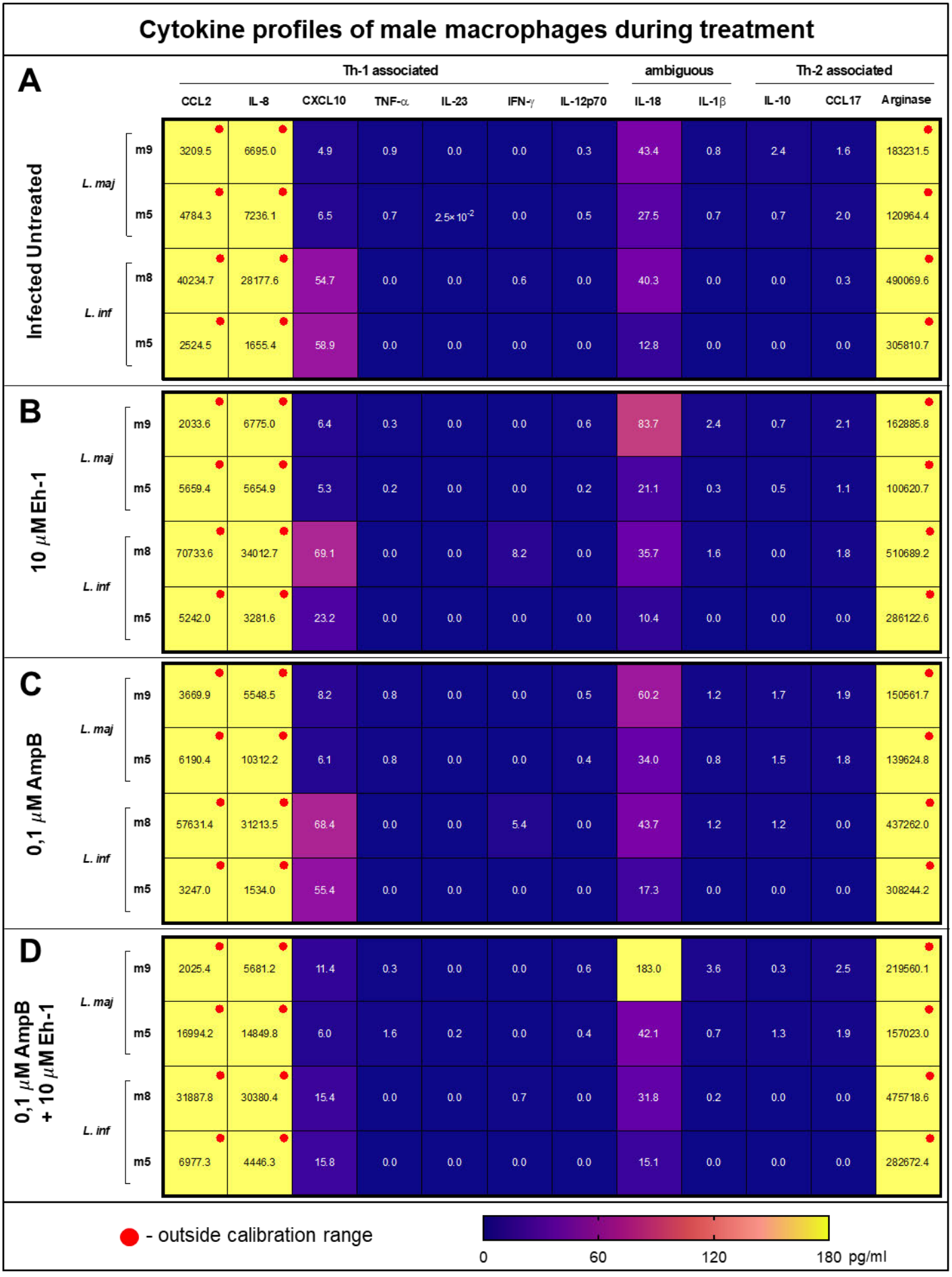
Cytokine profiles of male macrophages during treatment
A
B
C
D
Th-1 associated
ambiguous
Th-2 associated
CCL2
IL-8
CXCL10
TNF-α
IL-23
IFN-γ
IL-12p70
IL-18
IL-1β
IL-10
CCL17
Arginase
Infected Untreated
10 μM Eh-1
0,1 μM AmpB
0,1 μM AmpB + 10 μM Eh-1
L. maj
L. inf
m9
m5
m8
3209.5 6695.0 4.9 0.9 0.0 0.0 0.3 43.4 0.8 2.4 1.6 183231.5
4784.3 7236.1 6.5 0.7 2.5×10-2 0.0 0.5 27.5 0.7 0.7 2.0 120964.4
40234.7 28177.6 54.7 0.0 0.0 0.6 0.0 40.3 0.0 0.0 0.3 490069.6
2524.5 1655.4 58.9 0.0 0.0 0.0 0.0 12.8 0.0 0.0 0.0 305810.7
2033.6 6775.0 6.4 0.3 0.0 0.0 0.6 83.7 2.4 0.7 2.1 162885.8
5659.4 5654.9 5.3 0.2 0.0 0.0 0.2 21.1 0.3 0.5 1.1 100620.7
70733.6 34012.7 69.1 0.0 0.0 8.2 0.0 35.7 1.6 0.0 1.8 510689.2
5242.0 3281.6 23.2 0.0 0.0 0.0 0.0 10.4 0.0 0.0 0.0 286122.6
3669.9 5548.5 8.2 0.8 0.0 0.0 0.5 60.2 1.2 1.7 1.9 150561.7
6190.4 10312.2 6.1 0.8 0.0 0.0 0.4 34.0 0.8 1.5 1.8 139624.8
57631.4 31213.5 68.4 0.0 0.0 5.4 0.0 43.7 1.2 1.2 0.0 437262.0
3247.0 1534.0 55.4 0.0 0.0 0.0 0.0 17.3 0.0 0.0 0.0 308244.2
2025.4 5681.2 11.4 0.3 0.0 0.0 0.6 183.0 3.6 0.3 2.5 219560.1
16994.2 14849.8 6.0 1.6 0.2 0.0 0.4 42.1 0.7 1.3 1.9 157023.0
31887.8 30380.4 15.4 0.0 0.0 0.7 0.0 31.8 0.2 0.0 0.0 475718.6
6977.3 4446.3 15.8 0.0 0.0 0.0 0.0 15.1 0.0 0.0 0.0 282672.4
- outside calibration range
0
60
120
180 pg/ml

Figure 3-24: Cytokine concentrations in pg/ml per 1000 macrophages 72 h after infection of male macrophages with *L. infantum* or *L. major* and treatment with either nothing (A), 10 μM Eh-1 (B), 0,1 μM Amphotericin B (C) or 0,1 μM Amphotericin B + 10 μM Eh-1 (D) for 48 h at 24 h.p.i. Supernatants of macrophages from two female individuals were analyzed for both *Leishmania* ssp. (*L. infantum*: f3 & f5, *L. major*: f7 & f8). Red dots indicate cytokines that showed fluorescence signals higher than the maximum standard. MFIs of cytokines outside calibration range are shown in **Figure 3-23**.

3.5 Stimulation of hMDMs with Estradiol (E2) and Dihydrotestosterone (DHT) during *L. infantum* infection

Sex hormones have been shown to have a stimulating effect on various immune cells (Taneja 2018, Wilkinson, Chen et al. 2022). In parasitic diseases it has been shown that infection rate and disease severity follow a male bias and that DHT modulates immune response in parasitic infections (Sellau, Groneberg et al. 2019). For Leishmaniasis, DHT and E2 have been shown to influence immune response and parasite load (de Araujo Albuquerque, da Silva et al. 2021).

To test the impact of sex hormones on *Leishmania* infection, in a first step, a stimulation protocol for sex hormones must be established. Therefore, DHT and E2 were added in different concentrations ranging from 10 nM to 5 μM to male and female macrophages in a boost stimulation. High content screening readouts were generated with the use of Harmony™ image analysis sequence after immunofluorescence staining and confocal imaging.

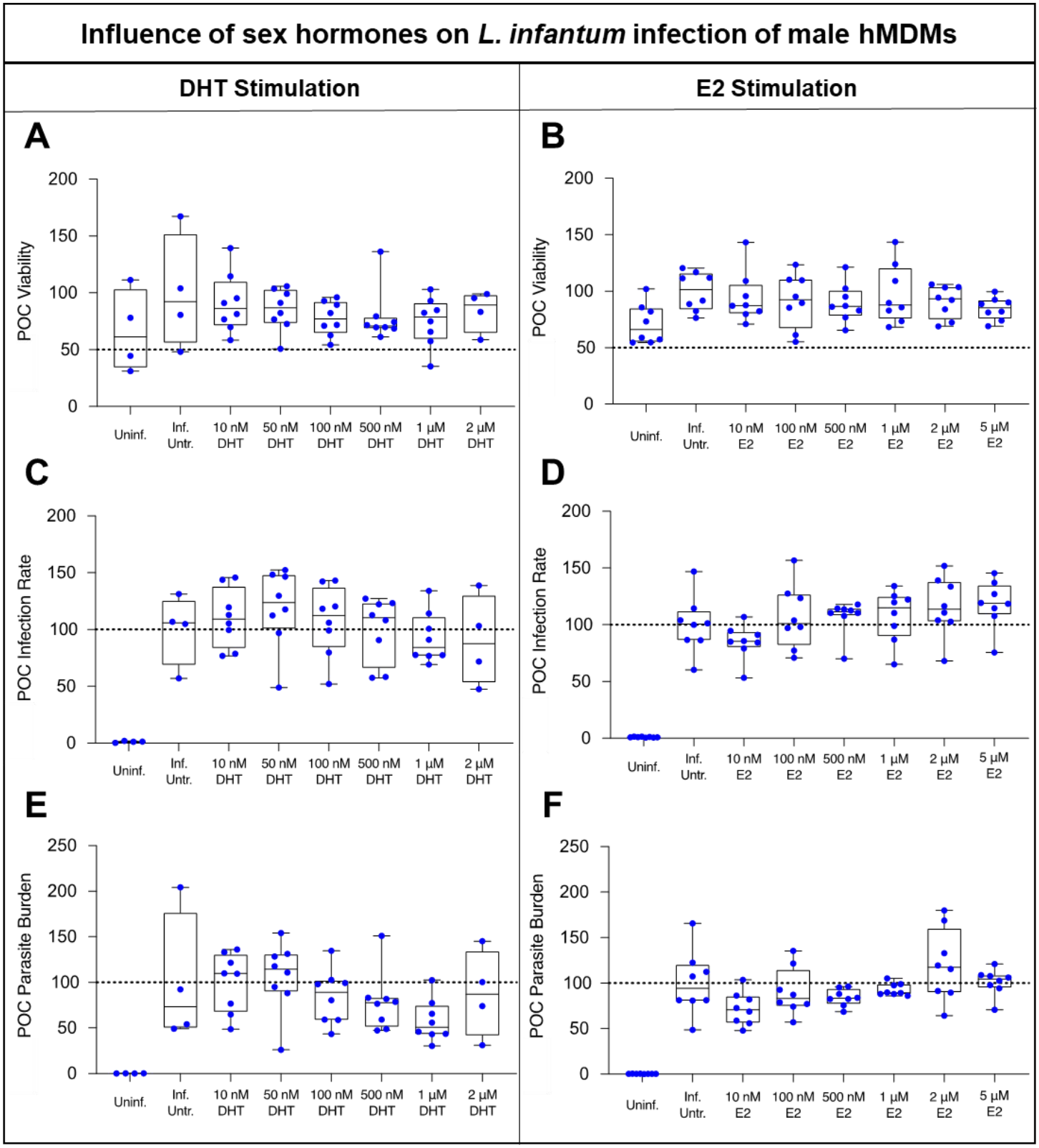

Figure 3-25: Overview of the drug screening readouts viability (A & B), infection rate (C & D) and parasite burden (E & F) in percent of infected untreated control after *L. infantum* infection (MOI 15:1) and boost stimulation with DHT (left) in the concentrations 10 nM, 50 nM, 100 nM, 500 nM, 1 µM and 2 µM, and E2 in the concentrations 10 nM, 100 nM, 500 nM, 1 µM, 2 µM and 5 µM for male macrophages. Macrophages for DHT and E2 stimulation were generated from different male individuals (n =1; DHT: m10, E2: f5). For viability, the toxicity threshold of 50 POC is shown as dotted line. For infection rate and parasite burden, dotted lines represent the mean of infected untreated control. Data is shown in box plots with the median represented by the centered line and standard deviation represented by box frame.

During DHT stimulation of male macrophages, uninfected cells showed a lower viability compared to unstimulated and stimulated cells (**Figure 3-25 A**). DHT stimulation led to slightly lower medians of cell viability in higher concentration compared to unstimulated cells, but without statistical significance. Single data points cross the toxicity threshold but no median of any DHT concentration shows a viability lower than 50 POC.

Infection rate of male macrophages stimulated with DHT showed higher median of around 120 POC in concentration of 50 nM and lower medians of around 80 POC in concentrations of 1 μM and 2 μM without statistical significance (**Figure 3-25 C**).

Parasite burden also showed an increase in median in concentrations of 10 nM and 50 nM, while a dose dependent decrease could be observed in concentrations from 100 nM - 1 μM up to a median of around 50 POC, but without statistical significance (**Figure 3-25 E**).

During E2 treatment cell viability of uninfected male macrophages was lower compared to infected untreated and stimulated cells (**Figure 3-25 B**). No data points crossed the toxicity threshold of 50 POC.

A slight increase of infection rate was observed in higher concentration of E2, while a minor decrease was seen in a concentration of 10 nM (**Figure 3-25 D**). No statistical significance could be observed.

Parasite burden of male macrophages was decreased cells stimulated with 10 nM E2 without statistical significance (**Figure 3-25 F**). In higher concentration no difference could be seen compared to infected untreated cells.

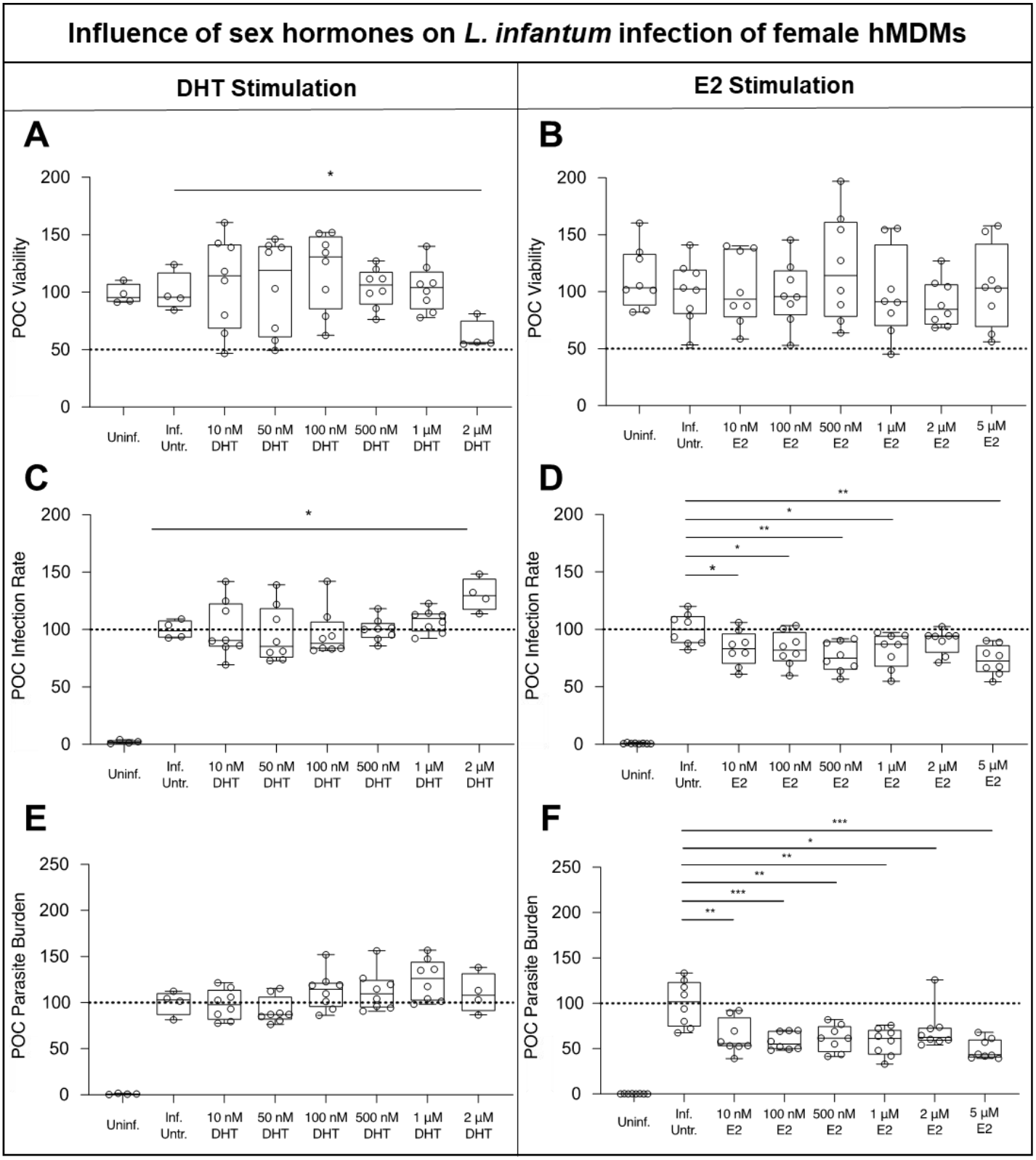

Figure 3-26: Overview of the drug screening readouts viability (A & B), infection rate (C & D) and parasite burden (E & F) in percent of infected untreated control after *L. infantum* infection (MOI 15:1) and boost stimulation with DHT (left) in the concentrations 10 nM, 50 nM, 100 nM, 500 nM, 1 µM and 2 µM, and E2 in the concentrations 10 nM, 100 nM, 500 nM, 1 µM, 2 µM and 5 µM for female macrophages. Macrophages for DHT and E2 stimulation were generated from different male individuals (n =1; DHT: f9, E2: f5). For viability, the toxicity threshold of 50 POC is shown as dotted line. For infection rate and parasite burden, dotted lines represent the mean of infected untreated control. Data is shown in box plots with the median represented by the centered line and standard deviation represented by box frame.

When comparing viability of female macrophages infected with *L. infantum* and stimulated with DHT, a significant impairment of cell viability in a concentration of 2 μM DHT could be observed compared to infected untreated cells, even though this did not cross the toxicity threshold of 50 POC (**Figure 3-26 A**). Generally, no median crossed the toxicity threshold, although single points showed a viability below 50 POC.

DHT significantly increased the infection rate of female hMDMs during *L. infantum* infection in a concentration of 2 μM (**Figure 3-26 C**). No other concentration showed an impact on infection rate.

Parasite burden showed a slight increase in mean in higher DHT concentrations, but without statistical significance (**Figure 3-26 E**).

For E2 treatment, again, single points showed viability near the toxicity threshold, but no median was found to be lower than 50 POC (**Figure 3-26 B**). No significant differences in cell viability could be observed.

Interestingly, female macrophages showed significantly reduced infection rates for all E2 concentrations except for 2 μM in with a reduction of around 10 - 30 POC (**Figure 3-26 D**). The highest effects were observed for concentrations of 500 nM and 5 μM.

Similar observations were made regarding parasite burden. Here, a strong, significant decrease was observed in all E2 concentrations with similar medians around 50 - 60 POC (**Figure 3-26 F**). The lowest mean and highest significance was observed for 5 μM E2.

4 Discussion

4.1 Effects of mono therapy with leishmanicidal drugs and immune response modifiers

To evaluate the efficacy of Amphotericin B and Miltefosine treatment combined with the immune response modifiers Imiquimod and Eh-1, it is important to understand the effects of the drugs during mono treatment. For the analysis of mono treatment effects, monocytes were purified from buffy coat samples and differentiated to hMDMs *in vitro*.

After the separation of PBMCs from buffy coat samples, monocytes were purified with anti-CD14 magnetic beads. FACS analysis could show the successful purification as monocyte populations were strongly increased. Since beads were directed against CD14 surface marker, a specific enrichment in classical monocytes could be seen while intermediate and non-classical monocyte populations were reduced compared to the sample before MACS purification. As expected, magnetic bead separation led to high monocyte purity and yield, as FACS data suggested that on average around 15 % of cells inside the PBMC samples were monocytes and average monocyte yields after MACS were 10 - 25 % with a purity of around 70 - 80 %.

After mono treatment, viability, infection rate and parasite burden of macrophages was compared between the drugs. Macrophage viability showed that treatments did not have relevant cytotoxic effects, as no drug led to a mean below the toxicity threshold. Infection rate and parasite burden of uninfected cells were used to verify the quality of staining and image analysis. In *L. infantum* infection, overall low infection rates and parasite burdens close to 0 POC were observed in uninfected cells for all treatments. This indicates, that staining, imaging and image analysis worked with a low error rate. For *L. major* infection on the other hand, for macrophages from one male individual (m7) high infection rates and parasite burdens of around 20 - 40 POC could be observed. After this was recognized, images of uninfected macrophages from this individual were checked and revealed that the staining of HSP-90 with Alexa647 showed high variation in fluorescence intensity with some very bright spots of intense fluorescence (**Figure 4-1**). These spots were much bigger than those found in infected cells and were found inside and outside cell cytoplasm, which indicates that the spots are not *Leishmania*. Moreover, high variation of fluorescence intensity indicates a high

degree of unspecific binding, which could be induced by inadequate blocking prior to antibody staining. In the analysis sequence these HSP-90 spots and some areas of higher fluorescence intensity were falsely recognized as *Leishmania* parasites explaining the high parasite numbers. Unfortunately, this problem was not recognized in time to repeat the experiment. Although the image analysis sequence did correctly identify most of the parasites present in the infected samples, data from this individual is tainted with a high error rate and must be viewed critically.

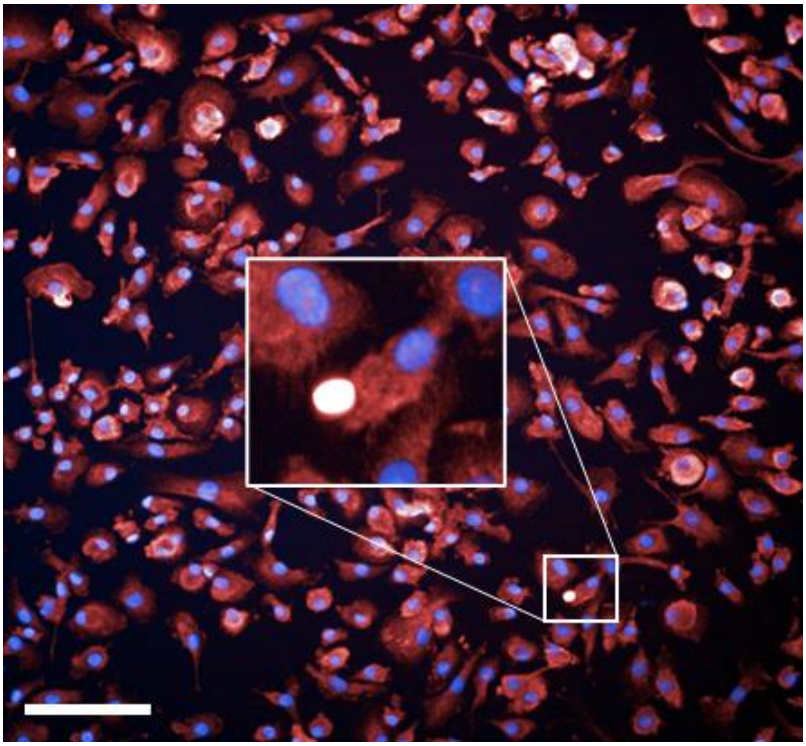

Figure 4-1: Exemplary image of inadequately stained uninfected macrophages from male individual m7. Fluorescence signals of HSP-90 (red) and DAPI (blue) were detected and visualized with the confocal microscopy unit of the Opera Phenix™ system as described in **2.3.1**. HSP-90 staining showed a high variation in Alexa647 signal with big, intense spots. Scale bar = 100 μm

During mono treatment, Amphotericin B in concentrations of 0,5 μM and 1 μM showed strong reductions in infection rate and parasite burden. This is caused by the formation of aqueous pores in *Leishmania* membranes since Amphotericin B concentration exceeds the threshold of 0,4 μM for their formation in *Leishmania* (Cohen 2016). This effect was observed to be stronger in *L. infantum* infection compared to *L. major* infection. It has been previously observed that viscerotropic *Leishmania* strains show higher susceptibility to Amphotericin B treatment than dermotropic strains (Berman and Wyler 1980). Viability was shown to be increased in the concentration of 1 μM for

L. infantum, which is most likely because of reduced parasite burden, as apoptosis occurs as a response mechanism to intracellular parasite infection (Solano-Galvez, Alvarez-Hernandez et al. 2021). Amphotericin B was the only drug that yielded a treatment response in all individuals.

Miltefosine induced dose-depended reduction of infection rate and parasite burden. Miltefosine has shown different modes of action regarding its leishmanicidal activity. Apoptosis-like cell death is observed in *Leishmania* after depletion of mitochondria membrane potential and inhibition of cytochrome C oxidase (Khademvatan, Gharavi et al. 2011, Khademvatan, Gharavi et al. 2011, Mollinedo 2014). Cytochrome C oxidase inhibition has been shown to be dose dependent explaining the dose dependent decline (Mollinedo 2014). Generally, for *L. major* treatment, responses were not as strong as in *L. infantum* infection. In cutaneous *L. braziliensis* strain lower uptake of Miltefosine dependent on the expression of the P-type ATPase subunit LbRos3, which shows lower expression in *L. braziliensis* compared to the visceral *L. donovani* strain, was observed indicating that cutaneous strains could show lower susceptibility to Miltefosine treatment (Sanchez-Canete, Carvalho et al. 2009).

Interestingly, Eh-1 showed an increase in viability for both, *L. infantum* and *L. major* infection. Since terminally differentiated macrophages do not proliferate in the given conditions, it is likely that treatment either induced proliferation or reduced parasite related cell death. Infection rates were reduced upon treatment with Eh-1 in *L. infantum*, but not in *L. major* infection. Depending on the species, *Leishmania* membranes are made to around 40-70 % of phospholipids (Beach, Holz et al. 1979, Wassef, Fioretti et al. 1985). Eh-1, as an analog of the phosphatidylinositol anchor *Eh*PIb, is very likely to interact with parasite membranes. Different membrane compositions could be an explanation for the different efficacy between the two parasite strains. *Eh*LPPG has been shown to induce IFN-γ response in NKT cells after interaction with TLR1/2/6 (Lotter, Gonzalez-Roldan et al. 2009). TLR2 has been associated with a protective role in Leishmaniasis (de Veer, Curtis et al. 2003) suggesting that Eh-1 might interact with TLRs in macrophages inducing the production of Th1 related cytokines to mediate parasite clearance.

During Imiquimod treatment of *L. infantum* infection, a slight dose-dependent decrease of infection rate was observed, while *L. major* infected hMDMs showed a non-significant decrease in median irrespective of concentration. Imiquimod is known to

bind to TLR7/8 and induce Th1 related cytokines (Bubna 2015). It has been shown to induce NO production in mouse models of Leishmaniasis facilitating parasite killing (Buates and Matlashewski 1999, Ghaffarifar, Foroutan et al. 2021). Parasite killing by induction of NO production explains the reductions in infection rate and parasite burden.

Generally, in *L. major* infection treatments showed lower efficacy. The *L. major* strain used was isolated from the spleen of a patient, although the preferential tissue for cutaneous strains is in the dermis indicating that this strain was especially resistant.

4.2 Analyzing the potential of combination therapy of Amphotericin B and Miltefosine with immune response modifiers

Current treatment of cutaneous and visceral Leishmaniasis heavily relies on drugs with strong adverse effects and high cost (Mann, Frasca et al. 2021). A trend in parasite drug resistance further increases the need for new treatment strategies (Mann, Frasca et al. 2021). Since Leishmaniasis course of disease has been shown to be altered by the degree of Th1 or Th2 immune response, an interesting opportunity is presented by combination treatments with immune response modifiers (Mann, Frasca et al. 2021).

To analyze the effects of drug combinations, Amphotericin B and Miltefosine were each combined with Imiquimod and Eh-1 in different concentrations for the treatment of *L. infantum* and *L. major* infection. Administration in mono treatment fashion allowed for the comparison of drug effects alone and in combination.

When combined with Amphotericin B in a concentration below the threshold for the formation of aqueous pores, no difference in leishmanicidal effect of Eh-1 could be observed. This indicates that membrane alteration by the formation of non-aqueous ion channels does not affect leishmanicidal effects of Eh-1. However, in concentrations that crossed the threshold for aqueous pore formation, Eh-1 mostly led to a significant increase in infection rate indicating that Eh-1 inhibits pore formation in the *Leishmania* membrane. As an amphiphilic molecule derived from a GPI anchor, Eh-1 is likely to associate with membranes altering pore formation by Amphotericin B.

In low concentrations of Miltefosine, combination with Eh-1 shows further reduction of infection rate and parasite burden in *L. infantum* infection. Since Miltefosine effect is dependent on its uptake by parasites, increased uptake mediated by Eh-1 could be an explanation (Pinto-Martinez, Rodriguez-Duran et al. 2018). They have similar structure with roughly the same length of alkyl chains and polar headgroups, similar to phospholipids found in parasite membranes, indicating that their association near or in parasite membranes is not unlikely (**Figure 1-5**). For *L. major* infection only in high Miltefosine concentration an effect of combination treatment could be found. Miltefosine uptake was shown to be lower in *Leishmania* strains that cause cutaneous disease (Sanchez-Canete, Carvalho et al. 2009). This could explain why a higher Miltefosine concentration is needed for *L. major* compared to *L. infantum* to induce leishmanicidal effects. Although cooperative reduction was found, combination of Miltefosine with Eh-1 also induced increased infection rates in some cases limiting the potential for this drug combination.

Combination of Amphotericin B concentrations below the threshold for aqueous pore formation with Imiquimod often showed increased infection rate and parasite burden compared to mono treatments indicating no cooperative function of their effects. In higher Amphotericin B concentrations however, in almost all cases reduction of infection rate compared to Amphotericin B mono treatment was seen. Imiquimod is a TLR receptor agonist, that induces Th1 response in macrophages (Bubna 2015), while Amphotericin B acts directly on *Leishmania* (Cohen 2016). Cooperative function of these drugs could be expected in cases where either TLR signaling is amplified by Amphotericin B interaction with hMDM membrane or Imiquimod stimulates NO production for cooperative killing of parasites. In high Amphotericin B concentrations, the latter was most likely observed.

Combining high concentrations of Miltefosine with Imiquimod showed increased reduction of infection rate and parasite burden compared to mono treatments except for one male individual, where combination treatment led to significant increase. This shows, that Imiquimod and Miltefosine can exert a cooperative effect during the clearance of *Leishmania*. Since effects of Miltefosine are not fully understood, it is hard to pinpoint how cooperative effects are achieved mechanistically. A hypothesis would be, that Imiquimod reduces the bioavailability of polyamines by induction of iNOS and NO production, which sequesters substrate from arginase reducing polyamine concentration for parasites (Bubna 2015). This could cooperate with Miltefosine to

further inhibit membrane anabolism (Pinto-Martinez, Rodriguez-Duran et al. 2018). Interestingly a phase 2 clinical study investigated use of Imiquimod as an addition to oral Miltefosine treatment for cutaneous Leishmaniasis in 2010 with no results, indicating that drugs show no cooperative effect *in vivo* (Soto 2010).

Although combination therapy with immune response modifiers theoretically has great potential and drugs showed convincing effects in their mono treatment, no drug combination provided convincing evidence of a strong cooperative effect during combination treatment. A slight potential was observed for the combination of Amphotericin B or Miltefosine with Imiquimod, but more experiments are needed to provide further evidence for these effects or to find drugs that mediate stronger leishmanicidal effects when combined. For this, it is important to understand drug effects mechanistically and investigate their effects *in vivo*.

4.3 Analyzing the role of hMDM cytokines during treatment of *L. infantum* and *L. major* infection

In Leishmaniasis diverse cytokines and effector molecules secreted by macrophages show important effects on the elimination or persistence of parasites and thus the course of disease. Many cytokines related to type 1 immune responses have been related to parasite elimination in macrophages (Liu and Uzonna 2012, Bogdan 2020). The most important player in parasite elimination is iNOS, which is upregulated after stimulation with IFN-γ and TNF-α (Liu and Uzonna 2012). But also, other inflammatory mediators like IL-12 and CXCL10 have been shown to be relevant to develop a protective immune response (Maspi, Abdoli et al. 2016). This is often linked to inhibition of effector molecules of type 2 immune responses. In Leishmaniasis IL-10 and Arg1 have been associated with disease progression (Maspi, Abdoli et al. 2016, Bogdan 2020). However, a cooperative role of Th1 and Th2 cytokines has been associated with the best disease outcome (Carneiro, Lopes et al. 2020).

To investigate if Amphotericin B and Eh-1 mono treatment and their combination could induce the expression of protective cytokines, LEGENDplex assays were used to determine cytokine concentrations in hMDM culture supernatants. Experiments with considerable leishmanicidal effect of treatments were picked and diverse cytokines with relevance in the context of Th1/Th2 responses were analyzed.

Generally, cytokine expression levels differed between the individuals of the same conditions, although the cytokines found are almost the same. This is likely because of age differences (Bajaj, Gadi et al. 2020) and epigenetic memory (Sun and Barreiro 2020). Aging leads to impaired function of immune cells including macrophages (Bajaj, Gadi et al. 2020). Especially activation of TLRs and their downstream pathways can be increased drastically resulting in higher inflammatory signaling (Bajaj, Gadi et al. 2020). Moreover, responses to pathogens differ substantially between human individuals because previous challenges with pathogens can lead to epigenetic memory of innate immune cells (Sun and Barreiro 2020). This does not only include previous challenge with the same pathogen, but also pathogens that interact with receptor pathways in a similar way (Sun and Barreiro 2020).

In infected untreated hMDMs, generally an induction of pro inflammatory cytokines and chemokines was observed. High levels of IL-18 and IL-8 indicate activation of macrophages and pro inflammatory signaling (Dayakar, Chandrasekaran et al. 2019). IL-12 is the major cytokine for the activation of pro inflammatory $CD4^+$ T cells (Muraille, Leo et al. 2014). Expression of IL-12 in *L. major* infection and not in *L. infantum* infection indicates a stronger initial Th1 response, which is consistent with the fact, that most infection with *L. major* are self-limiting (Mann, Frasca et al. 2021). Moreover, during *L. infantum* infection higher levels of Arg1 were observed suggesting a stronger active suppression of oxidative response for *L. infantum*, which is consistent with the observation that in visceral Leishmaniasis higher degree of M2 macrophage polarization and increased expression of Arg1 was observed (Kumar, Das et al. 2018). These immunosuppressive effects during the early stages of infection likely enables *L. infantum* parasites to persist in host cells until they are transported to the inner organs while *L. major* parasites are cleared by immediate induction of Th1 response and oxidative response.

Female macrophages showed stronger reduction of infection rate following treatment associated with higher concentrations of cytokines in *L. major* infection. Higher cytokine concentrations were also party observed in *L. infantum* infection. This will be further discussed in **4.4**.

During *L. major* infection expression of TNF-a, IL-1β and IL-12p70 indicate stimulation of mannose-fucose receptor, which initiates inflammatory response (Liu and Uzonna 2012, Elmahallawy, Alkhaldi et al. 2021). High expression IL-18 and IL-1β indicate

inflammasome formation, which in Leishmaniasis provided protection by NO mediated parasite killing (Liu and Uzonna 2012, Maspi, Abdoli et al. 2016, Tapia, Daniels et al. 2019, De Miguel, Pelegrin et al. 2021).

During Eh-1 treatment the expression of these inflammasome related cytokines is increased compared to untreated cells and infection rate reduced indicating increased inflammasome mediated NO response.

In Amphotericin B treatment, stronger reduction of infection rate was observed than in Eh-1 treatment, although cytokines related to inflammasome response showed lower levels. Amphotericin B is known to induce intracellular ROS production (Mesa-Arango, Trevijano-Contador et al. 2014) suggesting a combination of ROS and NO mediated parasite killing.

During combination treatment inflammasome related cytokines show higher levels and infection rate is further reduced compared to mono treatments suggesting cooperative induction of protective oxidative response with NO and ROS.

In two individuals (m5 and f8) generally lower reduction of infection rate was observed upon treatment. Here, Eh-1 led to reduced Arg1 level, but also reduced pro inflammatory and inflammasome related cytokines. This indicates a different mechanism for parasite removal which might be based on increased iNOS activity induced by reduction in Arg1 level. Arg1 sequesters substrate for NO production from iNOS (Liu and Uzonna 2012). More information would be needed to confirm this. Amphotericin B treatment showed higher levels of CCL2, IL-8 and IL-18 suggesting higher ROS production as the primary mechanism in these macrophages instead of inflammasome mediated NO production. In combination treatment, again a combination of oxidative responses led to slightly reduced infection rate compared to mono treatments.

During *L. infantum* infection two individuals (m8 and f3) showed expression of IFN-γ, which indicates the presence of other immune cells since hMDMs only produce IFN-γ upon simultaneous stimulation with IL-12 and IL-18 (Darwich, Coma et al. 2009) and IL-12p70 could not be detected. These individuals showed much higher concentrations of cytokines overall and can not be compared to the other samples. They will be excluded from this discussion since the goal was to analyze treatment effects on macrophages (for further discussion of samples with IFN-γ expression see **6.3**).

In supernatants that did not show IFN-γ expression, high expression of CXCL10 and Arg1 was found indicating high degree of immunosuppression that was accompanied by low expression of inflammatory mediators IL-8 and IL-18. CXCL10 expression could indicate activation of TLR2 and NF-κB pathway by LPG on *Leishmania* surface (Figueiredo, Viana et al. 2017, Elmahallawy, Alkhaldi et al. 2021).

Treatment with Eh-1 led to reduction of CXCL10 concentration but could induce higher levels of IL-8 and CCL2. In male and female macrophage Arg1 expression was also slightly reduced. Reduction of infection rate to around 65 POC was observed. These results indicate that Eh-1 mediates protection mostly independent of the cytokines analyzed as IL-8 and CCL2 have no direct effect on oxidative response, although reduction of immunosuppression by Arg1 might play a role.

Amphotericin B treatment did not induce relevant alteration in infection rate or cytokine profile indicating that ROS production induced by Amphotericin B is sufficiently counteracted by elevated Arg1 expression.

During combination treatment the effect of Eh-1 on cytokine expression dominated, but with higher levels of Arg1 and the reduction of infection rate was reduced compared to Eh-1 mono treatment. This indicates that during *L. infantum* infection Amphotericin B ameliorates Eh-1 mediated protection possibly by inhibiting Eh-1 effect on Arg1 expression.

The goal of this experiment was to see if treatment with Eh-1, Amphotericin B and their combination could induce a protective cytokine response in hMDMs.

These results suggest that Eh-1 leads to protection mediated by Th1 cytokine expression and inflammasome formation in *L. major*. A similar effect was observed for Amphotericin B, but higher treatment effect was observed likely induced by ROS production. For *L. major* infection combination therapy further increased protective cytokine expression and protective effects.

For *L. infantum* infection, treatment of hMDMs with Eh-1 led to reduction of infection rate without induction of the protective cytokines analyzed, although reduction of Arg1 level might contribute to this effect. Amphotericin B showed no effect on protective cytokine expression and reduced protective effect of Eh-1 when combined.

4.4 Analyzing sex specific differences during *L. infantum* and *L. major* infection and treatment of hMDMs

The infection rate and disease severity of Leishmaniasis shows a male bias indicating a role of male sex specific factors like androgens or genetic differences in immunity in disease development (Bernin and Lotter 2014). Sex specific differences could be observed in many experiments for this thesis. Infection rates, macrophage polarization and cytokine profiles were compared between male and female hMDMs to get information about infection characteristics of *L. major* and *L. infantum*. To analyze the impact of male and female sex hormones on the infection with *L. infantum* and establish a stimulation protocol, stimulation of hMDMs with DHT and E2 in different concentration was done.

During *L. infantum* infection significantly higher infection of male macrophages was observed compared to female macrophages. In mouse model experiments with *L. infantum*, 72 h.p.i. higher infection rates were observed in macrophages from male mice compared to female mice, although in the first 24 h no difference in uptake was observed (Lockard, Wilson et al. 2019). This indicates a better initial parasite control in female macrophages. Interestingly, in female, but not macrophages a significant increase in M1 macrophages was observed 72 h after infection with *L. infantum* accompanied by a decrease in M2 macrophage polarization. Increased number of M1 macrophages initiates a stronger oxidative response leading to better immediate control of parasites.

In mono treatments with Eh-1 and Miltefosine for *L. infantum* infection female hMDMs showed stronger reductions of infection rate indicating a difference in the efficacy of treatment for these drugs. This could be caused by differences in surface receptor composition. Escape from X-chromosome inactivation leads to higher TLR7 expression in women compared to men. Eh-1 is likely to interact with TLRs on macrophage surface as it is derived from *Eh*LPPG, which binds to TLRs or scavenger receptors (Fehling, Choy et al. 2020). Thus, stronger pro inflammatory response and parasite killing could be mediated by increased TLR7 stimulation. Miltefosine treatment was shown to increase TNF-α levels in human serum samples, which is majorly produced by macrophages (Mukhopadhyay, Das et al. 2011). Moreover, E2 stimulation

has been associated with epigenetic trained immunity and increased activation of non-canonical NF-κB pathway following pathogen challenge in murine BMDMs (Sun, Pan et al. 2020). Since TNF-α is a cytokine produced downstream of NF-kB signaling pathway, that has been associated with upregulation of NO production (Bogdan 2020), females might show stronger parasite removal following Miltefosine treatment.

During *L. major* infection, no sex specific difference in the percentage of infected macrophages was observed. This is consistent with literature as in human cutaneous leishmaniasis caused by *L. major* differences between sexes have not shown a clear bias (Lockard, Wilson et al. 2019).

Further differences in sex specific immune response were observed during analysis of cytokine profiles. Female macrophages generally showed higher levels of cytokine expression. Female mice and rats express more TLRs on the surface of macrophages indicating a stronger capacity for females to mount pro inflammatory response (Scotland, Stables et al. 2011). Moreover, in humans, monocytes from women are known to induce stronger cytokine expression in response to *ex vivo* stimulation with LPS (Jacobsen and Klein 2021). Together with the epigenetic trained immunity effect described above, this indicates that upon pathogen challenge women induce a faster and stronger cytokine response also explaining the difference in M1 macrophage polarization upon *L. infantum* infection.

Stimulation experiments with sex hormones showed no significant impact on infection rate or parasite burden during stimulation of male macrophages with either DHT or E2, while stimulation of female hMDMs with DHT led to increased infection rate and stimulation with E2 led to decreased infection rate. Stimulation with DHT was shown to increase parasite burden and infection rate in Leishmaniasis, although in this study parasites were stimulated instead of hMDMs (Lockard, Wilson et al. 2019). Moreover, in human macrophages NF-κB activity is suppressed by DHT leading to reduced production of proinflammatory cytokines and NO (Snider, Lezama-Davila et al. 2009). DHT can also induce expression of IL-10 and IL-4, which are associated with parasite growth and disease progression (Snider, Lezama-Davila et al. 2009). E2 on the other hand has been shown to have pro inflammatory properties by induction of TNF-α production mediating protection against *Leishmania* infection by stronger oxidative response (Karpuzoglu-Sahin, Hissong et al. 2001, Snider, Lezama-Davila et al. 2009).

The assay could successfully analyze the impact of sex hormones in different concentrations on the infection with *L. infantum*. A concentration of 2 µM DHT produced detectable effects during the infection. A concentration of 5 µM DHT could be tested in the future to analyze if higher effects could be observed. For E2 the strongest effect could be observed in the highest concentration of 5 µM. This concentration is well suited for future *in vitro* stimulation experiments.

Sex specific differences during *Leishmania* infection could be observed in different experiments. Higher infection rates were detected in men, while women showed higher expression of cytokines and stronger pro inflammatory polarization. Stimulation with sex hormones showed a protective role for E2 in women and a higher infection rate for DHT in women, while male hMDMs were not significantly affected by hormone stimulation.

5 Conclusion and Outlook

During this thesis different strategies for the treatment of hMDM infection with *Leishmania infantum* and *Leishmania major* were compared. Successful high content drug screening by image analysis after confocal imaging of infected, treated and stained hMDMs led to various data sets on different drug combinations. Further information about the characteristics of *Leishmania* strains during their infection and treatment of hMDMs were acquired by analyses of cytokine profiles. During these experiments various sex specific differences were observed.

Mono treatment analyses could show the potency of the leishmanicidal drugs Amphotericin B and Miltefosine, and the potential for the immune response modifier Imiquimod and drug candidate Eh-1 for the treatment of *Leishmania* infection. All drugs could lower infection rates without relevant cytotoxicity, but treatment efficacy was highly dependent on *Leishmania* strain and individual. Amphotericin B has proven to be more efficient in the removal of parasites compared to Miltefosine, as its effects show a clear, concentration dependent mechanism, that led to very efficient reduction of parasite load in both infections and all individuals, whereas Miltefosine showed an effect that was individual dependent and did not ensure efficient parasite removal. Eh-1 showed great potential in *L. infantum* infection with similar success as the FDA approved immune response modifier Imiquimod, although it did not alter the course of infection for *L. major*. Imiquimod showed effects for both parasite strains. Both immune response modifiers showed lower treatment response rates compared to leishmanicidal drugs.

The strain dependency of drug efficiency and response would be an interesting topic for further analyses, as drugs could maybe be chemically optimized for specific strains in the future. For future studies it could also be interesting to correlate age with treatment responsiveness especially to immune response modifiers, since age is a big factor influencing inflammatory responses. This could also give insights about the effector mechanisms of these drugs, since some mechanisms might be increased, reduced or lost with old age. To further specify the mechanisms of Eh-1, localization studies with fluorescent markers would be beneficial and could maybe also shed a light on the differences in treatment efficacy between *Leishmania* strains.

Combination treatments with leishmanicidal drugs and immune response modifiers did not reveal a combination that securely amplified leishmanicidal effects, however potential was observed for combinations of Amphotericin B or Miltefosine with Imiquimod. Further studies are needed to confirm this, as significant cooperative effects were only observed in particular concentrations. Combination therapy with drug candidate Eh-1 did not show convincing potential for combination therapy as inhibition of aqueous pore formation was observed in combination with Amphotericin B and combination with Miltefosine yielded minor reductions but in some cases also increases in infection rate. It is important to further elucidate drug mechanisms in order to combine drugs with cooperative effects and also to look at later timepoints after treatment to confirm successful clearance. Also, drug combination should be tested in more concentrations to get more information about concentration dependent effects. Moreover, testing combination treatments in the presence of other lymphocytes could be an interesting approach for the future.

Cytokine analyses showed that treatment of *L. major* infection with Amphotericin B and Eh-1 could induce the expression of protective cytokines and reduce infection rate. The cytokine profiles observed during *L. major* treatment indicate an inflammasome dependent oxidative response, that was amplified during treatment with Eh-1. Combination with Amphotericin B in a concentration below aqueous pore formation led to stronger parasite elimination likely mediated by ROS production. These effects seem to depend on the immune response of the respective individual, as treatment showed lower efficacy in individuals with less pronounced inflammasome response. In *L. infantum* infection Eh-1 could induce reduction of infection rate that was likely independent of protective pro inflammatory cytokine expression, although a minor effect on Arg1 expression could be observed. Amphotericin B and combination therapy showed no protective effect in a concentration below the threshold for aqueous pore formation.

Important sex differences were observed during infection with *L. infantum* and *L. major*, that reflect and confirm data presented in literature. During *L. infantum* infection a male bias of infection was observed with higher infection rate and stronger M1 differentiation of female hMDMs following infection. This is consistent with higher levels of protective cytokines observed in female cytokine profiles which most likely led to a more pronounced oxidative response. Treatments were also observed to have differing effect on female and male hMDMs, as female macrophages showed stronger cytokine

expression most likely linked to differences in TLR expression and epigenetic trained immunity induced by E2. This was represented in better response to Miltefosine and Eh-1.

By using different concentrations of the sex hormones DHT and E2 during the stimulation of hMDMs in *L. infantum* infection, 2 µM DHT and 5 µM E2 were identified as concentrations with relevant effect. It could be seen that E2 shows protecting effects especially in high concentration likely by stronger induction of oxidative response. Stimulation with DHT on the other hand led to a stronger infection by immunosuppression. These effects could be observed in female, but not male hMDMs. More data is needed on the infection under influence of sex hormones to confidently propose a difference in sex hormone response between male and female hMDMs, but a tendency towards stronger response was observed in female hMDMs. As higher infection rate after DHT stimulation of *Leishmania* prior to infection is reported in literature (Lockard, Wilson et al. 2019), it would be interesting to also test stimulation of parasites with both sex hormones before infection. Moreover, DHT could be tested in higher concentration. This could improve the efficacy of stimulation and show stronger effects for further *in vitro* analyses. Additionally, it would be interesting to test the influence of sex hormones on the infection with other *Leishmania* strains.

6 Appendix

6.1 Image Analysis Sequence parameters

Table 6-1: Image analysis sequence used during the experiments. Shown here are the individual image processing steps with their respective parameters.

Image Analysis		
Input Images	DAPI nuclear stain channel	AlexaFluor 647 HSP-90

Image Segmentation		
Find Nuclei	Detects Nuclei of host cell in the DAPI channel	
	Channel: ROI: Method: B Common Threshold: Area: Split Factor: Individual Threshold: Contrast: Output Population:	DAPI None B -0.02 > 40 µm² 16.9 0.14 > -0.71 **Macrophages**
Find Cytoplasm (M1 macrophages)	Detects host (M1 macrophages) cell cytoplasm and defines single cells of host cell in the Alexa 647 channel	
	Channel: Nuclei: Method: Individual Threshold: Output Population:	Alexa 647 Macrophages A 0.06 **Cytoplasm M1**
Find Cytoplasm (M2 macrophages)	Detects host (M2 macrophages) cell cytoplasm and defines single cells of host cell in the Alexa 647 channel	
	Channel: Nuclei:	Alexa 647 Macrophages

	Method: Individual Threshold: Output Population:	A 0.06 **Cytoplasm M2**

Definition of Regions of Interest			
Calculate Intensity Properties			
	Channel: Population: Region: Method: Mean Property Prefix:	DAPI Macrophages Nucleus Standard Nucleus DAPI	Alexa 647 Macrophages Cell Standard Cell Alexa 647
Calculate Morphology properties			
	Population: Region: Method: Mean Property Prefix:	Macrophages Nucleus Standard (area/ roundness) Nucleus	
Calculate Morphology properties for M1			
	Population: Region: Method: Mean Property Prefix:	Macrophages Cytoplasm Standard (area/ roundness) M1 macrophages	
Calculate Morphology properties for M2			
	Population: Region: Method: Mean Property Prefix:	Macrophages Cytoplasm Standard (area/ roundness) M2 macrophages	

Image Segmentation	
Find Spots	Detects intracellular spots within the region of interest in the Alexa 647 channel

	Channel:	Alexa 647
	ROI:	Macrophages
	ROI Region:	Cell
	Method:	B
	Detection Sensitivity:	0.11
	Splitting Coefficient:	0.844
	Calculate Spot Properties	
	Output Population:	**Spots**

Quantifying Properties in Regions			
Calculate Morphology Properties	Quantification and calculation of properties of spots		
	Input Population:	Spots	
	Region:	Spot	
	Method:	Standard (area/roundness/ width/length/ ratio width to length)	
	Output Property Prefix:	Spots	
Calculate Intensity Properties			
	Region:	Spot	Spot
	Method:	Standard (mean/ standard deviation/ coefficient of variance/ median)	Standard (mean)
	Output:	Intensity Spot	Intensity Spot
	Property Prefix:	Alexa 647	DAPI
Calculate Properties	Calculation of Properties		
	Population:	Spots	
	Method:	By Formula	
	Formula:	A/B	
	Variable A:	Spot Alexa 647 mean	

	Variable B:	Spot DAPI mean
	Output Property:	**Alexa/ DAPI intensity ratio**

Identification of intracellular *Leishmania* parasites:		
Select Population I	Selection of parasites from false-positive spots	
	Input Population:	**Spots**
	Method:	Linear Classifier
	Number of Classes:	2
	Relative Spot Intensity:	Spot Roundness
	Corrected Spot Intensity:	Spot Width [µm]
	Uncorrected Spot Peak Intensity:	Spot Length [µm]
	Spot Contrast:	Spot Ratio Width to Length
	Spot Background Intensity:	Spot Alexa 568 Mean
	Spot Area [px²]	Spot DAPI Mean
	Region Intensity:	ALEXA/DAPI intensity ratio
	Spot to Region Intensity:	Intensity Surrounding Alexa 568 Mean
	Spot Area [µm²]:	Intensity Surrounding Alexa 568 Median
	Output Population A:	**Likely Leishmania**
	Output Population B:	**False-positive**
	Population:	Spots
	Method:	Filter by property
	Likely Leishmania:	>0
	Output Population:	Spots selected
	Population:	Spots selected
	Method:	Filter by Property
	Spot Area [µm²]:	> 4
	ALEXA/DAPI intensity ratio:	> 0.3
	Spot Area [µm²]:	< 35
	Corrected Spot Intensity:	> 100 (Staining-dependent)
		Boolean
	Operations:	F1 and F2 and F3 and F4

Relation of macrophages and parasites		
Calculate Properties		
	Population: Method: Related Population: Number of *Leishmania* Output: Property Suffix:	Macrophages By related population *Leishmania* Per Cell
	Population: Method:	**Macrophages** Filter by Property

Identification of Subpopulation		
Select Population II		
	Number of Leishmania – per cell: Output Population: Number of Leishmania – per cell: Output Population: Number of Leishmania – per cell: Output Population:	 >0 Infected macrophages >=2 Double infected macrophages >0 Seriously infected macrophages

Identification of M1 and M2 macrophage subpopulations		
Select Population III **(M1 macrophages)**	Selection of M1-like macrophages from false-positive cells	
	Input Population: Method:	**Macrophages** Filter by Property
	M1 Cytoplasm Roundness: M1 Cytoplasm Length [µm]:	$0.38 \leq x \leq 0.62$ ≤ 0.25

	M1 Cytoplasm Width [µm]: M1 Cytoplasm Width to Length: Output population:	≤ 0.55 0.3 ≤ x ≤ 0.579 **M1 macrophages**
Select Population IV (M2 macrophages)	Selection of M2-like macrophages from false-positive cells	
	Input Population: Method:	**Macrophages** Filter by Property
	M1 Cytoplasm Roundness: M1 Cytoplasm Length [µm]: M1 Cytoplasm Width [µm]: M1 Cytoplasm Width to Length Output population:	0.15 ≤ x ≤ 0.51 ≤ 0.34 ≥ 0.48 ≤ 0.37 **M2 macrophages**

Readout Values		
Define Results		
	Method: Population: Population: Population: Population: Population:	List of outputs Macrophages - number of objects Leishmania - number of objects Infected macrophages - number of objects Seriously infected macrophages - number of objects M1 macrophages- number of objects

	Population:	M2 macrophages- number of objects
	Method: Formula: Population Type: Variable A: number of objects Variable B: number of objects Output name:	Formula Output 1. a/b 2. to 4. a/b*100 Objects 1. Leishmania 2. Infected macrophages 3. Seriously infected macrophages 4. Double infected macrophages Macrophages 1. Leishmania per infected macrophage 2. % infected macrophages 3. % seriously infected macrophages 4. Double infected Macrophages

6.2 P-value tables

POC Viability

L. infantum

A

Amphotericin B

Eh-1	-	0,01 µM	0,1 µM	0,5 µM	1 µM
-		0,6689	0,9927	0,0078	0,0033
1 µM	0,0055	0,4019	0,5207	0,0364	0,9648
5 µM	<0,0001	0,7462	0,0994	0,3817	0,1144
10 µM	0,0002	0,9243	0,2759	0,6909	0,1642

Miltefosin

Eh-1	-	1 µM	5 µM	10 µM	15 µM
-		0,3511	0,0506	0,6948	0,0143
1 µM	0,2016	0,0443	0,0656	0,2052	0,3585
5 µM	0,0012	0,1857	0,0378	0,0052	0,0092
10 µM	0,0868	0,1369	0,4916	0,4145	0,0024

Amphotericin B

Eh-1	-	0,01 µM	0,1 µM	0,5 µM	1 µM
-		0,0576	0,9423	0,4674	0,5355
1 µM	0,0031	0,3596	0,1916	0,3893	0,0158
5 µM	0,0003	0,4970	0,0555	0,9600	0,0841
10 µM	<0,0001	0,9944	0,0088	0,0436	0,0096

Miltefosin

Eh-1	-	1 µM	5 µM	10 µM	15 µM
-		0,2033	0,1097	0,9730	0,8125
1 µM	0,9558	0,2020	0,9099	0,5091	0,1666
5 µM	0,5906	0,0835	0,4665	0,3210	0,2674
10 µM	0,3083	0,4812	0,0415	0,3943	0,8698

Amphotericin B

Imiquimod	-	0,01 µM	0,1 µM	0,5 µM	1 µM
-		0,0044	0,0743	0,3798	0,5695
1 µM	0,8528	0,1544	0,5204	0,0971	0,3889
5 µM	0,0510	0,6352	0,1439	0,9465	0,4016
10 µM	0,0163	0,2647	0,0067	0,4755	0,1964

Miltefosin

Imiquimod	-	1 µM	5 µM	10 µM	15 µM
-		0,0237	0,1548	0,0802	0,9854
1 µM	0,4587	0,5773	0,1160	0,0348	0,0271
5 µM	0,0248	0,3133	0,0052	0,8846	0,0081
10 µM	0,3011	0,7321	0,0194	0,9314	0,0081

Amphotericin B

Imiquimod	-	0,01 µM	0,1 µM	0,5 µM	1 µM
-		0,1557	0,8997	0,8657	0,0699
1 µM	0,7625	0,0863	0,1185	0,3756	0,5096
5 µM	0,0005	0,1542	0,0014	0,9131	0,2042
10 µM	0,0002	0,3744	0,0124	0,6827	0,1363

Miltefosin

Imiquimod	-	1 µM	5 µM	10 µM	15 µM
-		0,0690	0,2967	0,0526	0,0621
1 µM	0,0568	0,1998	0,0215	0,8135	0,0007
5 µM	0,0408	0,7067	0,0017	0,0333	0,0013
10 µM	0,0011	0,9812	0,0004	0,3007	0,0009

C

L. major

B

Amphotericin B

	-	0,01 µM	0,1 µM	0,5 µM	1 µM
-		0,2843	0,137	0,5824	0,6812
1 µM	0,9777	0,662	0,0529	0,2269	0,6878
5 µM	0,7866	0,5582	0,0107	0,3234	0,3255
10 µM	0,7050	0,2264	0,0068	0,1774	0,4161

Miltefosin

	-	1 µM	5 µM	10 µM	15 µM
-		0,2950	0,8227	0,2951	0,1480
1 µM	0,9312	0,7531	0,0054	0,0351	0,3412
5 µM	0,1009	0,8204	0,0012	0,7767	0,025
10 µM	0,0105	0,2241	0,0214	0,1064	0,0331

male

Amphotericin B

	-	0,01 µM	0,1 µM	0,5 µM	1 µM
-		0,3758	0,9596	0,6938	0,7000
1 µM	0,7957	0,9432	0,1899	0,0686	0,7865
5 µM	0,0237	0,1358	0,0197	0,7239	0,1447
10 µM	0,0052	0,7108	0,0633	0,8903	0,0163

Miltefosin

	-	1 µM	5 µM	10 µM	15 µM
-		0,196	0,2184	0,0364	0,0764
1 µM	0,2597	0,5039	0,0537	0,7277	0,1367
5 µM	0,4040	0,8549	0,0884	0,3755	0,3364
10 µM	0,1099	0,6904	0,0843	0,1098	0,2317

female

Amphotericin B

	-	0,01 µM	0,1 µM	0,5 µM	1 µM
-		0,1978	0,2288	0,3616	0,6203
1 µM	0,1090	0,5043	0,2133	0,5346	0,7706
5 µM	0,0189	0,779	0,8058	0,5961	0,1692
10 µM	0,0754	0,1334	0,221	0,1463	0,8811

Miltefosin

	-	1 µM	5 µM	10 µM	15 µM
-		0,8626	0,819	0,1882	0,804
1 µM	0,9847	0,5749	0,8645	0,2037	0,8681
5 µM	0,5534	0,3500	0,8933	0,9854	0,7894
10 µM	0,126	0,5742	0,1081	0,5263	0,0816

male

Amphotericin B

	-	0,01 µM	0,1 µM	0,5 µM	1 µM
-		0,4823	0,4396	0,3578	0,8316
1 µM	0,4307	0,1520	0,2046	0,4408	0,0075
5 µM	0,6995	0,5049	0,0752	0,2681	0,0891
10 µM	0,3564	0,6576	0,0441	0,7872	0,1824

Miltefosin

	-	1 µM	5 µM	10 µM	15 µM
-		0,4975	0,9536	0,3349	0,7038
1 µM	0,2719	0,3461	0,0916	0,5436	0,0783
5 µM	0,0864	0,2385	0,1764	0,9508	< 0,0001
10 µM	0,2687	0,5556	0,0155	0,0093	0,0110

female

D

- tested against infected untreated
- tested against Eh-1/Imi
- tested against AmpB/Mil

Figure 6-1: Overview of p-values for the statistical significance calculations during combination treatment displayed in **Figure 3-16**.

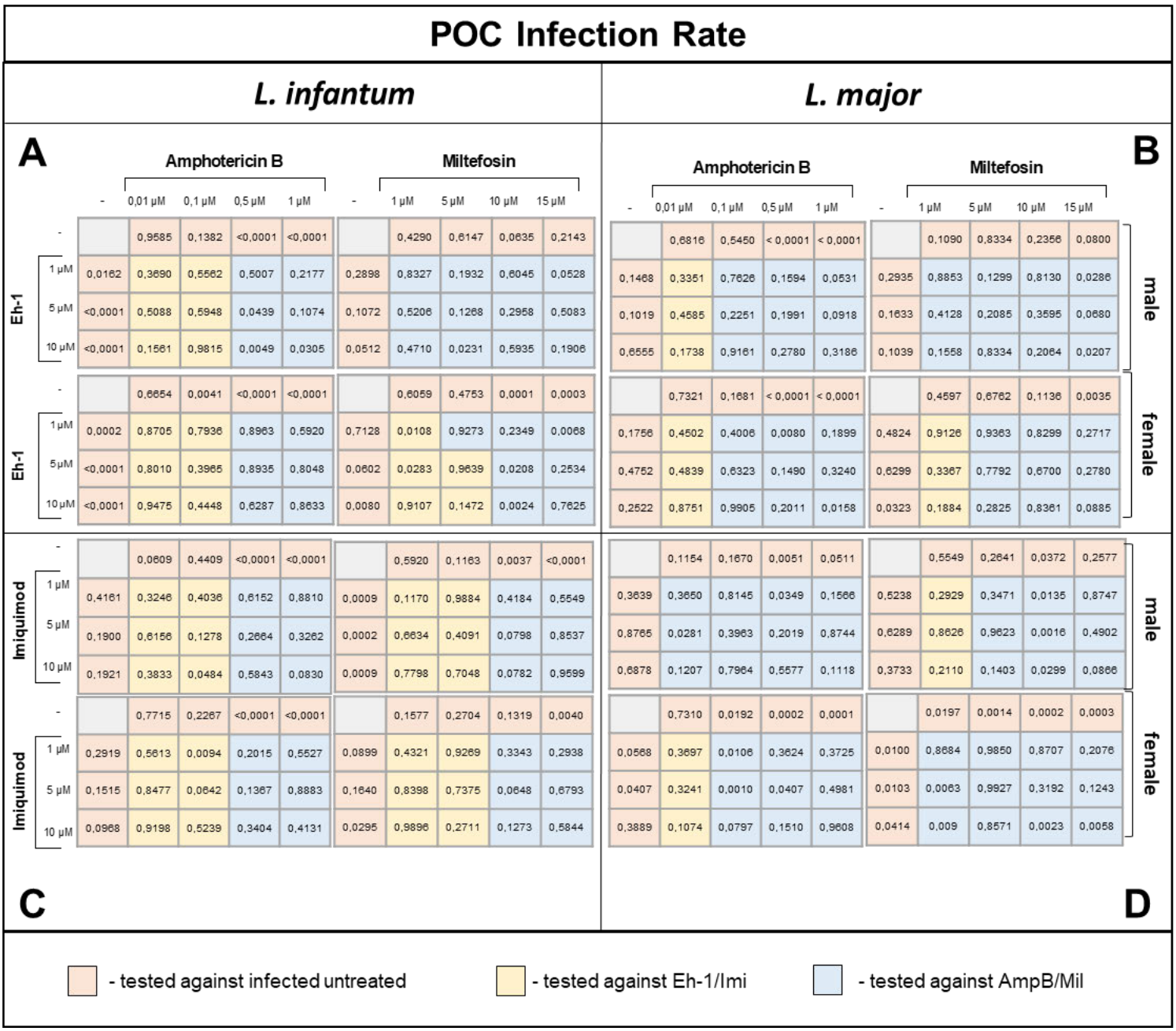

Figure 6-2: Overview of p-values for the statistical significance calculations during combination treatment displayed in **Figure 3-18**.

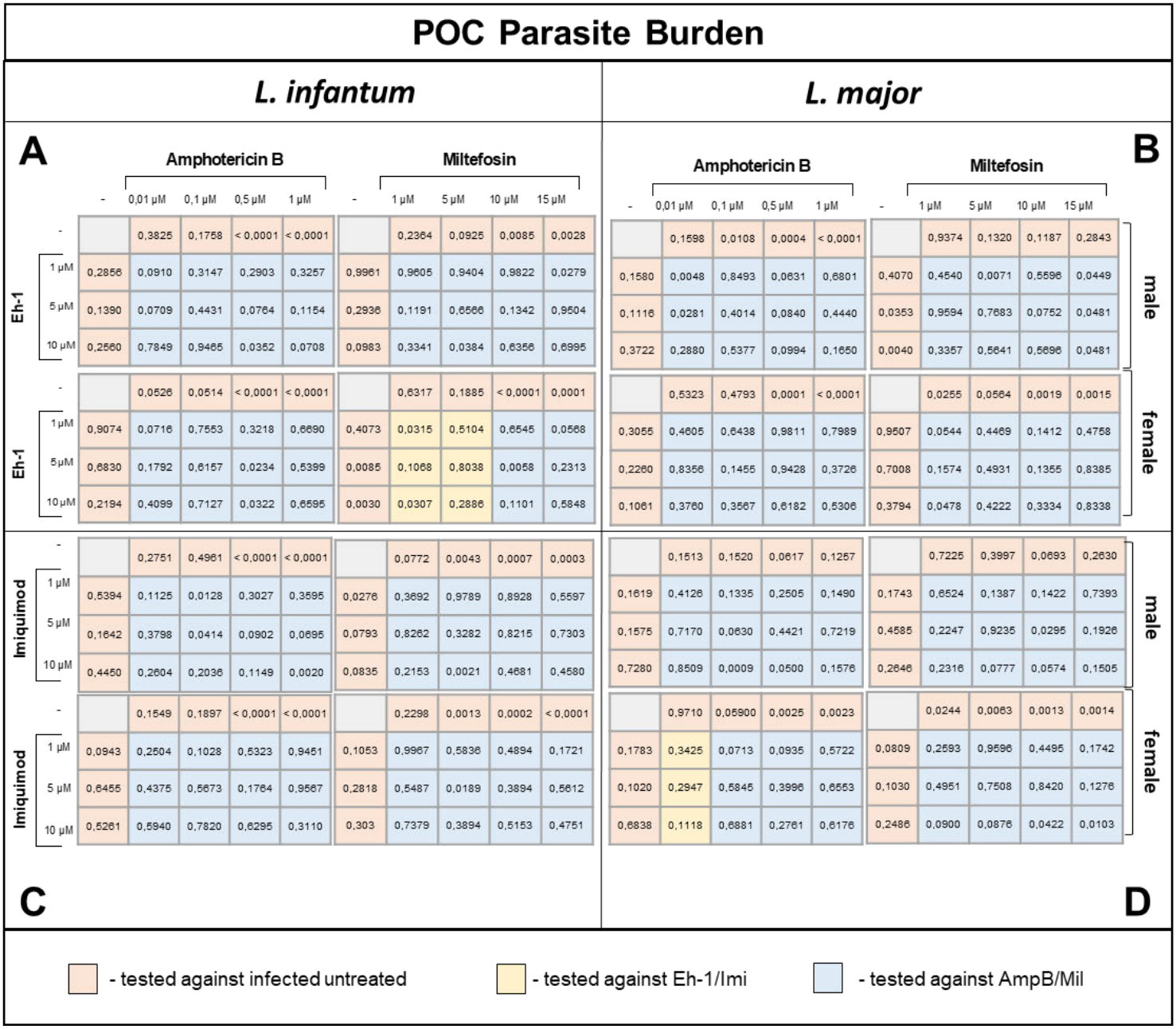

Figure 6-3: Overview of p-values for the statistical significance calculations during combination treatment displayed in **Figure 3-20**.

6.3 Discussion of supernatants with IFN-γ expression

For one female (f3) and one male (m8) individual IFN-γ could be detected in the supernatant after infection with *L. infantum*. Since the release of IFN-γ from macrophages is induced upon simultaneous stimulation with IL-12 and IL-18, and IL-12p70 was not present in supernatants, the most likely explanation for IFN-γ expression is the presence of other regulatory immune cells like e.g. NKT cells (Darwich, Coma et al. 2009). The FACS analysis of samples after MACS showed a low degree of impurity with other lymphocytes, which could induce IFN-γ production upon antigen presentation by macrophages. Further supporting this is the fact, that in these supernatants much higher levels of cytokines were detected.

Interestingly, Eh-1 treatment led to much higher production of IFN-γ compared to untreated cells for m8 and reduction of infection rate to around 60 POC. *Eh*LPPG was shown to induce IFN-γ production in NKT cells after presentation of *Eh*LPPG via CD1d (Fehling, Choy et al. 2020). This could indicate that macrophage cultures of m8 contained NKT cells, which showed IFN-γ production after presentation of Eh-1 by macrophages. IFN-γ is a potent inducer of NO production by iNOS (Bogdan 2020). High Arg1 levels could indicate a strong oxidative response causing parasite killing.

Interestingly, when treated with Eh-1, f3 showed an even stronger reduction of infection rate to around 35 POC. Since IL-4 is known to induce CCL17 expression (Wirnsberger, Hebenstreit et al. 2006), high CCL17 levels in samples of f3 suggest that IL-4 is present. This is accompanied by abrogation of IFN-γ expression and high Arg1 level. This is contradicting, since the absence of IFN-γ suggests lower induction of protective NO response, but high Arginase level could indicate high NO production and parasite killing. Together, this suggests that for f3 Eh-1 mediated protection to *L. infantum* infection independent of protective cytokine expression, although further evidence is needed to support this.

Upon treatment with Amphotericin B, for f3 IFN-γ expression was increased very strongly with high level of CXCL10 and low level of IL-10 associated with reduction of infection rate to around 75 POC. The cytokines found in the sample suggest a strong oxidative response. Interestingly, for high IFN-γ expression induced by Amphotericin B, a lower leishmanicidal effect was observed compared to Eh-1 treatment, where no

IFN-γ production was found, further supporting an effect independent of oxidative response during Eh-1 treatment of *L. infantum* infection in female macrophages.

On the other hand, strong reduction of infection rate to around 35 POC was observed for m8. Here, also a strong increase in IFN-γ was seen compared to uninfected cells with a reduction in Arg1 level. Also, no CCL17 could be detected in these samples, which indicates absence of IL-4 leading to stronger type 1 oxidative response, while IL-10 effect was likely ameliorated by CXCL10. Together, these effects showed high degree of protection.

In combination, the IFN-γ inducing effect of Amphotericin B seems to be suppressed by Eh-1 while CCL2 and CXCL10 show higher levels than during Eh-1 treatment. Arg1 and IL-10 levels are further reduced compared to both mono treatments indicating a stronger type 1 response and increased NO production. As infection rate is not lowered in combination compared to Eh-1 mono treatment, most likely the cytokine independent mechanism of Eh-1 shows a stronger protective effect than cytokine mediated NO production.

6.4 Declaration on oath

I confirm that I wrote this thesis on my own, without using any other than the declared sources, references and tools. All passages included from other publications or presentations, whether verbatim or in content, have been identified as such.

Signature: Max Hüppner

7 References

Ahmed, H., C. R. Curtis, S. Tur-Gracia, T. O. Olatunji, K. C. Carter and R. A. M. Williams (2020). "Drug combinations as effective anti-leishmanials against drug resistant Leishmania mexicana." RSC Med Chem **11**(8): 905-912.

Alberts, B. (2008). Molecular biology of the cell. New York, Garland Science.

Alexander, J., K. C. Carter, N. Al-Fasi, A. Satoskar and F. Brombacher (2000). "Endogenous IL-4 is necessary for effective drug therapy against visceral leishmaniasis." European Journal of Immunology **30**(10): 2935-2943.

Angelika Foitzik, K. B. t., Alexander Schreiner. (2015, 08.2015). "Opera Phenix High Content Screening System Technical Performance: Crosstalk Suppression." Retrieved 30.09.2022, 13:10, 2022.

Bajaj, V., N. Gadi, A. P. Spihlman, S. C. Wu, C. H. Choi and V. R. Moulton (2020). "Aging, Immunity, and COVID-19: How Age Influences the Host Immune Response to Coronavirus Infections?" Front Physiol **11**: 571416.

Bates, P. A. (2007). "Transmission of Leishmania metacyclic promastigotes by phlebotomine sand flies." Int J Parasitol **37**(10): 1097-1106.

Beach, D. H., G. G. Holz, Jr. and G. E. Anekwe (1979). "Lipids of Leishmania promastigotes." J Parasitol **65**(2): 201-216.

Behl, C., M. Widmann, T. Trapp and F. Holsboer (1995). "17-beta estradiol protects neurons from oxidative stress-induced cell death in vitro." Biochem Biophys Res Commun **216**(2): 473-482.

Berman, J. D. and D. J. Wyler (1980). "An in vitro model for investigation of chemotherapeutic agents in leishmaniasis." J Infect Dis **142**(1): 83-86.

Bernin, H. and H. Lotter (2014). "Sex bias in the outcome of human tropical infectious diseases: influence of steroid hormones." J Infect Dis **209 Suppl 3**: S107-113.

Berthois, Y., J. A. Katzenellenbogen and B. S. Katzenellenbogen (1986). "Phenol red in tissue culture media is a weak estrogen: implications concerning the study of estrogen-responsive cells in culture." Proc Natl Acad Sci U S A **83**(8): 2496-2500.

Besteiro, S., R. A. Williams, G. H. Coombs and J. C. Mottram (2007). "Protein turnover and differentiation in Leishmania." Int J Parasitol **37**(10): 1063-1075.

Biolegend. (2019, 30.05.2019). "Zombie UV™ Fixable Viability Kit." 4. Retrieved 22.10.2022, 17:00, 2022.

Biolegend. (2022). "LEGENDplex Multiplex Assays." Retrieved 18.08.2022, 12:30, 2022, from https://www.biolegend.com/en-us/legendplex.

Birmingham, A., L. M. Selfors, T. Forster, D. Wrobel, C. J. Kennedy, E. Shanks, J. Santoyo-Lopez, D. J. Dunican, A. Long, D. Kelleher, Q. Smith, R. L. Beijersbergen, P. Ghazal and C. E. Shamu (2009). "Statistical methods for analysis of high-throughput RNA interference screens." Nat Methods **6**(8): 569-575.

Bogdan, C. (2020). "Macrophages as host, effector and immunoregulatory cells in leishmaniasis: Impact of tissue micro-environment and metabolism." Cytokine X **2**(4): 100041.

BosterBIO. (2022). "FLOW CYTOMETRY PRINCIPLE." Retrieved 08.11.2022, 17:00, 2022, from https://www.bosterbio.com/protocol-and-troubleshooting/flow-cytometry-principle.

Brandau, S., A. Dresel and J. Clos (1995). "High constitutive levels of heat-shock proteins in human-pathogenic parasites of the genus Leishmania." Biochem J **310 (Pt 1)**: 225-232.

Broeren, C. P., G. S. Gray, B. M. Carreno and C. H. June (2000). "Costimulation light: activation of CD4+ T cells with CD80 or CD86 rather than anti-CD28 leads to a Th2 cytokine profile." J Immunol **165**(12): 6908-6914.

Buates, S. and G. Matlashewski (1999). "Treatment of experimental leishmaniasis with the immunomodulators imiquimod and S-28463: efficacy and mode of action." J Infect Dis **179**(6): 1485-1494.

Bubna, A. K. (2015). "Imiquimod - Its role in the treatment of cutaneous malignancies." Indian J Pharmacol **47**(4): 354-359.

Buxade, M., H. Huerga Encabo, M. Riera-Borrull, L. Quintana-Gallardo, P. Lopez-Cotarelo, M. Tellechea, S. Martinez-Martinez, J. M. Redondo, J. Martin-Caballero, J. M. Flores, E. Bosch, J. L. Rodriguez-Fernandez, J. Aramburu and C. Lopez-Rodriguez (2018). "Macrophage-specific MHCII expression is regulated by a remote Ciita enhancer controlled by NFAT5." J Exp Med **215**(11): 2901-2918.

Cai, J., Y. Hong, C. Weng, C. Tan, J. Imperato-McGinley and Y. S. Zhu (2011). "Androgen stimulates endothelial cell proliferation via an androgen receptor/VEGF/cyclin A-mediated mechanism." Am J Physiol Heart Circ Physiol **300**(4): H1210-1221.

Caldwell, R. W., P. C. Rodriguez, H. A. Toque, S. P. Narayanan and R. B. Caldwell (2018). "Arginase: A Multifaceted Enzyme Important in Health and Disease." Physiol Rev **98**(2): 641-665.

Carneiro, M. B., M. E. Lopes, L. S. Hohman, A. Romano, B. A. David, R. Kratofil, P. Kubes, M. L. Workentine, A. C. Campos, L. Q. Vieira and N. C. Peters (2020). "Th1-Th2 Cross-Regulation Controls Early Leishmania Infection in the Skin by Modulating the Size of the Permissive Monocytic Host Cell Reservoir." Cell Host Microbe **27**(5): 752-768 e757.

Carrera, L., R. T. Gazzinelli, R. Badolato, S. Hieny, W. Muller, R. Kuhn and D. L. Sacks (1996). "Leishmania promastigotes selectively inhibit interleukin 12 induction in bone marrow-derived macrophages from susceptible and resistant mice." J Exp Med **183**(2): 515-526.

Chakraborty, P., D. Ghosh and M. K. Basu (2001). "Modulation of Macrophage Mannose Receptor Affects the Uptake of Virulent and Avirulentleishmania Donovanipromastigotes." Journal of Parasitology **87**(5): 1023-1027.

Chavez-Galan, L., M. L. Olleros, D. Vesin and I. Garcia (2015). "Much More than M1 and M2 Macrophages, There are also CD169(+) and TCR(+) Macrophages." Front Immunol **6**: 263.

chemistds, T. (2012, 2012-10-08 15:38:13). "This is a revised image of amphotericin B, it replaces an image used on EN wikipedia that had several incorrect stereocentres." Retrieved 04.11.2022, 13:20, 2022, from https://de.wikipedia.org/wiki/Amphotericin_B#/media/Datei:Amphotericin_B_new.svg.

Chen, B., W. H. Piel, L. Gui, E. Bruford and A. Monteiro (2005). "The HSP90 family of genes in the human genome: insights into their divergence and evolution." Genomics **86**(6): 627-637.

Cohen, B. E. (2016). "The Role of Signaling via Aqueous Pore Formation in Resistance Responses to Amphotericin B." Antimicrob Agents Chemother **60**(9): 5122-5129.

Cunha, J. P. (2021, 9/28/2021). "ALDARA SIDE EFFECTS CENTER." Retrieved 08.11.2022, 18:50, 2022, from https://www.rxlist.com/aldara-side-effects-drug-center.htm#overview.

Dar, M. J., F. U. Din and G. M. Khan (2018). "Sodium stibogluconate loaded nano-deformable liposomes for topical treatment of leishmaniasis: macrophage as a target cell." Drug Deliv **25**(1): 1595-1606.

Darwich, L., G. Coma, R. Pena, R. Bellido, E. J. Blanco, J. A. Este, F. E. Borras, B. Clotet, L. Ruiz, A. Rosell, F. Andreo, R. M. Parkhouse and M. Bofill (2009). "Secretion of interferon-gamma by human macrophages demonstrated at the single-cell level after costimulation with interleukin (IL)-12 plus IL-18." Immunology **126**(3): 386-393.

Dayakar, A., S. Chandrasekaran, S. V. Kuchipudi and S. K. Kalangi (2019). "Cytokines: Key Determinants of Resistance or Disease Progression in Visceral Leishmaniasis: Opportunities for Novel Diagnostics and Immunotherapy." Front Immunol **10**: 670.

de Araujo Albuquerque, L. P., A. M. da Silva, F. M. de Araujo Batista, I. de Souza Sene, D. L. Costa and C. H. N. Costa (2021). "Influence of sex hormones on the immune response to leishmaniasis." Parasite Immunol **43**(10-11): e12874.

De Miguel, C., P. Pelegrin, A. Baroja-Mazo and S. Cuevas (2021). "Emerging Role of the Inflammasome and Pyroptosis in Hypertension." Int J Mol Sci **22**(3).

de Veer, M. J., J. M. Curtis, T. M. Baldwin, J. A. DiDonato, A. Sexton, M. J. McConville, E. Handman and L. Schofield (2003). "MyD88 is essential for clearance of Leishmania major: possible role for lipophosphoglycan and Toll-like receptor 2 signaling." Eur J Immunol **33**(10): 2822-2831.

Eiz-Vesper, B. and H. M. Schmetzer (2020). "Antigen-Presenting Cells: Potential of Proven und New Players in Immune Therapies." Transfus Med Hemother **47**(6): 429-431.

Ellis, D. (2002). "Amphotericin B: spectrum and resistance." J Antimicrob Chemother **49 Suppl 1**: 7-10.

Elmahallawy, E. K., A. A. M. Alkhaldi and A. A. Saleh (2021). "Host immune response against leishmaniasis and parasite persistence strategies: A review and assessment of recent research." Biomed Pharmacother **139**: 111671.

FDA. (2014, 03.2022). "IMPAVIDO (miltefosine) capsules, for oral use." Retrieved 13.10.2022, 16:50, 2022, from https://www.accessdata.fda.gov/drugsatfda_docs/label/2014/204684s000lbl.pdf.

FDA. (2022). "2021 First Generic Drug Approvals." Retrieved 13.10.2022, 16:50, 2022, from https://www.fda.gov/drugs/drug-and-biologic-approval-and-ind-activity-reports/2021-first-generic-drug-approvals.

Fehling, H., S. L. Choy, F. Ting, D. Landschulze, H. Bernin, S. C. Lender, M. Muhlenpfordt, E. Bifeld, J. Eick, C. Marggraff, N. Kottmayr, M. Groneberg, S. Hoenow, J. Sellau, J. Clos, C. Meier and H. Lotter (2020). "Antileishmanial Effects of Synthetic EhPIb Analogs Derived from the Entamoeba histolytica Lipopeptidephosphoglycan." Antimicrob Agents Chemother **64**(7).

Fehling, H., H. Niss, A. Bea, N. Kottmayr, C. Brinker, S. Hoenow, J. Sellau, T. W. Gilberger, F. Ting, D. Landschulze, C. Meier, J. Clos and H. Lotter (2021). "High Content Analysis of Macrophage-Targeting EhPIb-Compounds against Cutaneous and Visceral Leishmania Species." Microorganisms **9**(2).

Figueiredo, W. M. E., S. M. Viana, D. T. Alves, P. V. Guerra, Z. C. B. Coelho, H. S. Barbosa and M. J. Teixeira (2017). "Protection mediated by chemokine CXCL10 in BALB/c mice infected by Leishmania infantum." Mem Inst Oswaldo Cruz **112**(8): 561-568.

Fish, E. N. (2008). "The X-files in immunity: sex-based differences predispose immune responses." Nat Rev Immunol **8**(9): 737-744.

Frost, J. (2018). "How t-Tests Work: t-Values, t-Distributions, and Probabilities." Retrieved 22.09.22, 11:15, 2022, from https://statisticsbyjim.com/hypothesis-testing/t-tests-t-values-t-distributions-probabilities/.

Fuentes-Nava, G., A. Tirado-Sanchez, E. A. Fernandez-Figueroa, S. Sanchez-Montes, I. Becker and A. Bonifaz (2021). "Efficacy of imiquimod 5% cream as first-line management in cutaneous leishmaniasis caused by Leishmania mexicana." Rev Soc Bras Med Trop **54**: e0305-2020.

Gasteiger, G., A. D'Osualdo, D. A. Schubert, A. Weber, E. M. Bruscia and D. Hartl (2017). "Cellular Innate Immunity: An Old Game with New Players." J Innate Immun **9**(2): 111-125.

Ghaffarifar, F., M. Foroutan, S. Molaei and E. Moradi-Asl (2021). "Synergistic Anti-Leishmanial Activities of Morphine and Imiquimod on Leishmania infantum (MCAN/ES/98/LIM-877)." J Arthropod Borne Dis **15**(2): 236-254.

Global Health, D. o. P. D. a. M. (2020, February 14, 2020). "Parasites - Leishmaniasis." Retrieved 08.09.22, 15:20, 2022, from https://www.cdc.gov/parasites/Leishmaniasis/.

Guth, S. E., S. Bohm, B. H. Mussler and G. Eisenbrand (2004). "Sensitive in vitro test systems to determine androgenic/antiandrogenic activity." Mol Nutr Food Res **48**(4): 282-291.

Hemker, M. B., G. Cheroutre, R. van Zwieten, P. A. Maaskant-van Wijk, D. Roos, J. A. Loos, C. E. van der Schoot and A. E. von dem Borne (2003). "The Rh complex exports ammonium from human red blood cells." Br J Haematol **122**(2): 333-340.

Herwaldt, B. L. and J. D. Berman (1992). "Recommendations for treating leishmaniasis with sodium stibogluconate (Pentostam) and review of pertinent clinical studies." Am J Trop Med Hyg **46**(3): 296-306.

Inc., T. A. S. f. P. (2022). "Leishmania." Retrieved 09.09.22, 13:20, 2022, from http://parasite.org.au/para-site/text/leishmania-text.html.

Italiani, P. and D. Boraschi (2014). "From Monocytes to M1/M2 Macrophages: Phenotypical vs. Functional Differentiation." Front Immunol **5**: 514.

Jacobsen, H. and S. L. Klein (2021). "Sex Differences in Immunity to Viral Infections." Front Immunol **12**: 720952.

Jü. (2012). "Imiquimod Formula." Retrieved 03.11.2022, 13:35, 2022, from https://de.wikipedia.org/wiki/Imiquimod#/media/Datei:Imiquimod_Formula_V.1.svg.

Jü. (2013, 11. Februar 2013). "Miltefosine Structural Formula." Retrieved 03.11.2022, 13:30, 2022, from https://de.wikipedia.org/wiki/Miltefosin#/media/Datei:Miltefosine_Structural_Formula_V.2.svg.

Jü. (2020). "Dihydrotestosteron." Retrieved 07.11.2022, 17:10, 2022, from https://de.wikipedia.org/wiki/Dihydrotestosteron#/media/Datei:Dihydrotestosterone_Structural_Formula_V1.svg.

Kane, M. M. and D. M. Mosser (2001). "The role of IL-10 in promoting disease progression in leishmaniasis." J Immunol **166**(2): 1141-1147.

Karpuzoglu-Sahin, E., B. D. Hissong and S. Ansar Ahmed (2001). "Interferon-γ levels are upregulated by 17-β-estradiol and diethylstilbestrol." Journal of Reproductive Immunology **52**(1-2): 113-127.

Khademvatan, S., M. J. Gharavi, F. Rahim and J. Saki (2011). "Miltefosine-induced apoptotic cell death on Leishmania major and L. tropica strains." Korean J Parasitol **49**(1): 17-23.

Khademvatan, S., M. J. Gharavi and J. Saki (2011). "Miltefosine induces metacaspase and PARP genes expression in Leishmania infantum." The Brazilian Journal of Infectious Diseases **15**(5): 442-448.

Khattak, F. A., N. U. Akbar, M. Riaz, M. Hussain, K. Rehman, S. N. Khan and T. A. Khan (2021). "Novel IL-12Rbeta1 deficiency-mediates recurrent cutaneous leishmaniasis." Int J Infect Dis **112**: 338-345.

Komai, K., T. Shichita, M. Ito, M. Kanamori, S. Chikuma and A. Yoshimura (2017). "Role of scavenger receptors as damage-associated molecular pattern receptors in Toll-like receptor activation." Int Immunol **29**(2): 59-70.

Kumar, A., S. Das, A. Mandal, S. Verma, K. Abhishek, A. Kumar, V. Kumar, A. K. Ghosh and P. Das (2018). "Leishmania infection activates host mTOR for its survival by M2 macrophage polarization." Parasite Immunol **40**(11): e12586.

Laboratories, M. C. (2022, 2022). "Estradiol, Serum." Retrieved 09.11.2022, 19:10, 2022, from https://endocrinology.testcatalog.org/show/EEST.

Le P. Ngo, M. P., Jing Ge, and Bevin Engelward (2016). Whole blood hemolysis with isotonic ammonium chloride solution, nextgen-protocols.

Lee, G. T., J. H. Kim, S. J. Kwon, M. N. Stein, J. H. Hong, N. Nagaya, S. Billakanti, M. M. Kim, W. J. Kim and I. Y. Kim (2019). "Dihydrotestosterone Increases Cytotoxic Activity of Macrophages on Prostate Cancer Cells via TRAIL." Endocrinology **160**(9): 2049-2060.

Lee, S. J., S. Evers, D. Roeder, A. F. Parlow, J. Risteli, L. Risteli, Y. C. Lee, T. Feizi, H. Langen and M. C. Nussenzweig (2002). "Mannose receptor-mediated regulation of serum glycoprotein homeostasis." Science **295**(5561): 1898-1901.

Liu, D. and J. E. Uzonna (2012). "The early interaction of Leishmania with macrophages and dendritic cells and its influence on the host immune response." Front Cell Infect Microbiol **2**: 83.

Lockard, R. D., M. E. Wilson and N. E. Rodriguez (2019). "Sex-Related Differences in Immune Response and Symptomatic Manifestations to Infection with Leishmania Species." J Immunol Res **2019**: 4103819.

Lotter, H., N. Gonzalez-Roldan, B. Lindner, F. Winau, A. Isibasi, M. Moreno-Lafont, A. J. Ulmer, O. Holst, E. Tannich and T. Jacobs (2009). "Natural killer T cells activated by a lipopeptidophosphoglycan from Entamoeba histolytica are critically important to control amebic liver abscess." PLoS Pathog **5**(5): e1000434.

Mann, S., K. Frasca, S. Scherrer, A. F. Henao-Martinez, S. Newman, P. Ramanan and J. A. Suarez (2021). "A Review of Leishmaniasis: Current Knowledge and Future Directions." Curr Trop Med Rep **8**(2): 121-132.

Maspi, N., A. Abdoli and F. Ghaffarifar (2016). "Pro- and anti-inflammatory cytokines in cutaneous leishmaniasis: a review." Pathog Glob Health **110**(6): 247-260.

Melby, P. C., B. Chandrasekar, W. Zhao and J. E. Coe (2001). "The hamster as a model of human visceral leishmaniasis: progressive disease and impaired generation of nitric oxide in the face of a prominent Th1-like cytokine response." J Immunol **166**(3): 1912-1920.

Merck. (2022). "In Vitro Differentiation of Human PBMC Derived Monocytes into M1 or M2 Macrophages in a Serum-free and Xeno-free Cell Culture Media." Retrieved 04.07.22, 17:10, 2022, from https://www.sigmaaldrich.com/DE/de/technical-documents/protocol/cell-culture-and-cell-culture-analysis/primary-cell-culture/pbmc-macrophage-differentiation.

Mesa-Arango, A. C., N. Trevijano-Contador, E. Roman, R. Sanchez-Fresneda, C. Casas, E. Herrero, J. C. Arguelles, J. Pla, M. Cuenca-Estrella and O. Zaragoza (2014). "The production of reactive oxygen species is a universal action mechanism of Amphotericin B against pathogenic yeasts and contributes to the fungicidal effect of this drug." Antimicrob Agents Chemother **58**(11): 6627-6638.

Mogensen, T. H. (2009). "Pathogen recognition and inflammatory signaling in innate immune defenses." Clin Microbiol Rev **22**(2): 240-273, Table of Contents.

Mollinedo, F. (2014). "Alkylphospholipids and Leishmaniasis." Leishmaniasis - Trends in Epidemiology, Diagnosis and Treatment.

Moradin, N. and A. Descoteaux (2012). "Leishmania promastigotes: building a safe niche within macrophages." Front Cell Infect Microbiol **2**: 121.

Motulsky, H. J. (2016). "GraphPad Statistics Guide." Retrieved 09.08.2022, 2022, from https://www.graphpad.com/guides/prism/latest/statistics/index.htm.

Mukhopadhyay, D., N. K. Das, S. Roy, S. Kundu, J. N. Barbhuiya and M. Chatterjee (2011). "Miltefosine effectively modulates the cytokine milieu in Indian post kala-azar dermal leishmaniasis." J Infect Dis **204**(9): 1427-1436.

Muraille, E., O. Leo and M. Moser (2014). "TH1/TH2 paradigm extended: macrophage polarization as an unappreciated pathogen-driven escape mechanism?" Front Immunol **5**: 603.

Murphy, K. and C. Weaver (2016). Janeway's immunobiology. New York, NY, Garland Science/Taylor & Francis Group, LLC.

NEUROtiker. (2007, 29.07.2007). "Struktur von Estradiol (Östradiol)." Retrieved 07.11.2022, 17:30, 2022.

Nielsen, M. C., M. N. Andersen and H. J. Moller (2020). "Monocyte isolation techniques significantly impact the phenotype of both isolated monocytes and derived macrophages in vitro." Immunology **159**(1): 63-74.

Ong, S. M., K. Teng, E. Newell, H. Chen, J. Chen, T. Loy, T. W. Yeo, K. Fink and S. C. Wong (2019). "A Novel, Five-Marker Alternative to CD16-CD14 Gating to Identify the Three Human Monocyte Subsets." Front Immunol **10**: 1761.

Orecchioni, M., Y. Ghosheh, A. B. Pramod and K. Ley (2019). "Macrophage Polarization: Different Gene Signatures in M1(LPS+) vs. Classically and M2(LPS-) vs. Alternatively Activated Macrophages." Front Immunol **10**: 1084.

Parameswaran, N. and S. Patial (2010). "Tumor necrosis factor-alpha signaling in macrophages." Crit Rev Eukaryot Gene Expr **20**(2): 87-103.

Patel, A. A., F. Ginhoux and S. Yona (2021). "Monocytes, macrophages, dendritic cells and neutrophils: an update on lifespan kinetics in health and disease." Immunology **163**(3): 250-261.

Pentikainen, V., K. Erkkila, L. Suomalainen, M. Parvinen and L. Dunkel (2000). "Estradiol acts as a germ cell survival factor in the human testis in vitro." J Clin Endocrinol Metab **85**(5): 2057-2067.

Pigott, D. M., S. Bhatt, N. Golding, K. A. Duda, K. E. Battle, O. J. Brady, J. P. Messina, Y. Balard, P. Bastien, F. Pratlong, J. S. Brownstein, C. C. Freifeld, S. R. Mekaru, P. W. Gething, D. B. George, M. F. Myers, R. Reithinger and S. I. Hay (2014). "Global distribution maps of the leishmaniases." Elife **3**.

Pinto-Martinez, A. K., J. Rodriguez-Duran, X. Serrano-Martin, V. Hernandez-Rodriguez and G. Benaim (2018). "Mechanism of Action of Miltefosine on Leishmania donovani Involves the Impairment of Acidocalcisome Function and the Activation of the Sphingosine-Dependent Plasma Membrane Ca(2+) Channel." Antimicrob Agents Chemother **62**(1).

Rey-Giraud, F., M. Hafner and C. H. Ries (2012). "In vitro generation of monocyte-derived macrophages under serum-free conditions improves their tumor promoting functions." PLoS One **7**(8): e42656.

Rogers, A. and R. Eastell (2001). "The effect of 17β-estradiol on production of cytokines in cultures of peripheral blood." Bone **29**(1): 30-34.

Sacks, D. L., A. Barral and F. A. Neva (1983). "Thermosensitivity patterns of Old vs. New World cutaneous strains of Leishmania growing within mouse peritoneal macrophages in vitro." Am J Trop Med Hyg **32**(2): 300-304.

Sanchez-Canete, M. P., L. Carvalho, F. J. Perez-Victoria, F. Gamarro and S. Castanys (2009). "Low plasma membrane expression of the miltefosine transport complex renders Leishmania braziliensis refractory to the drug." Antimicrob Agents Chemother **53**(4): 1305-1313.

Sauder, D. N. (2004). "Mechanism of action and emerging role of immune response modifier therapy in dermatologic conditions." J Cutan Med Surg **8 Suppl 3**: 3-12.

Schwarz, T., K. A. Remer, W. Nahrendorf, A. Masic, L. Siewe, W. Muller, A. Roers and H. Moll (2013). "T cell-derived IL-10 determines leishmaniasis disease outcome and is suppressed by a dendritic cell based vaccine." PLoS Pathog **9**(6): e1003476.

Scotland, R. S., M. J. Stables, S. Madalli, P. Watson and D. W. Gilroy (2011). "Sex differences in resident immune cell phenotype underlie more efficient acute inflammatory responses in female mice." Blood **118**(22): 5918-5927.

Sellau, J., M. Groneberg, H. Fehling, T. Thye, S. Hoenow, C. Marggraff, M. Weskamm, C. Hansen, S. Stanelle-Bertram, S. Kuehl, J. Noll, V. Wolf, N. G. Metwally, S. H. Hagen, C. Dorn, J. Wernecke, H. Ittrich, E. Tannich, T. Jacobs, I. Bruchhaus, M. Altfeld and H. Lotter (2020). "Androgens predispose males to monocyte-mediated immunopathology by inducing the expression of leukocyte recruitment factor CXCL1." Nat Commun **11**(1): 3459.

Sellau, J., M. Groneberg and H. Lotter (2019). "Androgen-dependent immune modulation in parasitic infection." Semin Immunopathol **41**(2): 213-224.

Snider, H., C. Lezama-Davila, J. Alexander and A. R. Satoskar (2009). "Sex hormones and modulation of immunity against leishmaniasis." Neuroimmunomodulation **16**(2): 106-113.

Solano-Galvez, S. G., D. A. Alvarez-Hernandez, L. Gutierrez-Kobeh and R. Vazquez-Lopez (2021). "Leishmania: manipulation of signaling pathways to inhibit host cell apoptosis." Ther Adv Infect Dis **8**: 20499361211014977.

Soto, J. (2010). "Oral Miltefosine Plus Topical Imiquimod to Treat Cutaneous Leishmaniasis." Retrieved 21.10.2022, 16.10, 2022, from https://clinicaltrials.gov/ct2/show/NCT01380314.

Soto, J. and P. Soto (2006). "Miltefosine: oral treatment of leishmaniasis." Expert Rev Anti Infect Ther **4**(2): 177-185.

STEMCELL. (2022). "Cell Separation and Cell Isolation Methods." Retrieved 30.09.2022, 16:40, 2022, from https://www.stemcell.com/cell-separation/methods.

Stone, N. R., T. Bicanic, R. Salim and W. Hope (2016). "Liposomal Amphotericin B (AmBisome((R))): A Review of the Pharmacokinetics, Pharmacodynamics, Clinical Experience and Future Directions." Drugs **76**(4): 485-500.

Sun, S. and L. B. Barreiro (2020). "The epigenetically-encoded memory of the innate immune system." Curr Opin Immunol **65**: 7-13.

Sun, Z., Y. Pan, J. Qu, Y. Xu, H. Dou and Y. Hou (2020). "17beta-Estradiol Promotes Trained Immunity in Females Against Sepsis via Regulating Nucleus Translocation of RelB." Front Immunol **11**: 1591.

Sunyoto, T., J. Potet and M. Boelaert (2018). "Why miltefosine-a life-saving drug for leishmaniasis-is unavailable to people who need it the most." BMJ Glob Health **3**(3): e000709.

Swerdloff, R. S., R. E. Dudley, S. T. Page, C. Wang and W. A. Salameh (2017). "Dihydrotestosterone: Biochemistry, Physiology, and Clinical Implications of Elevated Blood Levels." Endocr Rev **38**(3): 220-254.

Taneja, V. (2018). "Sex Hormones Determine Immune Response." Front Immunol **9**: 1931.

Tapia, V. S., M. J. D. Daniels, P. Palazon-Riquelme, M. Dewhurst, N. M. Luheshi, J. Rivers-Auty, J. Green, E. Redondo-Castro, P. Kaldis, G. Lopez-Castejon and D. Brough (2019). "The three cytokines IL-1beta, IL-18, and IL-1alpha share related but distinct secretory routes." J Biol Chem **294**(21): 8325-8335.

Tomiotto-Pellissier, F., B. Bortoleti, J. P. Assolini, M. D. Goncalves, A. C. M. Carloto, M. M. Miranda-Sapla, I. Conchon-Costa, J. Bordignon and W. R. Pavanelli (2018). "Macrophage Polarization in Leishmaniasis: Broadening Horizons." Front Immunol **9**: 2529.

Travi, B. L., Y. Osorio, P. C. Melby, B. Chandrasekar, L. Arteaga and N. G. Saravia (2002). "Gender is a major determinant of the clinical evolution and immune response in hamsters infected with Leishmania spp." Infect Immun **70**(5): 2288-2296.

van Griensven, J., M. Balasegaram, F. Meheus, J. Alvar, L. Lynen and M. Boelaert (2010). "Combination therapy for visceral leishmaniasis." The Lancet Infectious Diseases **10**(3): 184-194.

Viola, A., F. Munari, R. Sanchez-Rodriguez, T. Scolaro and A. Castegna (2019). "The Metabolic Signature of Macrophage Responses." Front Immunol **10**: 1462.

von Stebut, E. and M. C. Udey (2004). "Requirements for Th1-dependent immunity against infection with Leishmania major." Microbes Infect **6**(12): 1102-1109.

Vouldoukis, I., P. A. Becherel, V. Riveros-Moreno, M. Arock, O. da Silva, P. Debre, D. Mazier and M. D. Mossalayi (1997). "Interleukin-10 and interleukin-4 inhibit intracellular killing of Leishmania infantum and Leishmania major by human macrophages by decreasing nitric oxide generation." Eur J Immunol **27**(4): 860-865.

Wassef, M. K., T. B. Fioretti and D. M. Dwyer (1985). "Lipid analyses of isolated surface membranes of Leishmania donovani promastigotes." Lipids **20**(2): 108-115.

Westrop, G. D., R. A. Williams, L. Wang, T. Zhang, D. G. Watson, A. M. Silva and G. H. Coombs (2015). "Metabolomic Analyses of Leishmania Reveal Multiple Species Differences and Large Differences in Amino Acid Metabolism." PLoS One **10**(9): e0136891.

WHO. (2022, 2022). "Neglected tropical diseases." Retrieved 12.09.2022, 12:15, 2022, from https://www.who.int/health-topics/neglected-tropical-diseases#tab=tab_1.

Wilkinson, N. M., H. C. Chen, M. G. Lechner and M. A. Su (2022). "Sex Differences in Immunity." Annu Rev Immunol **40**: 75-94.

Wirnsberger, G., D. Hebenstreit, G. Posselt, J. Horejs-Hoeck and A. Duschl (2006). "IL-4 induces expression of TARC/CCL17 via two STAT6 binding sites." Eur J Immunol **36**(7): 1882-1891.

Wyllie, S., M. L. Cunningham and A. H. Fairlamb (2004). "Dual action of antimonial drugs on thiol redox metabolism in the human pathogen Leishmania donovani." J Biol Chem **279**(38): 39925-39932.

Yang, J., L. Zhang, C. Yu, X. F. Yang and H. Wang (2014). "Monocyte and macrophage differentiation: circulation inflammatory monocyte as biomarker for inflammatory diseases." Biomark Res **2**(1): 1.

Zanoni, I. and F. Granucci (2013). "Role of CD14 in host protection against infections and in metabolism regulation." Front Cell Infect Microbiol **3**: 32.

Zheng, Z., J. Chen, G. Ma, A. R. Satoskar and J. Li (2020). "Integrative genomic, proteomic and phenotypic studies of Leishmania donovani strains revealed genetic features associated with virulence and antimony-resistance." Parasit Vectors **13**(1): 510.

Zizzo, G., B. A. Hilliard, M. Monestier and P. L. Cohen (2012). "Efficient clearance of early apoptotic cells by human macrophages requires M2c polarization and MerTK induction." J Immunol **189**(7): 3508-3520.

Gal-Oz, S.T., Maier, B., Yoshida, H. et al. ImmGen report: sexual dimorphism in the immune system transcriptome. Nat Commun 10, 4295 (2019)